Universiteit Leiden
The Netherlands

Development of potent and selective monoacylglycerol lipase inhibitors: SARs, structural analysis, and biological characterization

Butini, S.; Grether, U.; Jung, K.-M.; Ligresti, A.; Allara, M.; Postmus, A.G.J.; ... ; Campiani, G.

Citation

Butini, S., Grether, U., Jung, K. -M., Ligresti, A., Allara, M., Postmus, A. G. J., ... Campiani, G. (2024). Development of potent and selective monoacylglycerol lipase inhibitors: SARs, structural analysis, and biological characterization. *Journal Of Medicinal Chemistry*, *67*(3), 1758-1782. doi:10.1021/acs.jmedchem.3c01278

Version: Publisher's Version

License: Licensed under Article 25fa Copyright Act/Law (Amendment Taverne)

Downloaded from: https://hdl.handle.net/1887/3731683

Note: To cite this publication please use the final published version (if applicable).

Journal of Medicinal Chemistry

pubs.acs.org/jmc

Article

Development of Potent and Selective Monoacylglycerol Lipase Inhibitors. SARs, Structural Analysis, and Biological Characterization

Stefania Butini,* Uwe Grether, Kwang-Mook Jung, Alessia Ligresti, Marco Allarà, Annemarieke G. J. Postmus, Samuele Maramai, Simone Brogi, Alessandro Papa, Gabriele Carullo, David Sykes, Dmitry Veprintsev, Stefano Federico, Alessandro Grillo, Bruno Di Guglielmo, Anna Ramunno, Anna Floor Stevens, Dominik Heer, Stefania Lamponi, Sandra Gemma, Jörg Benz, Vincenzo Di Marzo, Mario van der Stelt, Daniele Piomelli, and Giuseppe Campiani*

Cite This: *J. Med. Chem.* 2024, 67, 1758−1782

Read Online

ACCESS | Metrics & More | Article Recommendations | Supporting Information

ABSTRACT: New potent, selective monoacylglycerol lipase (MAGL) inhibitors based on the azetidin-2-one scaffold ((±)-**5a−v**, (±)-**6a−j**, and (±)-**7a−d**) were developed as irreversible ligands, as demonstrated by enzymatic and crystallographic studies for (±)-**5d**, (±)-**5l**, and (±)-**5r**. X-ray analyses combined with extensive computational studies allowed us to clarify the binding mode of the compounds. **5v** was identified as selective for MAGL when compared with other serine hydrolases. Solubility, *in vitro* metabolic stability, cytotoxicity, and absence of mutagenicity were determined for selected analogues. The most promising compounds ((±)-**5c**, (±)-**5d**, and (±)-**5v**) were used for *in vivo* studies in mice, showing a decrease in MAGL activity and increased 2-arachidonoyl-*sn*-glycerol levels in forebrain tissue. In particular, **5v** is characterized by a high eudysmic ratio and (3*R*,4*S*)-**5v** is one of the most potent irreversible inhibitors of *h*/*m*MAGL identified thus far. These results suggest that the new MAGL inhibitors have therapeutic potential for different central and peripheral pathologies.

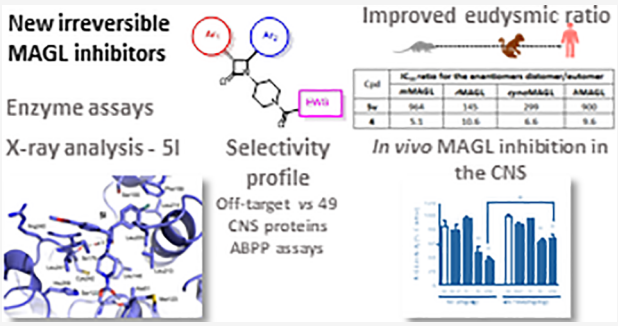

INTRODUCTION

The endocannabinoid system (ECS) is a key neuromodulatory network involved in the regulation of several pathophysiological processes throughout the body.[1,2] It consists of two G protein-coupled receptors (GPCRs), namely cannabinoid receptor type-1 and type-2 (CB_1R and CB_2R), their ligands, i.e., the endocannabinoids (ECs), such as anandamide (arachidonoylethanolamide, AEA), and 2-arachidonoylglycerol (2-AG), which activate CBRs, as well as various proteins responsible for the production, movement, and degradation of ECs.[1,3,4] ECs are generated upon demand and act as retrograde synaptic messengers (2-AG) or local mediators (AEA), modulating several biological processes including pain, stress, mood, cognition, and energy balance.[1,5] AEA signaling is terminated by transport into cells followed by intracellular hydrolysis, mediated by the serine hydrolase, fatty acid amide hydrolase (FAAH), which converts AEA into arachidonic acid (AA) and ethanolamine.[6] 2-AG is primarily deactivated by presynaptic monoacyl glycerol lipase (MAGL) and, to a lesser extent, by postsynaptic α/β-hydrolase domain-containing 6 (ABHD6).[7,8] MAGL is a ubiquitous serine hydrolase that makes use of a catalytic triad (Ser122, Asp239, His269) to hydrolyze 2-AG into AA and glycerol.[9] Considering the pivotal role of MAGL in 2-AG deactivation and ECS function, MAGL inhibition has emerged as a promising pharmacological strategy to enhance ECS activity while avoiding the typical side effects associated with direct CB_1R/CB_2R-agonism.[10,11] In the central nervous system (CNS), 2-AG is also an important source of AA, which can be converted into bioactive eicosanoids.[12] Accordingly, the key role played by MAGL in the control of 2-AG and AA levels strongly supports the therapeutic potential of MAGL inhibitors in the treatment of neuroinflammatory and neurodegenerative diseases.[13−15] As reported by several laboratories, including ours, potent, selective, and irreversible MAGL inhibitors are effective in rodent models of multiple sclerosis (MS) and neuropathic pain,[16,17] as well as in models of post-traumatic stress disorder.[4,18] Moreover, studies have shown that MAGL inhibitors such as JZL184 (**1**, Figure 1) may possess therapeutic

Received: July 14, 2023
Revised: December 15, 2023
Accepted: December 25, 2023
Published: January 19, 2024

Downloaded via LEIDEN UNIV on March 12, 2024 at 09:40:33 (UTC).
See https://pubs.acs.org/sharingguidelines for options on how to legitimately share published articles.

ACS Publications © 2024 American Chemical Society

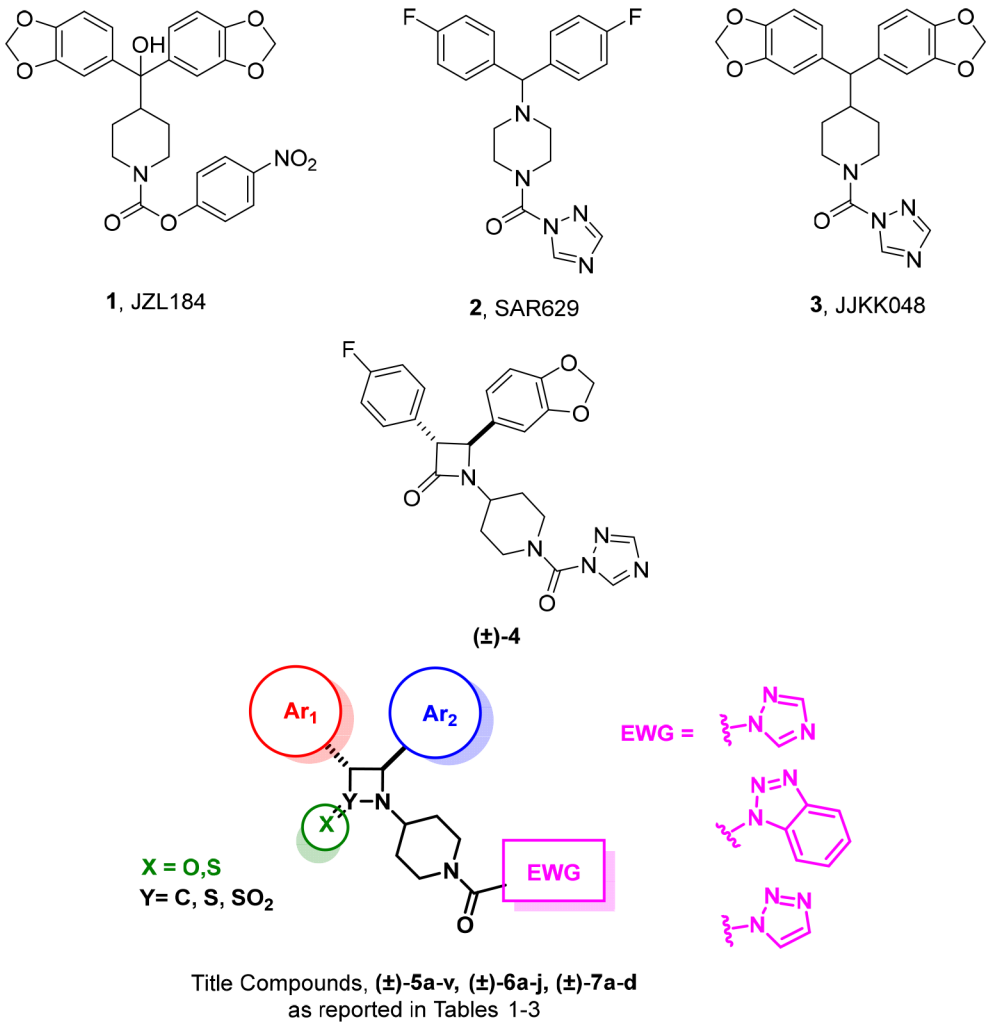

Figure 1. Representative diphenylmethane-based MAGL inhibitors (compounds **1**−**3**), the azetidinone-based MAGL inhibitor (±)-**4**, and the general structure of the title compounds (±)-**5a**−**v**, (±)-**6a**−**j**, and (±)-**7a**−**d**.

potential in different diseases including cancer,[18,19] chronic liver injuries,[20,21] and pain.[17]

MAGL is a homodimer in which a mobile "cap" (or "lid") domain confers to the enzyme the ability to adopt open or closed conformations.[19] The former allows access of 2-AG and other substrates (e.g., 2-oleoyl-*sn*-glycerol) to the enzyme binding pocket, which houses the catalytic triad responsible for hydrolytic activity.[19] The irreversible carbamate-based MAGL inhibitor JZL184 (**1**, Figure 1) acts by targeting the catalytic Ser122, leading to the formation of a tetrahedral intermediate preluding the formation of a carbamoylated enzyme with the subsequent release of 4-nitrophenol as leaving group.[20] However, the replacement of the 4-nitrophenoxy group with a triazole moiety led to the discovery of novel azole-urea-based MAGL inhibitors typified by SAR629 (**2**, Figure 1).[21] Several MAGL inhibitors were used as pharmacological tools and help in elucidating the key interaction points in the enzyme catalytic site. In particular, early reports were obtained by exploiting a piperazinyl amide-based reversible MAGL inhibitor developed by Janssen Pharmaceutica[22] that spans enzyme's lid-domain, thus impeding the substrate access to the catalytic pocket. This binding mode was demonstrated by one of the earliest X-ray analysis of MAGL in complex with an inhibitor.[23] Structurally all the early and more recent MAGL reversible inhibitors[24] lack the more classically employed moieties for interacting with the catalytic Ser122 such as piperazinyl-, piperidyl-, and azetidinyl-based carbamates or ureas with different leaving groups (e.g., as hexafluoroisopropanol, triazole, or benzotriazole).[24,25]

The analysis of the crystal structure of MAGL in complex with the covalent triazole-urea-based inhibitor **2** revealed that this compound binds to the active site by adopting a "Y shape" conformation in which the fluorophenyl substituents point in opposite directions.[21] These features guarantee elevated affinity and excellent selectivity. Similarly, the potent inhibitor JJKK048 (**3**, Figure 1) displays the same diphenylmethane arrangement[26] linked to a piperidine moiety supporting the electrophilic center. The steric hindrance of the biphenyl portion provides selectivity by interacting with hydrophobic residues, whereas the carbonyl group of the ureidic moiety (electrophilic center) sits in proximity of the catalytic triad.[21] More recently, a new carbamate-based MAGL inhibitor named ABX-1431 was developed and tested, unsuccessfully, for the treatment of Tourette syndrome or chronic motor tic disorder (NCT03625453).[27]

Modulation of the ECS throughout interference with FAAH and MAGL activities is part of our scientific interest. We have recently developed selective or dual-acting FAAH and MAGL inhibitors as pharmacological tools for exploring different potential therapeutic applications.[28−32] An example is the potent and selective MAGL inhibitor (±)-**4**[16] (Figure 1), in

https://doi.org/10.1021/acs.jmedchem.3c01278
J. Med. Chem. 2024, 67, 1758−1782

Table 1. Inhibition Potency of Compounds (±)-5a−v towards Human (*h*) and Rat (*r*) MAGL and FAAH Enzymes as IC_{50} (nM)[a]

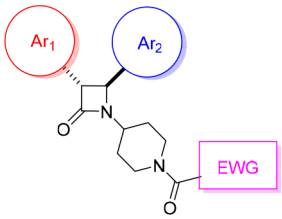

		EWG	IC50 (nM)		EWG	IC50 (nM)	
Ar1	Ar2	Cpds	*h*MAGL (*h*) *r*MAGL (*r*)	*h*FAAH (*h*) *r*FAAH (*r*)	Cpds	*h*MAGL (*h*) *r*MAGL (*r*)	*h*FAAH (*h*) *r*FAAH (*r*)
		5a	9.19 (*h*)	2977 (*h*) 368.1 (*r*)	**5n**	2682[b] (*r*)	-
		5b	6.95 (*h*)	3510 (*r*)	**5o**	2003[b] (*r*)	-
		5c	14.17 (*h*) 1.20[c] (*r*)	462.0 (*r*)	**5p**	2641[b] (*r*)	-
		5d	11.51 (*h*) 0.12[c] (*r*)	3227 (*h*) 266.2 (*r*)	**5q**	1863[b] (*r*)	-
		5e	9.75 (*h*)	1631 (*h*) 488.9 (*r*)	-	-	-
		5f	34.44 (*h*)	1232 (*r*)	-	-	-
	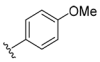	**5g**	12.52 (*h*)	1030 (*r*)	-	-	-
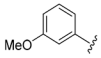	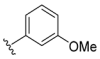	**5h**	8.34 (*h*)	4259 (*h*) 1435(*r*)	-	-	-
		5i	16.92 (*h*) 5.18 (*r*)	-	**5r**	20.54 (*h*) 80.6[b] (*h*) 8.40 (*r*) 592.3[b] (*r*)	-
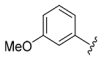		**5j**	35.43 (*h*) 137.8[b] (*h*) 5.53 (*r*) 372.7[b] (*r*)	-	**5s**	32.81 (*r*) 245.0[b] (*r*)	-
		5k	49.5 (*r*) 419.6[b] (*r*)	-	**5t**	19.48 (*r*) 557.5[b] (*r*)	-
	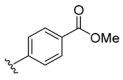	**5l**	54.6 (*r*) 2770[b] (*r*)	>1000 (*r*)	-	-	-
		-	-	-	**5u**	72.8 (*r*) 2730[b] (*r*)	61.0 (*r*)
		EWG **5m**	61.9 (*r*) 760.0[b] (*r*)	-	**5v**	12.19 (*h*) 0.22[c] (*r*)	300.7 (*r*)
		4[16]	7.4 (*h*) 0.25 (*r*)				

[a]Tests were performed as described in the Experimental Section after 20 min of preincubation unless otherwise noted, for MAGL inhibition, method A was followed unless otherwise noted; values are means of three experiments and all SD are within 10%. [b]Value obtained without preincubation. [c]For MAGL inhibition, method B was followed.

which the Y shape of the diphenylmethane derivatives **1**−**3** was mimicked and challenged by exploiting the *trans*-3,4-diaryl-substituted *β*-lactam structural motif. The azetidin-2-one could support the aromatic rings (namely the key pharmacophoric elements), allowing their correct reciprocal orientation and distance for interaction in their enzymatic binding site. The previous results obtained with the covalent (as demonstrated by enzymatic and top-down bottom-up mass studies) MAGL inhibitor (±)-**4**[16] spurred us to further explore the structure−activity relationships (SARs) of azetidin-2-one-based inhibitors in order to identify the optimal combinations of substituents on the azetidin-2-one core and the leaving groups supported on the piperidinyl-based ureidic moiety. The newly developed analogues can be clustered into different structural sets, 3,4-diphenylazetidin-2-one derivatives ((±)-**5a**−**v**, Figure 1 and Table 1), pyridine-containing inhibitors synthesized in order to ameliorate the drug-like properties of the newly developed compounds ((±)-**6a**−**j**, Figure 1 and Table 2), and sulfur-containing analogues ((±)-**7a**−**d**, Figure 1 and Table 3).

https://doi.org/10.1021/acs.jmedchem.3c01278
J. Med. Chem. 2024, 67, 1758−1782

Table 2. Inhibition Potency of Pyridine-Containing Compounds (±)-6a–j towards Rat (*r*) MAGL and Rat FAAH Enzymes as IC_{50} (nM).[a]

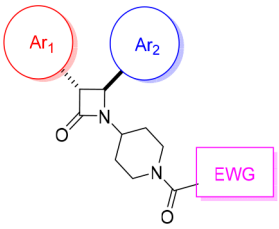

		EWG	IC_{50} (nM)		EWG	IC_{50} (nM)	
Ar_1	Ar_2	Cpds	*r*MAGL	*r*FAAH	Cpds	*r*MAGL	*r*FAAH
		6a	10040[b]		**6f**	124.8 5570[b]	310.5
		6b	95.0 7380[b]	>1000	**6g**	409.0 8020[b]	>1000
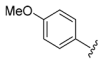		**6c**	9320[b]	-	**6h**	4740[b]	-
		-	-	-	**6i**	4080[b]	-
		6d	4820[b]	-	-	-	-
		6e	105.7 4570[b]	>1000	-	-	-
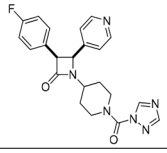		**6j**	99.5 3560[b]	>1000	-	-	-

[a]Tests were performed as described in the Experimental Section after 20 min of preincubation unless otherwise noted, for MAGL inhibition, method A was followed; values are means of three experiments and all SD are within 10%; [b]Value obtained without preincubation.

Furthermore, the effect of different leaving groups, including the bulky benzotriazole, were investigated (vide infra).

Covalent bond formation relies on the potency of the first reversible binding event and the maximum potential rate of inactivation.[33] The irreversible mechanism of action of these urea-based inhibitors was tested by time-dependent MAGL inhibition studies and dilution assays performed on selected analogues (±)-**5c**, (±)-**5d**, and (±)-**5v**. To confirm the irreversible enzyme inhibition mechanism and binding mode of these new compounds, the crystal structures of derivatives (±)-**5d**, (±)-**5l**, and (±)-**5r** in complex with *human* MAGL were solved. Based on these data, molecular docking studies and enzymatic assays (performed on MAGL enzyme of different species, Table 4) coupled with the determination of the ratio of the IC_{50} values of the enantiomers (distomer/eutomer), furnished new insight about the role of enantioselective interaction of azetidine-2-one based compounds against MAGL.

The selectivity profile, preliminary absorption distribution metabolism excretion (ADME) properties, of the most promising analogues were assessed. Toxicity was evaluated in murine fibroblasts, and the absence of mutagenicity was assessed using Ames tests. Endogenous levels of 2-AG, AA, AEA, and other lipids were measured in mouse forebrain tissue after ip administration of the most promising analogues (±)-**5c**, (±)-**5d**, and (±)-**5v**, confirming the value of these compounds as novel pharmacological tools for MAGL inhibition.

RESULTS AND DISCUSSION

Chemistry. The synthesis of compounds (±)-**5a–v** is reported in Scheme 1; the synthesis of compounds (±)-**6a–j**, of the *β*-sultame (±)-**7**, and of the thio-derivatives (±)-**7b–d** is reported in Schemes S1–S3 of the Supporting Information (SI).

The synthesis of compounds (±)-**5a–v** (Scheme 1) started with the appropriately substituted aldehydes **8a–g**, which reacted with 4-amino-1-benzylpiperidine to afford the imines **9a–g**. These latter and **9h**[16] were subjected to Staudinger reaction with suitable phenylacetic acids, to obtain the *β*-lactams (±)-**10a–l** exclusively in the *trans*-configuration as determined by NMR studies (coupling constant of H_3 and H_4 in azetidin-2-one ring proton are $JH_3,H_4 \leq 3.0$ Hz for the *trans* stereoisomer). The cleavage of the benzyl group led to amines (±)-**11a–l**. These latter and (±)-**11m**[34] were reacted with appropriate heterocycles (i.e., 1*H*-1,2,3 triazole, 1*H*-1,2,4-triazole, or 1*H*-1,2,3-benzotriazole) in the presence of phosgene and DMAP, providing compounds (±)-**5a–v** as reported in Table 1. The enantiomerically pure amines (3*R*,4*S*)-**11n** and (3*S*,4*R*)-**11n** were obtained from (±)-**11n**, after chiral HPLC enantioseparation (absolute configuration was determined as reported[16]). These two enantiomeric amines were used in the reaction with phosgene and 1*H*-benzotriazole, for obtaining the pure enantiomers (3*R*,4*S*)-**5v** and (3*S*,4*R*)-**5v**.

Based on our experience in the synthesis of azetidin-2-one-based compounds, in this work we embarked on the optimization of the reaction conditions of compounds

https://doi.org/10.1021/acs.jmedchem.3c01278
J. Med. Chem. 2024, 67, 1758–1782

Table 3. Inhibition Potency of Sulfur-Containing Compounds (±)-7a−d towards Rat (*r*) MAGL and Rat FAAH Enzymes as IC_{50} (nM).[a]

Cpds	Structure	IC_{50} (nM) *r*MAGL	*r*FAAH
7a	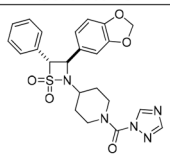	40.5	-
7b	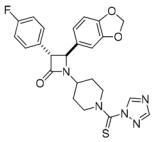	>10000 *cos*	>10000
7c	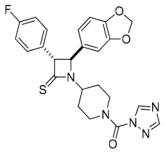	18.38 *cos* 11.08	>1000
7d	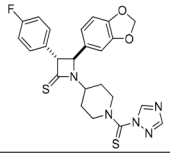	5570 *cos*	7980

[a]Tests were performed as described in the Experimental Section after 20 min of preincubation, for MAGL inhibition, method A was followed; values are means of three experiments and all SD are within 10%.

(±)-**11m**[34] and (±)-**11n**,[16] previously described by us, and here used for the synthesis of the most potent MAGL inhibitors of the series (±)-**5d** and (±)-**5v** (Table 1). Our efforts were dedicated to the optimization of the Staudinger protocol, in terms of a sustainable protocol (SI, Scheme S4). In particular, the (2 + 2) ketene−imine cycloaddition reaction was conducted under two different conditions. For compounds (±)-**11m,n**, imines **25** (for (±)-**11m**) and **26** (for (±)-**11n**), obtained after refluxing in EtOH, were added to a mixture of suitable phenylacetic acid and triphosgene. The original conditions performed DCM at 50 °C were modified using green solvents such as 2-methyl-THF or MeCN[35] combined with no heating (room temperature) and in the presence of the green base DBU[36] in place of TEA. Gratifyingly, under these conditions the azetidin-2-ones (±)-**27** and (±)-**28** (from **25** and **26**, respectively) were obtained with a notable improvement of the reaction yields of 15% (80%, new method, vs 65%, old method, SI, Table S1) and 21% (82%, new method, vs 61%, old method, SI, Table S1), respectively. Compounds (±)-**27** and (±)-**28** underwent hydrogenolysis to afford (±)-**11m,n**, and from these latter, we synthesized the target compounds (±)-**5d** and (±)-**5v**, respectively. For the synthesis of (±)-**5d**, the amine (±)-**11m** was treated with 1,1′-carbonyl-di-(1,2,4-triazole) in MeCN, in the absence of the base catalyst, providing (±)-**5d** in an improved yield compared with the original method (81%, new method, vs 61%, old method, SI, Table S1). For the synthesis of compound (±)-**5v**, the amine (±)-**11n** was treated with triphosgene (instead of phosgene of the original method) in MeCN and DBU. The mixture was then added to 1*H*-benzotriazole to afford (±)-**5v** and improving the reaction yields also in this case (51%, new method, vs 42%, old method, SI, Table S1). Overall yields for the synthesis of (±)-**5d** and (±)-**5v** resulted improved. The compounds (±)-**5d** and (±)-**5v** were obtained, following the original procedures, with an overall yield of 40% and 26%, respectively. Gratifyingly, the newly developed sustainable methods improved the overall yields (calculated in mg scale) for both (±)-**5d** and (±)-**5v** by 65% and 42% (SI, Table S1), respectively.

Structure−Activity Relationship, Irreversible Mode of MAGL Inhibition, and Computational Studies. In order to identify potent and selective small-molecule MAGL inhibitors,[16] we investigated the SAR of azetidin-2-one-based compounds following three main lines.

1. We interrogated the effect of introducing differently functionalized aromatic groups and heteroaromatic systems on C3 and C4 of the azetidin-2-one core (compounds (±)-**5a−v**, Table 1, and (±)-**6a−j**, Table 2).
2. As per the mechanism of action on triazole-urea derivatives (e.g., the carbamoylation of the enzyme prompted by the nucleophilic attack of the catalytic Ser122),[25,37] the SARs were also explored in relation to the nature of the leaving groups by comparing the fusion

Table 4. Inhibition Potency of Compounds (±)-5d, (±)-5l, (±)-5r, (±)-5v, (3*R*,4*S*)-5v, and (3*S*,4*R*)-5v against Different MAGL Isoforms[a]

MAGL isoform → Cmpds ↓	IC_{50} nM *m*MAGL	*h*MAGL	*r*MAGL	*cyno*MAGL
(±)-**5d**	0.081	0.180	-	-
(±)-**5l**	1.053	2.730	-	-
(±)-**5r**	0.049	0.050	-	-
(±)-**5v**	0.072	0.050	-	-
(*3R,4S*)-**5v**	0.026	0.021	0.240	0.067
(*3S,4R*)-**5v**	25.07	18.90	34.90	20.01
IC_{50} ratio for the enantiomers of **5v** distomer/eutomer	**964**	**900**	**145**	**299**
(±)-**4**	0.105	0.198	0.159	0.255
(*3R,4S*)-**4**	0.070	0.086	0.078	0.168
(*3S,4R*)-**4**	0.357	0.825	0.827	1.117
IC_{50} ratio for the enantiomers of **4** distomer/eutomer	**5.1**	**9.6**	**10.6**	**6.6**

[a]Tests were performed after 15 min of incubation, as described in the Experimental Section; values are means of three experiments and all SD are within 10%.

https://doi.org/10.1021/acs.jmedchem.3c01278
J. Med. Chem. 2024, 67, 1758−1782

Scheme 1. Synthesis of Compounds (±)-5a−v[a]

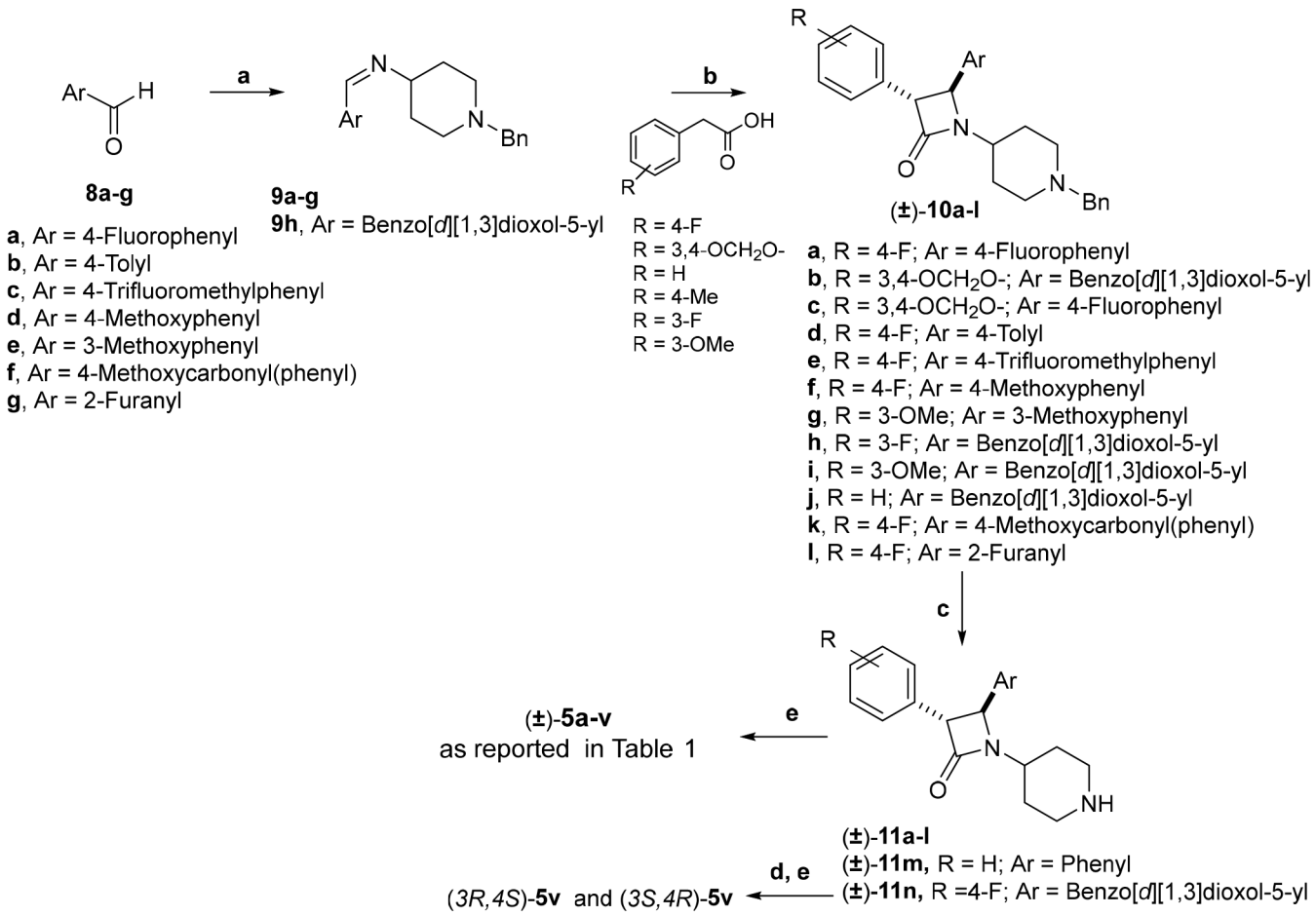

[a]Reagents and conditions: (a) 4-amino-*N*-benzylpiperidine, EtOH, 80 °C, 12 h (quantitative yield); (b) appropriate phenylacetic acid, triphosgene, dry DCM, 50 °C, 30′, then TEA, 50 °C, 12 h (42−65% yield); (c) H_2, Pd/C 10%, MeOH, 25 °C, 2 h (quantitative yield); (d) enantiomeric separation by chiral HPLC (cellulose-carbamate (OD) column (Daicel) eluted with a mixture of 50% of 2-propanol in *n*-hexane as eluent, flow 1 mL/min, injection volume 50 μL); (e) 1*H*-1,2,4-triazole for compounds (±)-**5a−l**, 1*H*-1,2,3-triazole for compound (±)-**5m**, 1*H*-1,2,3-benzotriazole for compounds (±)-**5n−v**, phosgene (20% soln. in toluene), DMAP, dry DCM, 25 °C, rt, 12 h (32−66% yield).

of several carbamoylating moieties with various azoles: a 1,2,4-triazole system (compounds (±)-**5a−l**, Table 1), a 1,2,3-triazole system (compound (±)-**5m**, Table 1), and a 1,2,3-benzotriazole (compounds (±)-**5n−v**, Table 1). In line with our previously reported data,[16] we selected these leaving groups considering the ideal pK_a values of the corresponding conjugated acids after carbamoylation (10.0 for 1,2,4-triazole, 9.4 for 1,2,3-triazole, and 8.2 for 1,2,3-benzotriazole).[26]

3. As a further analysis, we synthesized sulfur-containing compounds ((±)-7**a−d**, Table 3), where we explored the replacement of the azetidin-2-one core system with a *β*-sultame (compound (±)-7**a**) and an azetidin-2-thione ((±)-7**c**). A thiourea moiety was also inserted in compounds (±)-7**b** and (±)-7**d** for exploring its effect on the electrophilic center.

As illustrated in Tables 1−3, most compounds displayed nanomolar or subnanomolar inhibitory potencies toward *human* and *rat* MAGL, thus confirming the value of the azetidin-2-one scaffold.

Furthermore, in line with several literature examples,[38] the more sterically hindered aryl groups supported on the *β*-lactam system could be responsible for very high values of MAGL versus FAAH selectivity. However, the selectivity is intrinsically high for this class of compounds and, when evaluated, was never lower than 3 orders of magnitude.

In more detail, in the set of compounds (±)-**5a−v** (Table 1), different aromatic systems were combined at C3 and C4 positions in order to investigate the space available within the catalytic cleft of the enzyme. The presence of fluorophenyl rings was mostly introduced on C3 of the lactam core and combined with differently decorated phenyl systems at C4. In fact, at C4, we introduced different aromatic rings in terms of size, and the nature of the *para* substituents was modified, starting from the unsubstituted benzene ring and carrying on substitutions with fluorine, methyl, methoxy, trifluoromethyl, COOMe groups, and the benzodioxole system. Para *versus* meta substitutions were also investigated (e.g., (±)-**5h−j**). The introduction of a furan-2-yl moiety at C4 of the azetidin-2-one core was also explored in (±)-**5u**.

In particular, in the 1,2,4-triazoleurea series ((±)-**5a−m**), the symmetrical substitution at C3 and C4 (e.g., (±)-**5a**, (±)-**5b**, (±)-**5d**, and (±)-**5h**, Table 1) generated MAGL inhibitors of similar nanomolar potency. When compared with compound (±)-**4**, several SARs were examined. Notably, the inversion of the substituents at C3 and C4 as in (±)-**5c** slightly decreased the

https://doi.org/10.1021/acs.jmedchem.3c01278
J. Med. Chem. 2024, 67, 1758−1782

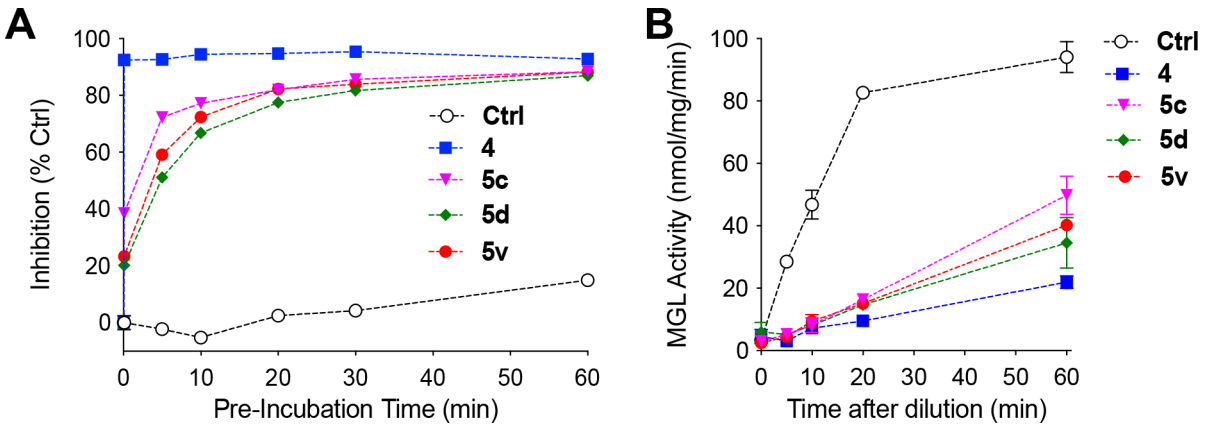

Figure 2. *In vitro* characterization of MAGL inhibition by azetidin-2-one-based compounds. Time-dependent *r*MAGL inhibition studies (A), and rapid dilution studies on *r*MAGL for compounds (±)-**5c**, (±)-**5d**, (±)-**5v**, and (±)-**4** (B). Activity assays were conducted using homogenates of HeLa cells overexpressing wild-type rat MGL.

inhibition potency (*h*MAGL IC_{50} 14.17 vs 7.4 nM, and *r*MAGL IC_{50} 1.20 vs 0.25 for (±)-and **5c** and (±)-**4**, respectively). The same was true when the benzodioxole at C4 of compound (±)-**4** was replaced by 4-tolyl ((±)-**5e**) and 4-methoxyphenyl ((±)-**5g**). The introduction of the trifluoromethyl group ((±)-**5f**) decreased the potency toward *h*MAGL. Shifting of the fluorine atom from the *para* to the *meta* position, as in (±)-**5i**, almost halved the inhibition potency as compared to (±)-**4**. When the fluorine of (±)-**5i** was substituted by a methoxy group in (±)-**5j**, the inhibition potency was further weakened. The high potency of (±)-**5d**, when one phenyl system was replaced by a benzodioxole ((±)-**5k**), was diminished by 3 orders of magnitude and (±)-**5k** was a two-digit nM *r*MAGL inhibitor. The same was true when 4-methoxycarbonyl(phenyl) was introduced at C4 ((±)-**5l**, *r*MAGL IC_{50} = 54.63 nM, Table 1).

Regarding the nature of the leaving group, the 1,2,3-benzotriazoleurea-based compounds ((±)-**5n−v**) generally demonstrated slightly weakened or similar inhibition potencies than their 1,2,4-triazoleurea counterparts (Table 1). A remarkable exception was observed with compounds (±)-**5t** and (±)-(3*R*,4*S*)-**5v**, which were more potent MAGL inhibitors than (±)-**5k** and (±)-**5m**, respectively. In fact, when the single enantiomers of compound **5v** (obtained after chiral HPLC) were tested on human and murine MAGL, they exhibited a noticeable stereoselectivity of interaction being (3*R*,4*S*)-**5v** the eutomer with nearly 900 times improved potency than the distomer in *human* and *murine* MAGL orthologues (see later Table 4 and related discussion).

Compounds (±)-**5n−q**, showed inhibitory potencies in the micromolar range when preliminarily tested without preincubation and were not further tested. When a furan system was introduced at C4 ((±)-**5u**), a sensible decrease in MAGL inhibition potency and selectivity toward FAAH was observed, thus confirming the relevance of the size of the aryl substituents for increasing potency and MAGL/FAAH selectivity. When the same substitutions on the azetidin-2-one core of (±)-**4** and (±)-**5v** were combined with a 1,2,3-triazole system ((±)-**5m**), a decrease in inhibition potency was observed.

For further analysis, we tested the effect of introducing pyridine systems into the azetidin-2-one core ((±)-**6a−j**, Table 2) in combination with 1,2,4-triazole and 1,2,3-benzotriazole as leaving groups. In general, with respect to the most potent compounds of the series (Table 1), the insertion of a pyridine was not beneficial. Among the sulfur-containing compounds ((±)-**7a−d**, Table 3), consistent with the mechanism of enzyme inhibition, the presence of a thiourea caused a dramatic drop in potency (more comments are in the Supporting Information).

From this initial inhibitory potency exploration of the SARs on three main sets of compounds ((±)-**5a−v**, (±)-**6a−j**, and (±)-**7a−d** Tables 1−3), three interesting analogues, (±)-**5c**, (±)-**5d**, and (±)-**5v**, were selected for further analysis.

Evaluation of MAGL Inhibition against Species-Specific Enzyme Orthologues: Stereoselective Interaction and the Improved IC_{50} Ratio of the Enantiomers Ratio of 5v. To cross-validate the pharmacodynamic (PD) properties of the newly developed azetidin-2-one-based MAGL inhibitors, the efficacy of the best performing analogues was evaluated with a different experimental protocol and using a panel of different MAGL isoforms (Table 4). The final aim of this investigation was to validate the *in vitro* potency of the compounds on *murine* MAGL before conducting *in vivo* target engagement studies in mice. To prepare for putative later studies in other species, enzyme inhibition data have been generated on rat and cynomolgus monkey MAGL isoforms for the most promising ligand (3*R*,4*S*)-**5v** and its enantiomer (3*S*,4*R*)-**5v**. For this analysis, compounds (±)-**5d**, (±)-**5l**, (±)-**5r**, and (±)-**5v** were tested. Moreover, enantiomers of **5v**, the most promising analogue, were synthesized, and the single enantiomers (3*R*,4*S*)-**5v** and (3*S*,4*R*)-**5v** were tested against *murine* and *human* MAGL, and the IC_{50} ratio of the enantiomers (distomer/eutomer) were determined and compared with that of the enantiomers of **4** that have been resynthesized and tested under the same conditions for performing a direct comparison. A high eudysmic ratio is an important property in the discovery and design of chiral drugs. In fact, enantiomers of a single drug may have different pharmacokinetic and PD properties, and the use of an eutomer may improve efficacy and safety.[39] Accordingly, by combining computer-aided drug design (CADD) and biological tests, compound **5v** was synthesized with the specific objective of improving the IC_{50} ratio of the enantiomers of compound **4**, investigating the chiral cliff of enantiomers in enzymatic assays. The enantiomers of **5v** demonstrated a clear-cut stereoselective interaction with the *h*/*m*MAGL, with the eutomer (3*R*,4*S*)-**5v** being about 900 times more potent than its distomer (Table 4). In contrast, the enantiomers of **4** showed an IC_{50} ratio of 5.1 and 9.6 for *m*MAGL and *h*MAGL, respectively. The same trend was observed with *r*MAGL and *cyno*MAGL

https://doi.org/10.1021/acs.jmedchem.3c01278
J. Med. Chem. 2024, 67, 1758−1782

orthologues where the IC_{50} ratios for the enantiomers of **5v** were calculated as 145 and 299 were sensibly higher that those of **4** (calculated as 10.6 and 6.6). In general, the data shown in Table 4 confirmed the role played by the benzotriazole moiety in stereoselectivity of interaction with the MAGL enzymes, with (3*R*,4*S*)-**5v** as one of the most potent inhibitors of *h*/*m*MAGL known to date. The steric hindrance of the leaving group might be responsible for the high IC_{50} ratio of **5v**, than that of compound **4**.

Mode of Action of the New MAGL Inhibitors. The mechanism of action of the newly synthesized compounds was confirmed by means of additional enzymatic studies performed on selected analogues ((±)-**5c**, (±)-**5d**, and (±)-**5v**). As all new compounds had shown greater inhibitory potency when tested after a 10 min preincubation, according to the structural features of these triazoleurea-based MAGL inhibitors,[26] and in analogy with compound **4**, we hypothesized that they might act through an irreversible mechanism. In fact, the time-course studies illustrated in Figure 2A, which show that compounds (±)-**5c**, (±)-**5d**, and also the benzotriazole-based analogue (±)-**5v** inhibit *r*MAGL in a time-dependent manner, whereas inhibition by compound (±)-**4** is ostensibly instantaneous. As a further test of reversibility, we performed the dilution assays reported in Figure 2B. The results of this experiment show that MAGL activity, inhibited by compounds (±)-**5c**, (±)-**5d**, (±)-**5v**, and (±)-**4**, did not fully recover 60 min after dilution, confirming the irreversible mode of inhibition of these compounds.

Crystal Structure of MAGL in Complex with Compounds 5d, 5l, and 5r. With all these data in hand, the most interesting analogues were subjected to X-ray crystallography to confirm their mechanisms of action and assess their binding mode. We succeeded in obtaining crystal structures for compounds **5d**, **5l**, and **5r** in complex with *h*MAGL (Figure 3). Unfortunately, **5v** did not provide any valuable crystal.

In line with the enzymatic studies (**5v** enantiomers), the X-ray data confirmed that MAGL prefers the (3*R*,4*S*)-isomers of the azetidin-2-one-based inhibitors. After incubating the enantiomeric mixtures of compounds (±)-**5d**, (±)-**5l**, and (±)-**5r** with the *h*MAGL, the enzyme selected the (3*R*,4*S*)-isomers of all the crystallized compounds, and in all the resulting structures, the catalytic serine (Ser122) covalently bound to the (3*R*,4*S*)-isomers.

All three MAGL structures are highly similar and superimpose with a RMSD for all atoms of about 0.7 Å. The largest structural differences were observed in the position of helix 4 (**5d**) and in parts of the lid domain. Only for **5d** the loop region extending from Leu167 to Ser176 is defined in the structure, whereas for **5l**, **5r**, no electron density is visible, indicating the introduction of some flexibility for this area. The electron density in the structures of all three compounds confirms the formation of a covalent bond with catalytic Ser122. No electron density is observed for the triazole (**5d**, **5l**) and benzotriazole groups (**5r**), pointing toward a complete turnover of the compounds and removal of the polar moiety. The carbonyl oxygen of the carbamate function is hydrogen bonded to the main chain atoms of Ala51 and Met123. The side chains of Leu148 and Leu241 embed the piperidine group through van der Waals interactions, and the azetidin-2-one participates in a hydrogen bonding network via a water molecule with the backbone carbonyl of Leu150 (**5r** and **5l**). In the structure of **5d**, this hydrogen bond cannot be formed because of a shift in the position of the carbonyl of Leu150 by about 3 Å related to a movement in the position of helix 4. The benzodioxole (**5r**) and the 4-methoxycarbonyl(phenyl) (**5l**) substituents on the azetidin-2-one core point toward the solvent region, both of which are located close to the side chain of Arg240, and in addition form van der Waals interactions with Ile179 of the lid domain. In **5r**, the 3-fluorophenyl group occupies a hydrophobic pocket lined up by residues Leu213, Leu214, and Val217, which could explain the improved potency compared with **5l** and **5d**. In

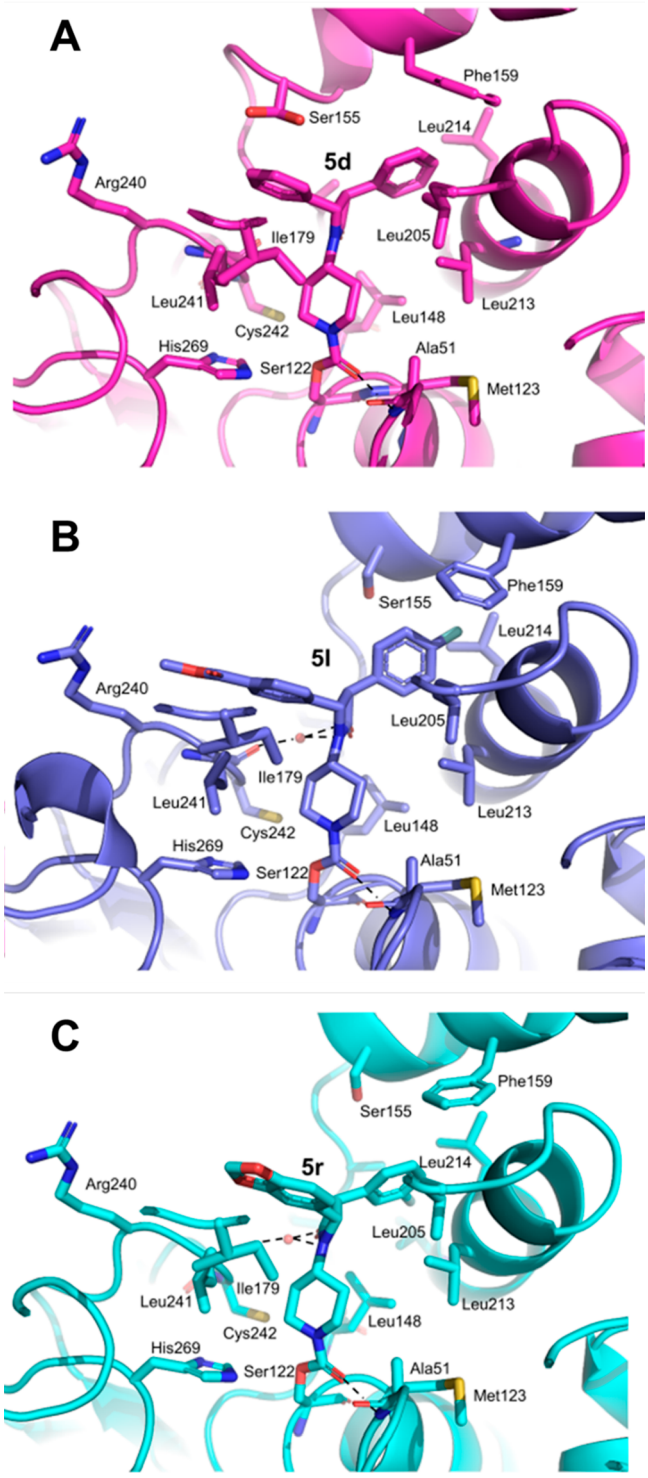

Figure 3. Crystal structures of *h*MAGL in complex with **5d** (PDB 8PTC), **5l** (PDB 8PTQ), and **5r** (PDB 8PTR). View of the active site with **5d** shown in magenta, with **5l** in blue, and with **5r** in cyan. Selected hydrogen bonds are depicted as black dashes.

https://doi.org/10.1021/acs.jmedchem.3c01278
J. Med. Chem. 2024, 67, 1758−1782

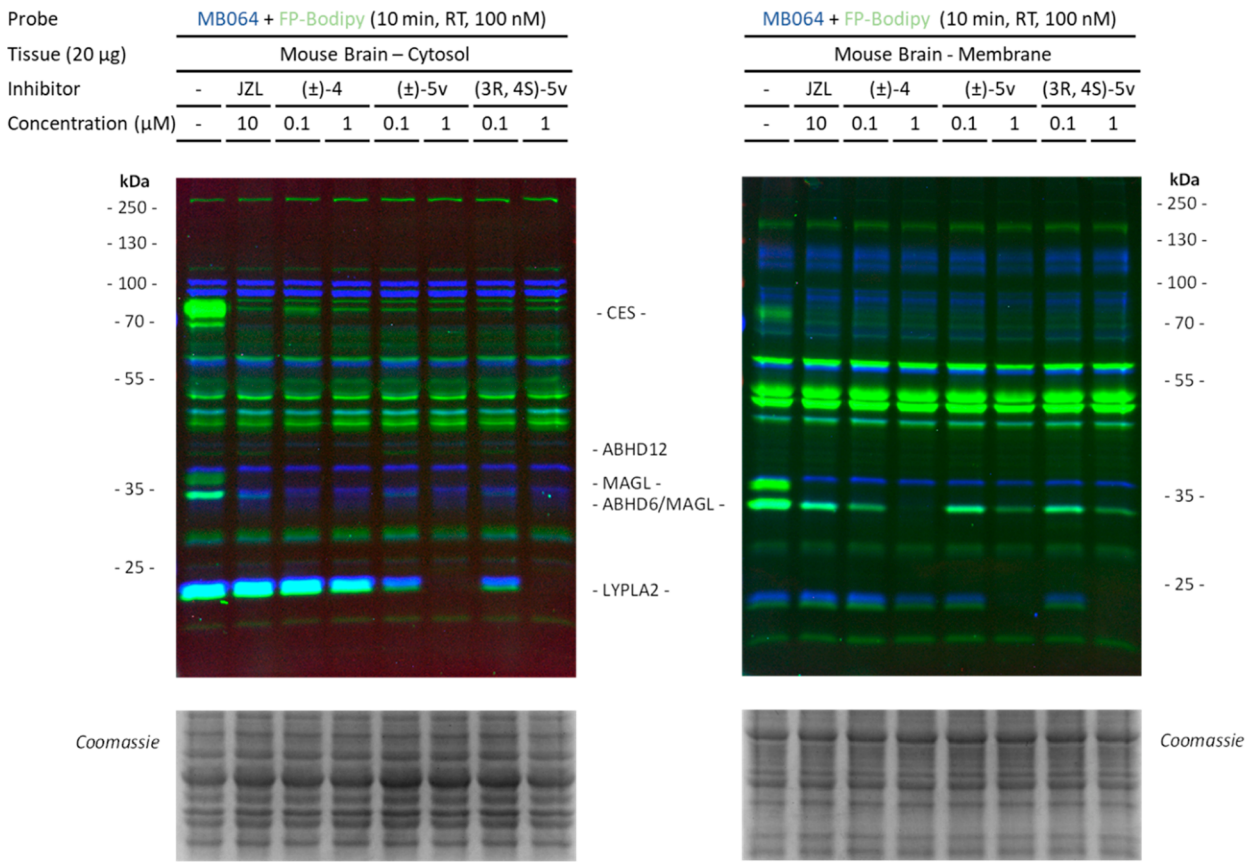

Figure 4. Competitive gel-based ABPP analysis of 44 proteins in treated mouse brain lysates with MAGL inhibitors. Selectivity of the presented compounds was assessed at 0.1 and 1 μM final concentration on membrane and cytosol fractions of mouse brain lysate using MB064 and FP-Bodipy (100 nM final, 20 min, rt). JZL-184 at a final concentration of 10 μM was taken along as control. Indicated are the target (MAGL) and off-targets (carboxyl esterases (CES), ABHD12, ABHD6, and LYPLA2).

comparison to **5r**, the 4-fluorophenyl moiety of **5l** moves by about 2.5 Å toward Phe159 of helix 4, thereby avoiding close contact with the backbone atoms of Gly210 of helix 6. The X-ray analysis undoubtedly demonstrated that these compounds are covalent *h*MAGL ligands, behaving as carbamoylating agents for the catalytic Ser122.

In a comparative analysis with the X-ray structure of **2** (namely, SAR629, PDB code 3JWE),[21] we observed that the covalent interaction with the catalytic triad is similar for **2** and the new compounds **5d**, **5l**, and **5r**, but the way the two (hetero)aryl substituents populate the Y-shaped part of the binding pocket bear substantial differences. These relay on the different exit vectors of the central β-lactam compared with the tertiary carbon of **2** (see SI, Figure S1, Table S2).

Notably, filling different spatial segments of the MAGL binding pocket has significant implications on the SAR of this new class of compounds, e.g., with regards to exploring different ligand protein interactions to modulate binding affinity as well as fine-tuning ADMET properties.

Computational Studies on New Azetidin-2-one-Based MAGL Inhibitors. With the crystal structures in our hand (PDBs 8PTC, 8PTQ, and 8PTR), we decided to expand the information about the binding mode of all the compounds by performing molecular docking studies. Starting from the solved 3D structure of the MAGL enzyme in complex with **5d** (PDB 8PTC), the new compounds were docked employing Glide software (Glide release 2018, Schrödinger, LLC, New York, NY) using XP (extra precision) as the scoring function.[16] Because the title compounds behave as suicide MAGL inhibitors, the molecular dockings were needed to complement the crystallographic data, as they relate to the whole molecule and may shed light on the approach of the electrophilic center to the catalytic serine. Starting from our prototypic azetidin-2-one derivative **4**, we investigated the effects of different EWGs and the effects of different substituents on the azetidin-2-one ring, detailed comments and SI, Figures S2−S5.

In order to provide further details about the different degrees of inhibition shown by selected analogues against MAGL enzymes belonging to different species, we analyzed the structural differences among *h*MAGL, *cyno*MAGL, *m*MAGL, and *r*MAGL (alignment and the superposition reported in SI, Figure S6) and conducted comparative docking studies on these MAGL orthologues. Despite no crucial differences were found in the proximity of the catalytic site, a different arrangement of the helix encircled in SI, Figure S6, that in *h*MAGL was found. This may reflect the possibility of enclosing a Phe residue in the binding site of the developed inhibitors that could produce fruitful interactions with our compounds.

Using the 3D model of MAGL enzymes, we conducted molecular docking studies of selected derivatives (**5c**, **5d**, and **5v**), considering *r*FAAH, *h*ABHD6, and *h*LYPLA2 for assessing the selectivity issues. In line with the high inhibition potencies of the tested analogues, very slight differences were found with MAGL orthologues dockings (SI, Table S3). This analysis also confirmed that the compounds can moderately bind to the *r*FAAH enzyme. Finally, considering *h*ABHD6 and *h*LYPLA2,

https://doi.org/10.1021/acs.jmedchem.3c01278
J. Med. Chem. 2024, 67, 1758−1782

the compounds **5c**, **5d**, and **5v** showed docking scores consistent with the *in vitro* assessment.

CB_1R, CB_2R, and Off-Target Selectivity Profiling. The privileged MAGL inhibitors (±)-**5d** and (±)-**5v** were interrogated to assess their selectivity toward CBRs and were found to exhibit excellent selectivity over these key ECS GPCRs.

Both compounds were found to be very weak ligands for CB_1R and CB_2R. Binding studies were conducted on CB_1R by testing compounds (±)-**5d** and (±)-**5v** at 10 μM (see SI, Table S4). The two analogues were also investigated in the newly developed time resolved fluorescence resonance energy transfer (TR-FRET)-based CB_2R binding assays[40] and were found to be ligands of micromolar potency for CB_2R ((±)-**5d** K_i = 2.1 ± 0.9 μM, and (±)-**5v** K_i > 10 μM; SI, Figure S7).

To identify potential off-targets at this early stage of drug development, the most promising compounds (±)-**5d** and (±)-**5v** were tested against a customized panel of 50 representative proteins (SI, Table S4).[41] At the high test concentration of 10 μM (±)-**5d** exhibited a weak interaction with the kappa opioid receptor (with inhibition % of 65.2 for (±)-**5d** and 73.03 for (±)-**5v**), which was considered not relevant due to the high inhibition potency for the MAGL enzymes ((±)-**5d** *h*MAGL IC_{50} = 11.5 nM, *r*MAGL IC_{50} = 0.12 nM; (±)-**5v** *h*MAGL IC_{50} = 12.19 nM, *r*MAGL IC_{50} = 0.22 nM, Table 1). The same is true when considering the subnanomolar IC_{50} of (±)-**5d** on *r*MAGL (*r*MAGL IC_{50} = 0.12 nM) and compared with the reported 55% inhibition of the *rat* Ca^{2+} channel that can be neglected. MAGL inhibitor (±)-**5v** showed a substantial inhibition of the *rat* Ca^{2+} channel at 10 μM. Thus, we followed up at 1 μM, where the inhibition of *rat* Ca^{2+} channel was absent. In the light of the 220 pM rat IC_{50} toward the MAGL enzyme, this activity will therefore not impact the PD read-outs. In addition, 73% inhibition of the kappa opioid receptor was derisked at 1 μM (63% inhibition), whereas weaker off-target interactions were considered less relevant. In summary, both ligands exhibit a favorable selectivity profile.

Activity-Based Protein Profiling. Compound (±)-**5v** showed high inhibitory potency against the MAGL enzyme in a competitive activity-based protein profiling (ABPP) assay for 44 proteins in the *mouse* brain proteome at concentrations of 0.1 and 1 μM. Compounds (±)-**5v** and (3*R*,4*S*)-**5v** showed off-target effects for other serine hydrolases, including ABHD12, ABHD6, carboxyl esterases, and LYPLA2 at both concentrations, as shown in Figure 4.

In summary, the novel and potent MAGL inhibitors (±)-**5d** and (±)-**5v** exhibit an acceptable overall selectivity when tested against a large set of putative off-targets and were therefore subjected to early absorption distribution metabolism excretion and toxicology (ADMET) profiling.

Early ADMET Profiling of (±)-5d, (±)-5v and Reference (±)-4. To exploit the potential of the newly developed azetidinone-based MAGL inhibitors for *in vivo* proof of concept (PoC) studies, we determined some of the most relevant early ADMET features of the best performing compounds (±)-**5d**, (±)-**5v**, and (±)-**4** (Table 5).

The triazoleurea-based analogue (±)-**5d** exhibits a favorable log *D* value of 2.6, which translated into a high solubility of 52 μg/mL. (±)-**5d** is the most soluble of the tested analogues. In fact, when compared with (±)-**4**, this latter is less soluble probably because of the presence of substitution in the two aryl moieties. In line with this result, the analogue (±)-**5v**, which presents benzotriazoleurea as the carbamoylating function, is the least soluble of the analyzed compounds.

Table 5. Solubility and *in Vitro* Metabolic Stability of Compounds (±)-5d, (±)-5v, and (±)-4

compounds → property ↓	(±)-**5d**	(±)-**5v**	(±)-**4**
log *D* @ pH 7.4	2.6	3.4 (mlLogD)[a]	2.7
solubility (μg/mL)	52	<1	24
Cl mouse microsomes (μL/min/mg)	164.5	101.3	273.2
Cl human microsomes (μL/min/mg)	10.3	106.6	123.8
Cl mouse hepatocytes (μL/min/mg)	200.0	114.0	200.0
Cl human hepatocytes (μL/min/mg)	60.5	101.7	91.9
mouse P-gp P_{app} [nm/s]	301	60	297
mouse P-gp efflux ratio	1.4	1.1	2.1
CYP2C9% inh 10 μM	69.5	69.5	75.0
CYP2D6% inh 10 μM	89.5	66.0	64.8
CYP3A4% inh 10 μM	78.0	63.0	74.5

[a]Machine-learning distribution coefficient (mlLogD at pH = 7.4).

Furthermore, (±)-**5d** is stable in human microsomes and hepatocytes. In contrast, mouse hepatocyte clearance was lowest for (±)-**5v**. Overall, mouse clearance data suggest the administration of MAGL inhibitors iv or ip for rodent *in vivo* studies, as already successfully demonstrated in case of (±)-**4**.[16]

All the molecules permeate well through membranes as indicated by machine-learning parallel artificial membrane permeability assay (PAMPA)[42] data in which all the tested ligands score high, and the experimental P-glycoprotein (P-gp) assay permeability values P_{app} is particularly favorable for (±)-**5d** (mouse P-gp P_{app} = 301 nm/s). Moreover, the two novel MAGL inhibitors (±)-**5d** and (±)-**5v** do not serve as substrates for the mouse P-gp (Mdr1a) transporter and therefore have a high propensity to cross the blood−brain barrier (BBB) in rodents, which is instrumental for performing *in vivo* PoC studies. *In vivo* profiling of (±)-**5d**, (±)-**5v**, and (±)-**4** is further supported by single point 2C9, 2D6, and 3A4 cytochrome P450 interaction data at 10 μM. As a further investigation, cytotoxicity and mutagenicity (Ames test) assays were performed to exclude any side effects for the investigated compounds (see SI, Table S5−S6 and Figure S8).

***In Vivo* Activity of Azetidin-2-one-Based Compounds (±)-5c, (±)-5d, and (±)-5v, and (±)-4.** Due to their covalent mode of action, the pharmacodynamics effects of the new inhibitors are expected to be decoupled from exposure levels. For this reason, and to save resources, we turned to *in vivo* pharmacodynamics experiments without conducting formal pharmacokinetics studies. *In vivo* administration of compounds (±)-**5c**, (±)-**5d**, and (±)-**5v** and (±)-**4** (5 mg/kg, ip) in male mice produced an approximately 50% inhibition of brain MAGL activity, which was assessed *ex vivo* 1 h after compound administration (Figure 5A). This effect was accompanied by a greater than 10-fold increase in brain 2-AG content (Figure 5B) as well as by a marked decrease in the levels of nonesterified arachidonic acid (Figure 5C). No statistically detectable change was noted in the levels of other nonesterified fatty acids, including docosahexaenoic (22:6), oleic (18:1), palmitic (16:0), and stearic (18:0) acids (Figure 5D−G). Similarly, compounds (±)-**4**, (±)-**5d**, and (±)-**5v** had no statistically detectable effect on the levels of AEA, oleoylethanolamide (OEA), and palmitoylethanolamide (PEA) (Figure 5H−J). A significant increase in brain PEA content was observed with compound (±)-**5c** (Figure 5J), which is suggestive of interference with FAAH or *N*-acylethanolamide acid amidase activity.

Next, we compared the compounds (±)-**5v** and **1** (JZL-184) for their ability to inhibit brain MAGL activity *in vivo* in a dose-

https://doi.org/10.1021/acs.jmedchem.3c01278
J. Med. Chem. 2024, 67, 1758−1782

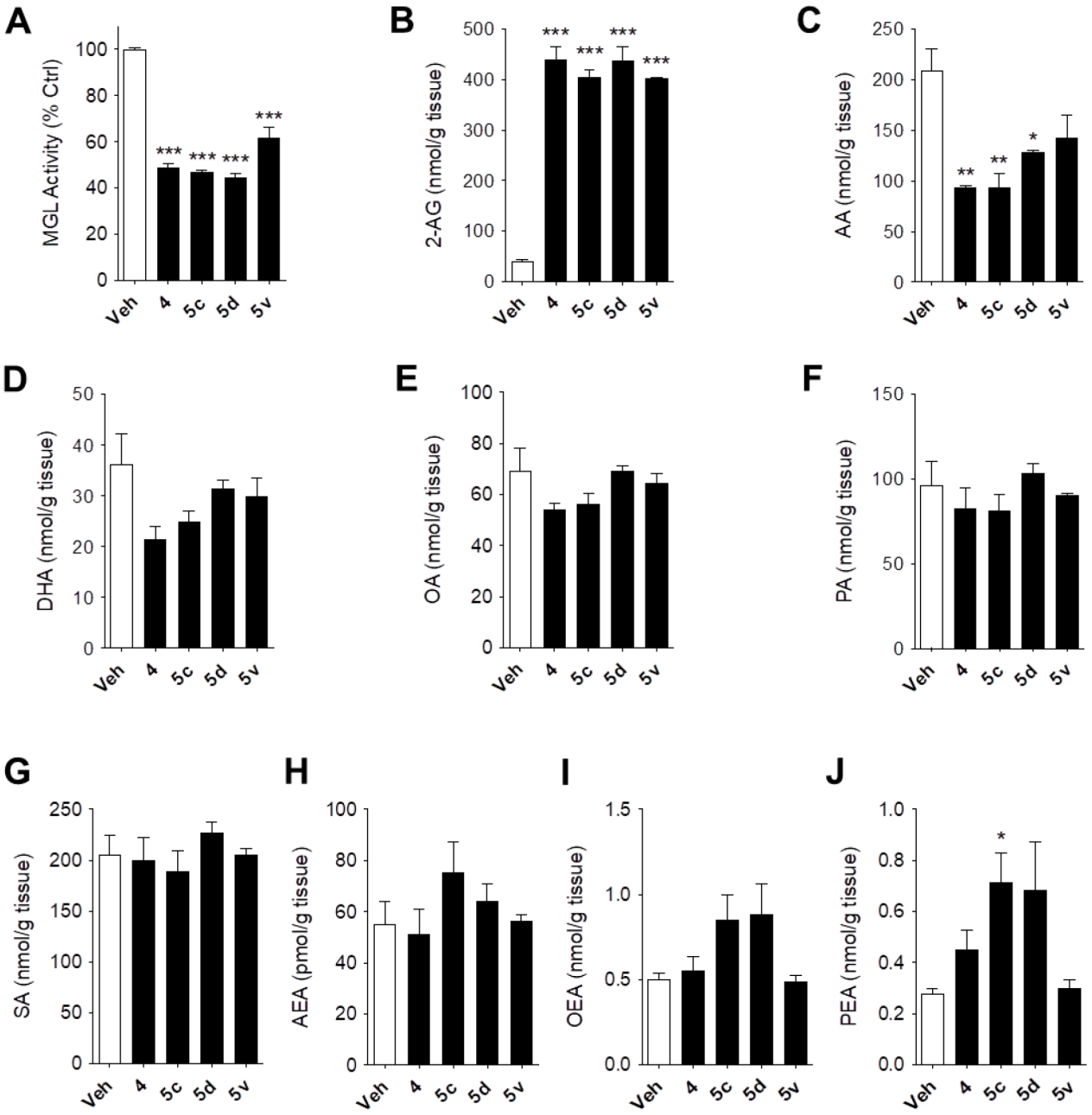

Figure 5. *In vivo* activity of azetidin-2-one-based compounds (±)-**5c**, (±)-**5d**, and (±)-**5v** and (±)-**4**. Drugs were ip injected to adult male mice at the dose of 5 mg/kg ($n = 3$/group). After 1 h from the injection, mice were killed and the half brains were taken for lipid analyses by LC-MS. The other half brains were used for MAGL assay using the homogenate. $^{*}P < 0.05$, $^{**}P < 0.01$, and $^{***}P < 0.001$ by two-tailed t test compared to the vehicle (DMSO).

dependent manner. Both compounds inhibited MAGL activity and elevated 2-AG levels in brain tissue at the doses of 5 and 20 mg/kg ip (Figure 6A,B). No such effect was observed at lower doses (0.2, 1 mg/kg).

■ CONCLUSIONS

This study reports the development and initial preclinical characterization of a set of potent MAGL inhibitors. The new inhibitors ((±)-**5a−v**, (±)-**6a−j**, and (±)-**7a−d**) allowed an extensive SAR analysis (enzymatic studies), leading to the identification of highly potent and selective prototype small molecules to be further characterized as valuable pharmacological tools for *in vivo* studies. For the best performing compounds, an alternative greener protocol has been developed in order to optimize yields and avoid the use of more toxic solvents and catalysts. Time-dependent MAGL inhibition and dilution assays performed using analogues (±)-**5c**, (±)-**5d**, and (±)-**5v** compared to (±)-**4** pointed to an irreversible mechanism of action. The resolution of the crystal structures of (±)-**5d**, (±)-**5l**, and (±)-**5r** in complex with *h*MAGL confirmed their irreversible mode of action, and the stereoselective preference of the *h*MAGL enzyme for the (3*R*,4*S*)-isomers. This evidence matched the hints from the enzymatic studies that highlighted the very high IC_{50} ratio for (3*R*,4*S*)-**5v** (≥900) for *h*/*m*MAGL, with respect to the previously developed azetidine-2-one **4**. The analogue (3*R*,4*S*)-**5v** proved to be one of the most potent MAGL inhibitors known to date. MAGL selectivity was demonstrated, for key analogues toward

https://doi.org/10.1021/acs.jmedchem.3c01278
J. Med. Chem. 2024, 67, 1758−1782

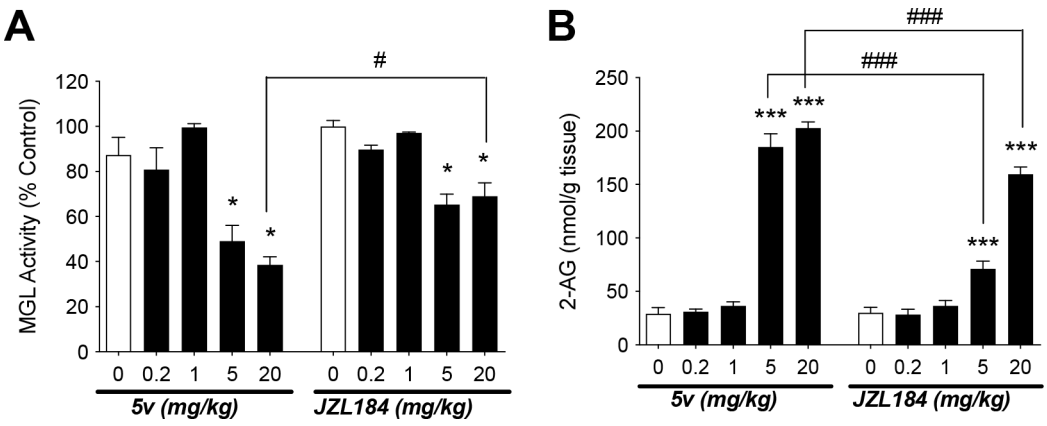

Figure 6. Dose-dependent MAGL inhibition of compound (±)-**5v** *in vivo*. Drugs were ip injected to adult male mice as indicated (n = 3/group). We used DMSO or PEG/Tween (4:1) as vehicles, for (±)-**5v** and JZL-184, respectively. After 1 h from injection, mice were killed and their brains were taken, cut by half, and immediately frozen. One half of the brains were used for 2-AG analyses by LC-MS. The other half brains were used for MAGL assay using the homogenate. No statistic difference was observed between the vehicles. *P < 0.05 and ***P < 0.001 by two-tailed t test compared to the vehicle (0 mg/kg); $^{\#}P$ < 0.05 and $^{\#\#\#}P$ < 0.001 by two-way ANOVA with Bonferroni post-test.

the most relevant proteins of the ECS (e.g., FAAH and CBRs) and various serine hydrolases (ABPP studies on **5v**). Off-target liabilities were excluded by testing (±)-**5d** and (±)-**5v** on a panel of 50 receptors. For the same analogues, the preliminary ADME properties and metabolic stability were assessed with positive outcomes, displaying a superior profile when compared with (±)-**4**. The lack of cell toxicity was evaluated in murine fibroblasts, and the absence of mutagenicity was evaluated using the Ames test. Together, these results suggested that (±)-**5c**, (±)-**5d**, and (±)-**5v** are suitable pharmacological tools for *in vivo* administration in order to measure their effect on the endogenous levels of 2-AG, AEA, and other brain lipids. The data confirmed that the novel ligands produce strong MAGL inhibition after *in vivo* administration. These azetidin-2-one-based compounds are promising tools suitable for further investigation in various rodent models in human disease models.

■ EXPERIMENTAL SECTION

Chemistry. Unless otherwise specified, materials were purchased from commercial suppliers and used without further purification. Reaction progress was monitored by TLC using Silica Gel 60 F254 (0.040−0.063 mm) with detection by UV. Silica Gel 60 (0.040−0.063 mm) or aluminum oxide 90 (0.063−0.200 mm) were used for column chromatography. ^{1}H NMR and ^{13}C NMR spectra were recorded on a Varian 300 MHz spectrometer by using the residual signal of the deuterated solvent as internal standard. Splitting patterns are described as singlet (s), doublet (d), double doublet (dd), triplet (t), quartet (q), quintet (p), and broad (br); the value of chemical shifts (δ) is given in ppm and coupling constants (J) in hertz (Hz). ESI-MS spectra were performed by an Agilent 1100 series LC/MSD spectrometer. Melting points were determined in Pyrex capillary tubes using an Electrothermal 8103 apparatus and are uncorrected. Yields refer to purified products and are not optimized. All moisture-sensitive reactions were performed under argon atmosphere using oven-dried glassware and anhydrous solvents. Mass spectra were recorded utilizing an electron spray ionization (ESI) Agilent 1100 series LC/MSD spectrometer. ESI-HRMS spectra were acquired by a linear ion-trap-Orbitrap hybrid mass spectrometer (LTQOrbitrap XL) (Thermo Fisher Scientific, Bremen, Germany) operating in positive electrospray ionization mode. Data were collected and analyzed using the Xcalibur 2.2 software provided by the manufacturer. Yields refer to purified products and are not optimized. The purity of final products (>95%) was determined by an analytical HPLC Merk Purospher STAR RP-18e (5 μm) LiChroCART 250-4 column; detection at 254 nm; flow rate = 1.0 mL/min; mobile phase A, 0.1% trifluoroacetic acid (TFA) (v/v) in water; mobile phase B, acetonitrile; gradient, 90/10−10/90 A/B in 20 min. The gradient was optimized based on compound polarity.

General Procedures. *General Procedure A. Formation of the Intermediate Imines **9a−g**, **9i**, **13**, **17**, and **23**.* A solution of the appropriate aldehyde (1 equiv) and 4-amino-1-benzylpiperidine (1 equiv) in absolute ethanol (15 mL/mmol) was heated at 80 °C for 12 h. The mixture was cooled to 25 °C, and the solvent was removed under reduced pressure. The crude imines (quantitative yields) were used in the following step with no further purification.

*General Procedure B. Staudinger Reaction for the Synthesis of Azetidin-2-one Derivatives (±)-**10a−l**, (±)-**14a−f**, and (±)-**18**.* A solution of the suitable phenylacetic acid (1.5 equiv) and triphosgene (0.5 equiv) in dry DCM (5.0 mL/mmol) was heated at 50 °C for 30 min. Then, a solution of the appropriate imine (1 equiv) in dry DCM (5.0 mL/mmol) was added dropwise, followed by the addition of TEA (3 equiv), and the mixture was heated at 50 °C for 12 h. The solvent was removed under reduced pressure, and the crude was purified by means of flash chromatography on silica gel, eluting as indicated for each analogue.

*General Procedure C. Catalytic Hydrogenation for the Cleavage of the Benzyl Group and Obtainment of Free Bases (±)-**11a−l**, (±)-**15a−f**, and (±)-**19**.* To a solution of the appropriate benzyl-intermediate in MeOH (10 mL/mmol), a catalytic amount of Pd/C 10% was added, and the mixture was stirred under H_2 atmosphere at 1 atm for 4 h. Pd/C was filtered off, and the solvent was removed under reduced pressure. The crude transparent oils (quantitative yield) were used in the following step with any further purification.

*General Procedure D. Synthesis of Final Compounds (Urea Formation) (±)-**5a−v**, (±)-**6a−j**, and (±)-**7c,d**.* To a solution of the appropriate heterocycle (2 equiv) in dry DCM (20 mL/mmol), phosgene 20% solution in toluene (2 equiv) and DMAP (4 equiv) were added, and the mixture was stirred at 25 °C for 12 h. Then a solution of the suitable amine (1 equiv) in dry DCM (10 mL/mmol) was added, and the reaction was stirred at rt for 12 h. The solvent was removed under reduced pressure, and the crude was purified by means of chromatography on silica gel, eluting as indicated for each analogue, to afford the target compounds.

*N-(4-Fluorobenzylidene)-1-benzylpiperidin-4-amine (**9a**).* The title compound was obtained via general procedure A starting from 4-fluorobenzaldehyde (**8a**, 180 μL, 1.66 mmol). ESI-MS m/z 323 [M + H]$^{+}$.

*N-(4-Methylbenzylidene-1-benzylpiperidin-4-amine (**9b**).* The title compound was obtained via general procedure A starting from 4-tolualdehyde (**8b**, 195 μL, 1.66 mmol). ESI-MS m/z 293 [M + H]$^{+}$.

*N-(4-(Trifluoromethyl)benzylidene)-1-benzylpiperidin-4-amine (**9c**).* The title compound was obtained via general procedure A starting from 4-(trifluoromethyl)benzaldehyde (**8c**, 225 μL, 1.66 mmol). ESI-MS m/z 345 [M + H]$^{+}$.

https://doi.org/10.1021/acs.jmedchem.3c01278
J. Med. Chem. 2024, 67, 1758−1782

*N-(4-Methoxybenzylidene)-1-benzylpiperidin-4-amine (**9d**).* The title compound was obtained via general procedure A starting from 4-methoxybenzaldehyde (**8d**, 200 μL, 1.66 mmol). ESI-MS *m/z* 309 [M + H]$^+$.

*N-(3-Methoxybenzylidene)-1-benzylpiperidin-4-amine (**9e**).* The title compound was obtained via general procedure A starting from 3-methoxybenzaldehyde (**8e**, 200 μL, 1.66 mmol). ESI-MS *m/z* 309 [M + H]$^+$.

*(±)-Methyl 4-(((1-Benzylpiperidin-4-yl)imino)methyl)benzoate (**9f**).* The title compound was obtained via general procedure A, starting from methyl 4-formylbenzoate (**8f**, 270 mg, 1.66 mmol). ESI-MS *m/z* 337 [M + H]$^+$.

*N-(1-Benzylpiperidin-4-yl)-1-(furan-2-yl)methanimine (**9g**).* The title compound was obtained via general procedure A, starting from furan-2-carbaldehyde (**8g**, 150 mg, 1.56 mmol). ESI-MS *m/z* 269 [M + H]$^+$.

*(±)-trans-1-(1-Benzylpiperidin-4-yl)-3,4-bis(4-fluorophenyl)-azetidin-2-one (**10a**).* The title compound was obtained via general procedure B starting from imine **9a** (491 mg, 1.66 mmol) and 4-fluorophenylacetic acid (385 mg, 2.49 mmol). Purification: 2:1 PE/EtOAc. Yield: 63%, 450 mg, yellow oil. ^{1}H NMR (300 MHz, $CDCl_3$) δ 7.41−7.14 (m, 9H), 7.14−6.94 (m, 4H), 4.42 (d, *J* = 2.2 Hz, 1H), 4.01 (d, *J* = 2.0 Hz, 1H), 3.59 (m, 1H), 3.44 (s, 2H), 2.82 (dd, *J* = 39.0, 10.6 Hz, 2H), 2.00 (m, 4H), 1.63 (dd, *J* = 12.7, 3.0 Hz, 1H), 1.45 (qd, *J* = 11.8, 4.0 Hz, 1H). ESI-MS *m/z*: 433 [M + H]$^+$.

*(±)-trans-3,4-bis(Benzo[d][1,3]dioxol-5-yl)-1-(1-benzylpiperidin-4-yl)azetidin-2-one (**10b**).* The title compound was obtained via general procedure B starting from **9h**[16] (534 mg, 1.66 mmol) and 3,4-(methylendioxy)phenylacetic acid (450 mg, 2.49 mmol). Purification: 2:1 PE/EtOAc. Yield: 59%, 470 mg, yellow oil. ^{1}H NMR (300 MHz, $CDCl_3$) δ 7.43−7.07 (m, 5H), 6.86 (s, 1H), 6.79 (m, 2H), 6.74 (s, 1H), 6.70 (m, 2H), 5.98 (s, 2H), 5.93 (s, 2H), 4.34 (d, *J* = 2.2 Hz, 1H), 3.94 (d, *J* = 2.0 Hz, 1H), 3.9 (m, 1H), 3.44 (m, 2H), 2.82 (dd, *J* = 36.1, 10.5 Hz, 2H), 1.98 (m, 4H), 1.70 (dd, *J* = 12.8, 2.8 Hz, 1H), 1.50 (qd, *J* = 11.7, 3.9 Hz, 1H). ESI-MS *m/z*: 485 [M + H]$^+$, 507 [M + Na]$^+$.

*(±)-trans-3-(Benzo[d][1,3]dioxol-5-yl)-1-(1-benzylpiperidin-4-yl)-4-(4-fluorophenyl)azetidin-2-one (**10c**).* The title compound was obtained via general procedure B starting from **9a** (491 mg, 1.66 mmol) and (3,4-methylendioxy)phenylacetic acid (450 mg, 2.49 mmol). Purification: 2:1 PE/EtOAc. Yield: 55%, 420 mg, yellow oil. ^{1}H NMR (300 MHz, $CDCl_3$) δ 7.42−7.14 (m, 7H), 7.08 (t, *J* = 8.3 Hz, 2H), 6.72 (m, 3H), 5.93 (s, 2H), 4.43 (d, *J* = 1.4 Hz, 1H), 3.96 (d, *J* = 1.6 Hz, 1H), 3.59 (m, 1H), 3.43 (m, 2H), 2.82 (dd, *J* = 37.7, 11.2 Hz, 2H), 2.00 (m, 4H), 1.70 (m, 1H), 1.46 (qd, *J* = 12.0, 3.8 Hz, 1H). ESI-MS *m/z*: 459 [M + H]$^+$, 481 [M + Na]$^+$.

*(±)-trans-1-(1-Benzylpiperidin-4-yl)-3-(4-fluorophenyl)-4-(p-tolyl)azetidin-2-one (**10d**).* The title compound was obtained via general procedure B starting from imine **9b** (486 mg, 1.66 mmol) and 4-fluorophenylacetic acid (385 mg, 2.49 mmol). Purification: 2:1 PE/EtOAc. Yield: 60%, 415 mg, yellow oil. ^{1}H NMR (300 MHz, $CDCl_3$) δ 7.36−7.08 (m, 11H), 7.02 (t, *J* = 8.6 Hz, 2H), 4.40 (d, *J* = 2.1 Hz, 1H), 4.02 (d, *J* = 1.7 Hz, 1H), 3.58 (m, 1H), 3.43 (s, 2H), 2.81 (dd, *J* = 40.8, 10.9 Hz, 2H), 2.37 (s, 3H), 1.99 (m, 4H), 1.67 (dd, *J* = 12.1, 3.1 Hz, 1H), 1.48 (qd, *J* = 12.2, 4.0 Hz, 1H). ESI-MS *m/z*: 429 [M + H]$^+$.

*(±)-trans-1-(1-Benzylpiperidin-4-yl)-3-(4-fluorophenyl)-4-(4-(trifluoromethyl)phenyl)azetidin-2-one (**10e**).* The title compound was obtained via general procedure B starting from imine **9c** (572 mg, 1.66 mmol) and 4-fluorophenylacetic acid (**4a**, 385 mg, 2.49 mmol). Purification: 2:1 PE/EtOAc. Yield: 63%, 500 mg, yellow oil. ^{1}H NMR (300 MHz, $CDCl_3$) δ 7.67 (d, *J* = 8.2 Hz, 2H), 7.51 (d, *J* = 8.1 Hz, 2H), 7.35−7.10 (m, 7H), 7.04 (t, *J* = 8.7 Hz, 2H), 4.50 (d, *J* = 1.8 Hz, 1H), 4.02 (d, *J* = 2.0 Hz, 1H), 3.62 (m, 1H), 3.44 (s, 2H), 2.83 (dd, *J* = 38.4, 10.7 Hz, 2H), 1.99 (m, 4H), 1.68 (dd, *J* = 12.4, 3.5 Hz, 1H), 1.45 (qd, *J* = 10.9, 4.1 Hz, 1H). ESI-MS *m/z*: 483 [M + H]$^+$.

*(±)-trans-1-(1-Benzylpiperidin-4-yl)-3-(4-fluorophenyl)-4-(4-methoxyphenyl)azetidin-2-one (**10f**).* The title compound was obtained via general procedure B starting from imine **9d** (512 mg, 1.66 mmol) and 4-fluorophenylacetic acid (385 mg, 2.49 mmol). Purification: 2:1 PE/EtOAc. Yield: 61%, 425 mg, yellow oil. ^{1}H NMR (300 MHz, $CDCl_3$) δ 7.37−7.16 (m, 9H), 7.06−6.83 (m, 4H), 4.40 (d, *J* = 2.1 Hz, 1H), 4.03 (d, *J* = 1.8 Hz, 1H), 3.81 (s, 3H), 3.59 (m, 1H), 3.43 (s, 2H), 2.81 (dd, *J* = 38.7, 11.3 Hz, 2H), 1.97 (m, 4H), 1.67 (dd, *J* = 12.8, 3.0 Hz, 1H), 1.48 (qd, *J* = 11.8, 3.9 Hz, 1H). ESI-MS *m/z*: 445 [M + H]$^+$.

*(±)-trans-1-(1-Benzylpiperidin-4-yl)-3,4-bis(3-methoxyphenyl)-azetidin-2-one (**10g**).* The title compound was obtained via general procedure B starting from imine **9e** (512 mg, 1.66 mmol) and 3-methoxyphenylacetic acid (415 mg, 2.49 mmol). Purification: 2:1 PE/EtOAc. Yield: 46%, 350 mg. ^{1}H NMR (300 MHz, $CDCl_3$) δ 7.26 (m, 7H), 6.95 (m, 3H), 6.86 (m, 3H), 4.49 (d, *J* = 2.1 Hz, 1H), 4.06 (d, *J* = 2.0 Hz, 1H), 3.82 (s, 3H), 3.79 (s, 3H), 3.61 (m, 1H), 3.44 (s, 2H), 2.83 (dd, *J* = 37.2, 9.6 Hz, 2H), 2.00 (m, 4H), 1.73 (dd, *J* = 12.7, 2.9 Hz, 1H), 1.54 (qd, *J* = 11.8, 3.9 Hz, 1H). ESI-MS *m/z*: 457 [M + H]$^+$.

*(±)-trans-4-(Benzo[d][1,3]dioxol-5-yl)-1-(1-benzylpiperidin-4-yl)-3-(3-fluorophenyl)azetidin-2-one (**10h**).* The title compound was obtained via general procedure B starting from imine **9h**[16] (534 mg, 1.66 mmol) and 3-fluorophenylacetic acid (385 mg, 2.49 mmol). Purification: 2:1 PE/EtOAc. Yield: 65%, 470 mg, yellow oil. ^{1}H NMR (300 MHz, $CDCl_3$) δ 7.34−7.20 (m, 6H), 7.08−6.92 (m, 3H), 6.87 (s, 1H), 6.82−6.78 (m, 2H), 6.00 (s, 2H), 4.39 (d, *J* = 2.2 Hz, 1H), 4.02 (d, *J* = 2.2 Hz, 1H), 3.71−3.49 (m, 1H), 3.45 (s, 2H), 2.83 (dd, *J* = 35.7, 10.8 Hz, 2H), 1.97 (m, 4H), 1.78−1.43 (m, 2H). ESI-MS *m/z*: 459 [M + H]$^+$, 481 [M + Na]$^+$.

*(±)-trans-4-(Benzo[d][1,3]dioxol-5-yl)-1-(1-benzylpiperidin-4-yl)-3-(3-methoxyphenyl)azetidin-2-one (**10i**).* The title compound was obtained via general procedure B starting from imine **9h**[16] (534 mg, 1.66 mmol) and 3-methoxyphenylacetic acid (410 mg, 2.49 mmol). Purification: 2:1 PE/EtOAc. Yield: 58%, 450 mg, yellow oil. ^{1}H NMR (300 MHz, $CDCl_3$) δ 7.39−7.10 (m, 6H), 6.96−6.67 (m, 6H), 5.96 (s, 2H), 4.43 (d, *J* = 2.1 Hz, 1H), 4.01 (d, *J* = 1.7 Hz, 1H), 3.77 (s, 3H), 3.69−3.49 (m, 1H), 3.44 (s, 2H), 2.82 (dd, *J* = 34.0, 10.1 Hz, 2H), 2.11−1.82 (m, 4H), 1.71 (dd, *J* = 12.7, 2.8 Hz, 1H), 1.53 (qd, *J* = 12.0, 3.8 Hz, 1H). ESI-MS *m/z*: 471 [M + H]$^+$, 493 [M + Na]$^+$.

*(±)-trans-4-(Benzo[d][1,3]dioxol-5-yl)-1-(1-benzylpiperidin-4-yl)-3-phenylazetidin-2-one (**10j**).* The title compound was obtained via general procedure B starting from imine **9h**[16] (534 mg, 1.66 mmol) and phenylacetic acid (315 μL, 2.49 mmol). Purification: 10:1 DCM/acetone. Yield: 53%, 390 mg, yellow oil. ^{1}H NMR (300 MHz, $CDCl_3$) δ 7.45−7.16 (m, 10H), 6.90 (s, 1H), 6.87−6.72 (m, 2H), 5.98 (s, 2H), 4.43 (d, *J* = 2.1 Hz, 1H), 4.04 (d, *J* = 2.1 Hz, 1H), 3.80−3.51 (m, 1H), 3.45 (s, 2H), 2.84 (dd, *J* = 35.9, 10.5 Hz, 2H), 2.10−1.86 (m, 4H), 1.81−1.67 (m, 1H), 1.53 (qd, *J* = 11.9, 3.6 Hz, 1H). ESI-MS *m/z*: 441 [M + H]$^+$, 463 [M + Na]$^+$.

*(±)-Methyl 4-(trans-1-(1-benzylpiperidin-4-yl)-3-(4-fluorophenyl)-4-oxoazetidin-2-yl)benzoate (**10k**).* The title compound was obtained via general procedure B starting from imine **9f** (560 mg, 1.66 mmol) and 4-fluorophenylacetic acid (415 mg, 2.49 mmol). Purification: 1:1 PE/EtOAc. Yield: 42%, 330 mg, yellow oil. ^{1}H NMR (300 MHz, $CDCl_3$) δ 8.07 (d, *J* = 8.2 Hz, 2H), 7.46 (d, *J* = 8.2 Hz, 2H), 7.33−7.13 (m, 7H), 7.03 (t, *J* = 8.6 Hz, 2H), 4.49 (d, *J* = 2.1 Hz, 1H), 4.04 (d, *J* = 1.9 Hz, 1H), 3.93 (s, 3H), 3.69−3.53 (m, 1H), 3.43 (s, 2H), 2.80 (dd, *J* = 39.6, 11.5 Hz, 2H), 2.03−1.82 (m, 4H), 1.74−1.51 (m, 1H), 1.51−1.32 (m, 1H). ESI-MS *m/z*: 473 [M + H]$^+$, 495 [M + Na]$^+$.

*trans-1-(1-Benzylpiperidin-4-yl)-3-(4-fluorophenyl)-4-(furan-2-yl)azetidin-2-one (**10l**).* The title compound was obtained via general procedure B starting from imine **9g** (420 mg, 1.56 mmol) and 4-fluorophenylacetic acid (361 mg, 2.34 mmol). Purification: 1:1 PE/EtOAc. Yield 50%, 315 mg. ^{1}H NMR (300 MHz, $CDCl_3$) δ 7.44 (d, *J* = 1.4 Hz, 1H), 7.33−7.17 (m, 7H), 7.06−6.94 (m, 2H), 6.37 (s, 2H), 4.51 (d, *J* = 1.6 Hz, 1H), 4.39 (d, *J* = 2.4 Hz, 1H), 3.66−3.48 (m, 1H), 3.43 (s, 2H), 2.89−2.68 (m, 2H), 2.08−1.81 (m, 4H), 1.75−1.62 (m, 1H), 1.51−1.37 (m, 1H). ESI-MS *m/z*: 405 [M + H]$^+$, 427 [M + Na]$^+$.

*(±)-trans-3,4-bis(4-Fluorophenyl)-1-(piperidin-4-yl)azetidin-2-one (**11a**).* The title compound was obtained via general procedure C starting from **10a** (150 mg, 0.35 mmol). ^{1}H NMR (300 MHz, $CDCl_3$) δ 7.35 (m, 2H), 7.21 (m, 2H), 7.05 (m, 4H), 4.42 (d, *J* = 2.1 Hz, 1H), 4.02 (d, *J* = 1.9 Hz, 1H), 3.64 (m, 1H), 3.01 (dd, *J* = 35.6, 12.5 Hz, 2H), 2.54 (m, 2H), 1.95 (m, 1H), 1.75 (m, 3H), 1.34 (m, 1H). ESI-MS *m/z*: 343 [M + H]$^+$.

*(±)-trans-3,4-bis(Benzo[d][1,3]dioxol-5-yl)-1-(piperidin-4-yl)-azetidin-2-one (**11b**).* The title compound was obtained via general

https://doi.org/10.1021/acs.jmedchem.3c01278
J. Med. Chem. 2024, 67, 1758−1782

procedure C starting from **10b** (150 mg, 0.31 mmol). ^{1}H NMR (300 MHz, $CDCl_3$) δ 6.97−6.59 (m, 6H), 5.99 (s, 2H), 5.94 (s, 2H), 4.35 (d, *J* = 2.2 Hz, 1H), 3.96 (d, *J* = 2.1 Hz, 1H), 3.65 (m, 1H), 3.04 (dd, *J* = 32.8, 12.6 Hz, 2H), 2.57 (m, 2H), 1.95 (m, 2H), 1.77 (m, 2H), 1.41 (m, 1H). ESI-MS *m/z*: 395 [M + H]$^+$.

*(±)-trans-3-(Benzo[d][1,3]dioxol-5-yl)-4-(4-fluorophenyl)-1-(piperidin-4-yl)-azetidin-2-one (**11c**).* The title compound was obtained via general procedure C starting from **10c** (150 mg, 0.33 mmol). ^{1}H NMR (300 MHz, $CDCl_3$) δ 7.34 (m, 2H), 7.09 (m, 2H), 6.72 (m, 3H), 5.95 (s, 2H), 4.42 (d, *J* = 1.9 Hz, 1H), 3.97 (d, *J* = 1.8 Hz, 1H), 3.67 (m, 1H), 3.04 (dd, *J* = 36.7, 12.7 Hz, 2H), 2.59 (m, 2H), 1.98 (m, 2H), 1.79 (m, 2H), 1.30 (m, 1H). ESI-MS *m/z*: 369 [M + H]$^+$.

*(±)-trans-3-(4-Fluorophenyl)-1-(piperidin-4-yl)-4-(p-tolyl)-azetidin-2-one (**11d**).* The title compound was obtained via general procedure C starting from **10d** (150 mg, 0.35 mmol). ^{1}H NMR (300 MHz, $CDCl_3$) δ 7.23 (m, 6H), 7.01 (m, 2H), 4.41 (d, *J* = 2.1 Hz, 1H), 4.04 (d, *J* = 1.5 Hz, 1H), 3.63 (m, 1H), 3.03 (m, 2H), 2.58 (m, 2H), 2.36 (s, 3H), 1.83 (m, 4H), 1.35 (m, 1H). ESI-MS *m/z*: 339 [M + H]$^+$.

*(±)-trans-3-(4-Fluorophenyl)-1-(piperidin-4-yl)-4-(4-(trifluoromethyl)phenyl)azetidin-2-one (**11e**).* The title compound was obtained via general procedure C starting from **10e** (150 mg, 0.31 mmol). ^{1}H NMR (300 MHz, $CDCl_3$) δ 7.59 (m, 4H), 7.13 (m, 4H), 4.50 (d, *J* = 1.8 Hz, 1H), 4.04 (d, *J* = 1.6 Hz, 1H), 3.67 (m, 1H), 3.03 (dd, *J* = 35.0, 12.4 Hz, 2H), 2.56 (m, 2H), 1.84 (m, 4H), 1.34 (m, 1H). ESI-MS *m/z*: 393 [M + H]$^+$.

*(±)-trans-3-(4-Fluorophenyl)-4-(4-methoxyphenyl)-1-(piperidin-4-yl)azetidin-2-one (**11f**).* The title compound was obtained via general procedure C starting from **10f** (150 mg, 0.34 mmol). ^{1}H NMR (300 MHz, $CDCl_3$) δ 7.28 (m, 2H), 7.21 (m, 2H), 7.03 (m, 2H), 6.91 (m, 2H), 4.41 (d, *J* = 2.2 Hz, 1H), 4.05 (d, *J* = 2.1 Hz, 1H), 3.82 (s, 3H), 3.65 (m, 1H), 3.03 (m, 2H), 2.56 (m, 2H), 1.80 (m, 4H), 1.32 (m, 1H). ESI-MS *m/z*: 355 [M + H]$^+$.

*(±)-trans-3,4-bis(3-Methoxyphenyl)-1-(piperidin-4-yl)azetidin-2-one (**11g**).* The title compound was obtained via general procedure C starting from **10g** (150 mg, 0.33 mmol). ^{1}H NMR (300 MHz, $CDCl_3$) δ 7.27 (m, 2H), 6.87 (m, 6H), 4.47 (d, *J* = 2.1 Hz, 1H), 4.06 (d, *J* = 2.0 Hz, 1H), 3.81 (s, 3H), 3.77 (s, 3H), 3.68 (m, 1H), 3.02 (dd, *J* = 35.0, 12.6 Hz, 2H), 2.56 (m, 2H), 1.99 (m, 1H), 1.79 (m, 3H), 1.36 (qd, *J* = 12.1, 4.1 Hz, 1H). ESI-MS *m/z*: 367 [M + H]$^+$.

*(±)-trans-4-(Benzo[d][1,3]dioxol-5-yl)-3-(3-fluorophenyl)-1-(piperidin-4-yl)azetidin-2-one (**11h**).* The title compound was obtained via general procedure C starting from **10h** (150 mg, 0.33 mmol). ^{1}H NMR (300 MHz, $CDCl_3$) δ 7.33−7.24 (m, 1H), 7.05−6.90 (m, 3H), 6.90−6.76 (m, 3H), 5.98 (s, 2H), 4.40 (d, *J* = 2.3 Hz, 1H), 4.04 (d, *J* = 2.2 Hz, 1H), 3.72−3.51 (m, 1H), 3.20−2.91 (m, 2H), 2.74−2.41 (m, 2H), 1.96−1.68 (m, 3H), 1.36 (qd, *J* = 11.4, 2.6 Hz, 1H). ESI-MS *m/z*: 369 [M + H]$^+$.

*(±)-trans-4-(Benzo[d][1,3]dioxol-5-yl)-3-(3-methoxyphenyl)-1-(piperidin-4-yl)azetidin-2-one (**11i**).* The title compound was obtained via general procedure C starting from **10i** (150 mg, 0.32 mmol). ^{1}H NMR (300 MHz, $CDCl_3$) δ 7.34−7.10 (m, 1H), 6.89−6.65 (m, 6H), 5.94 (s, 2H), 4.42 (d, *J* = 1.8 Hz, 1H), 4.02 (d, *J* = 2.0 Hz, 1H), 3.70 (m, 3H), 3.67−3.39 (m, 3H), 2.92 (d, *J* = 8.0 Hz, 2H), 2.30 (d, *J* = 10.2 Hz, 1H), 2.16 (d, *J* = 16.4 Hz, 1H), 1.88 (s, 2H). ESI-MS *m/z*: 381 [M + H]$^+$.

*(±)-trans-4-(Benzo[d][1,3]dioxol-5-yl)-3-phenyl-1-(piperidin-4-yl)azetidin-2-one (**11j**).* The title compound was obtained via general procedure C starting from **10j** (150 mg, 0.34 mmol). ^{1}H NMR (300 MHz, $CDCl_3$) δ 7.33−7.21 (m, 3H), 7.20−7.15 (m, 2H), 6.85−6.71 (m, 3H), 5.93 (s, 2H), 4.41 (d, *J* = 1.7 Hz, 1H), 4.03 (d, *J* = 2.1 Hz, 1H), 3.64−3.37 (m, 3H), 3.12−2.72 (m, 2H), 2.47−2.14 (m, 3H), 1.99−1.89 (m, 1H). ESI-MS *m/z*: 351[M + H]$^+$.

*(±)-Methyl 4-(trans-1-(Piperidin-4-yl)-3-(4-fluorophenyl)-4-oxoazetidin-2-yl)benzoate (**11k**).* The title compound was obtained via general procedure C starting from **10k** (150 mg, 0.32 mmol). ^{1}H NMR (300 MHz, $CDCl_3$) δ 8.10 (d, *J* = 8.2 Hz, 2H), 7.47 (d, *J* = 8.2 Hz, 2H), 7.20 (dd, *J* = 8.5, 5.4 Hz, 2H), 7.06 (t, *J* = 8.6 Hz, 2H), 4.53 (d, *J* = 2.1 Hz, 1H), 4.14 (d, *J* = 1.5 Hz, 1H), 3.94 (s, 3H), 3.84−3.64 (m, 1H), 3.48 (d, *J* = 9.0 Hz, 1H), 3.30 (d, *J* = 11.3 Hz, 1H), 2.91 (m, 3H), 2.37−2.22 (m, 2H), 1.93−1.80 (m, 1H). ESI-MS *m/z*: 383 [M + H]$^+$.

*(±)-trans-3-(4-Fluorophenyl)-4-(furan-2-yl)-1-(piperidin-4-yl)-azetidin-2-one (**11l**).* The title compound was obtained via general procedure C starting from **10l** (315 mg, 1.0 mmol).^{1}H NMR (300 MHz, $CDCl_3$) δ 7.40 (t, *J* = 1.5 Hz, 1H), 7.34−7.27 (m, 2H), 7.10−7.02 (m, 2H), 6.32 (s, 2H), 5.12 (d, *J* = 7.5 Hz, 1H), 4.56 (dd, *J* = 7.5, 0.8 Hz, 1H), 4.30−4.20 (m, 1H), 3.10−2.93 (m, 2H), 2.91−2.72 (m, 2H), 2.68−2.50 (m, 1H), 2.03−1.83 (m, 2H), 1.75−1.53 (m, 2H). ESI-MS *m/z*: 315[M + H]$^+$.

*(±)-trans-1-(1-(1H-1,2,4-Triazole-1-carbonyl)piperidin-4-yl)-3,4-bis(4-fluorophenyl)azetidin-2-one (**5a**).* The title compound was obtained via general procedure D starting from amine **11a** (50 mg, 0.15 mmol) and 1*H*-1,2,4-triazole (21 mg, 0.30 mmol). Purification: 1:1 PE/EtOAc. Yield: 59%, 40 mg, amorphous white solid. ^{1}H NMR (300 MHz, $CDCl_3$) δ 8.73 (s, 1H), 7.95 (s, 1H), 7.36 (m, 2H), 7.19 (m, 2H), 7.10 (m, 2H), 7.02 (m, 2H), 4.70−4.28 (m, 3H), 4.08 (d, *J* = 2.0 Hz, 1H), 3.77 (m, 1H), 3.09 (m, 2H), 2.07 (m, 2H), 1.85 (dd, *J* = 13.2, 3.0 Hz, 1H), 1.59 (qd, *J* = 11.7, 4.1 Hz, 1H). ^{13}C NMR (75 MHz, $CDCl_3$) δ 168.3, 163.2 (d, J_{C-F} = 248.5 Hz), 162.5 (d, J_{C-F} = 246.9 Hz), 152.3, 148.6, 146.9, 134.2 (d, J_{C-F} = 3.2 Hz), 130.6 (d, J_{C-F} = 3.3 Hz), 129.1 (d, J_{C-F} = 8.1 Hz), 128.3 (d, J_{C-F} = 8.3 Hz), 116.6 (d, J_{C-F} = 21.8 Hz), 116.22 (d, J_{C-F} = 21.6 Hz), 64.2, 62.9, 50.8, 30.4, 30.2. ESI-MS *m/z*: 438 [M + H]$^+$, 460 [M + Na]$^+$.

*(±)-trans-1-(1-(1H-1,2,4-Triazole-1-carbonyl)piperidin-4-yl)-3,4-bis(benzo[d][1,3]dioxol-5-yl)azetidin-2-one (**5b**).* The title compound was obtained via general procedure D starting from amine **11b** (50 mg, 0.13 mmol) and 1*H*-1,2,4-triazole (19 mg, 0.26 mmol). Purification: 1:1 PE/EtOAc. Yield: 56%, 40 mg, amorphous white solid. ^{1}H NMR (300 MHz, $CDCl_3$) δ 8.77 (s, 1H), 7.99 (s, 1H), 6.94−6.56 (m, 6H), 6.01 (s, 2H), 5.95 (s, 2H), 4.72−4.30 (m, 3H), 4.01 (d, *J* = 1.8 Hz, 1H), 3.71 (m, 1H), 3.14 (m, 2H), 2.08 (m, 2H), 1.89 (m, 1H), 1.63 (m, 1H). ^{13}C NMR (75 MHz, $CDCl_3$) δ 168.7, 152.5, 148.9,148.8, 148.5, 148.4, 147.4, 132.2, 128.6, 120.9, 120.6, 108.9 (2C), 107.6 (2C), 106.3, 101.7, 101.4, 64.6, 63.7, 50.6, 45.4, 30.4, 30.2. ESI-MS *m/z*: 490 [M + H]$^+$, 512 [M + Na]$^+$.

*(±)-trans-1-(1-(1H-1,2,4-Triazole-1-carbonyl)piperidin-4-yl)-3-(benzo[d][1,3]dioxol-5-yl)-4-(4-fluoro phenyl)azetidin-2-one (**5c**).* The title compound was obtained via general procedure D starting from amine **11c** (50 mg, 0.14 mmol) and 1*H*-1,2,4-triazole (20 mg, 0.28 mmol). Purification: 1:1 PE/EtOAc. Yield: 56%, 36 mg, amorphous white solid. ^{1}H NMR (300 MHz, $CDCl_3$) δ 8.74 (s, 1H), 7.97 (s, 1H), 7.36 (m, 2H), 7.11 (t, *J* = 8.5 Hz, 2H), 6.83−6.63 (m, 3H), 5.95 (s, 2H), 4.76−4.32 (m, 3H), 4.01 (d, *J* = 2.1 Hz, 1H), 3.78 (m, 1H), 3.12 (m, 2H), 2.07 (m, 2H), 1.86 (m, 1H), 1.58 (m, 1H). ^{13}C NMR (75 MHz, $CDCl_3$) δ 168.9, 163.4 (d, J_{C-F} = 248.4 Hz), 152.5, 148.8, 148.6, 147.7, 147.1, 134.5 (d, J_{C-F} = 3.1 Hz), 128.6, 128.5 (d, J_{C-F} = 8.3 Hz), 121.1, 116.7 (d, J_{C-F} = 21.8 Hz), 109.1, 107.8, 101.6, 65.0, 63.2, 50.9, 30.6, 30.4. ESI-MS *m/z*: 464 [M + H]$^+$.

*(±)-trans-1-(1-(1H-1,2,4-Triazole-1-carbonyl)piperidin-4-yl)-3,4-diphenylazetidin-2-one (**5d**).* The title compound was obtained via general procedure D starting from amine **11m**[34] (50 mg, 0.16 mmol) and 1*H*-1,2,4-triazole (22 mg, 0.32 mmol). Purification: 1:1 PE/EtOAc. Yield: 61%, 39 mg, amorphous white solid. ^{1}H NMR (300 MHz, $CDCl_3$) δ 8.75 (s, 1H), 7.97 (s, 1H), 7.54−7.18 (m, 10H), 4.73−4.24 (m, 3H), 4.15 (d, *J* = 2.1 Hz, 1H), 3.81 (m, 1H), 3.14 (m, 2H), 2.12 (m, 2H), 1.89 (dd, *J* = 13.5, 2.9 Hz, 1H), 1.63 (qd, *J* = 11.3, 3.7 Hz, 1H). ^{13}C NMR (75 MHz, $CDCl_3$) δ 168.7, 152.3, 148.7, 146.9, 138.6, 135.1, 129.5, 129.3, 129.2, 128.0, 127.5, 126.7, 64.8, 63.4, 50.8, 30.4, 30.2. ESI-MS *m/z*: 402 [M + H]$^+$, 424 [M + Na]$^+$.

*(±)-trans-1-(1-(1H-1,2,4-Triazole-1-carbonyl)piperidin-4-yl)-3-(4-fluorophenyl)-4-(p-tolyl)azetidin-2-one (**5e**).* The title compound was obtained via general procedure D starting from amine **11d** (50 mg, 0.15 mmol) and 1*H*-1,2,4-triazole (21 mg, 0.30 mmol). Purification: 1:1 PE/EtOAc. Yield: 59%, 38 mg, amorphous white solid. ^{1}H NMR (300 MHz, $CDCl_3$) δ 8.72 (s, 1H), 7.94 (s, 1H), 7.23 (m, 6H), 7.01 (m, 2H), 4.68−4.24 (m, 3H), 4.09 (d, *J* = 2.1 Hz, 1H), 3.76 (m, 1H), 3.11 (m, 2H), 2.36 (s, 3H), 2.08 (m, 2H), 1.85 (m, 1H), 1.60 (m, 1H). ^{13}C NMR (75 MHz, $CDCl_3$) δ 168.5, 162.5 (d, J_{C-F} = 246.5 Hz), 152.2, 148.6, 146.8, 139.2, 135.2, 131.0 (d, J_{C-F} = 3.2 Hz), 130.2, 129.1 (d, J_{C-F} = 8.1 Hz), 126.6, 116.1 (d, J_{C-F} = 21.5 Hz), 63.9, 63.4, 50.7, 30.4, 30.1, 21.4. ESI-MS *m/z*: 434 [M + H]$^+$, 456 [M + Na]$^+$.

https://doi.org/10.1021/acs.jmedchem.3c01278
J. Med. Chem. 2024, 67, 1758−1782

*(±)-trans-1-(1-(1H-1,2,4-Triazole-1-carbonyl)piperidin-4-yl)-3-(4-fluorophenyl)-4-(4-(trifluoromethyl)phenyl)azetidin-2-one (**5f**).* The title compound was obtained via general procedure D starting from amine **11e** (50 mg, 0.15 mmol) and 1*H*-1,2,4-triazole (21 mg, 0.30 mmol). Purification: 1:1 PE/EtOAc. Yield: 66%, 48 mg, amorphous white solid. ^{1}H NMR (300 MHz, $CDCl_3$) δ 8.74 (s, 1H), 7.96 (s, 1H), 7.70 (d, J = 8.4 Hz, 2H), 7.52 (d, J = 8.1 Hz, 2H), 7.22 (m, 2H), 7.05 (m, 2H), 4.67−4.31 (m, 3H), 4.09 (d, J = 2.1 Hz, 1H), 3.78 (m, 1H), 3.09 (m, 2H), 2.12 (m, 2H), 1.88 (m, 1H), 1.60 (qd, J = 11.7, 4.2 Hz, 1H). ^{13}C NMR (75 MHz, $CDCl_3$) δ 168.2, 162.6 (d, J_{C-F} = 247.3 Hz), 152.3, 148.6, 146.9, 142.6 (2C), 131.6 (q, J_{C-CF3} = 32.8 Hz), 130.3 (d, J_{C-F} = 3.3 Hz), 129.2 (d, J_{C-F} = 8.2 Hz), 126.9, 126.6 (q, J_{CF3} = 3.7 Hz), 125.8, 116.3 (d, J_{C-F} = 21.6 Hz), 64.3, 62.9, 53.7, 51.0, 45.3, 30.4, 30.2. ESI-MS m/z: 488 [M + H]$^+$, 510 [M + Na]$^+$.

*(±)-trans-1-(1-(1H-1,2,4-Triazole-1-carbonyl)piperidin-4-yl)-3-(4-fluorophenyl)-4-(4-methoxyphenyl) azetidin-2-one (**5g**).* The title compound was obtained via general procedure D starting from amine **11f** (50 mg, 0.14 mmol) and 1*H*-1,2,4-triazole (20 mg, 0.28 mmol). Purification: 1:1 PE/EtOAc. Yield: 60%, 37 mg, amorphous white solid. ^{1}H NMR (300 MHz, $CDCl_3$) δ 8.74 (s, 1H), 7.96 (s, 1H), 7.30 (m, 2H), 7.20 (m, 2H), 7.03 (m, 2H), 6.94 (m, 2H), 4.68−4.24 (m, 3H), 4.10 (d, J = 1.9 Hz, 1H), 3.83 (s, 3H), 3.76 (m, 1H), 3.12 (m, 2H), 2.10 (m, 2H), 1.86 (m, 1H), 1.60 (qd, J = 11.5, 4.2 Hz, 1H). ^{13}C NMR (75 MHz, $CDCl_3$) δ 168.65, 162.5 (d, J_{C-F} = 246.6 Hz), 160.4, 152.3, 148.6, 146.9, 131.0 (d, J_{C-F} = 3.3 Hz), 130.1, 129.1 (d, J_{C-F} = 8.1 Hz), 127.9, 116.1 (d, J_{C-F} = 21.5 Hz), 114.9, 64.0, 63.2, 55.6, 50.6, 30.4, 30.2. ESI-MS m/z: 450 [M + H]$^+$.

*(±)-trans-1-(1-(1H-1,2,4-Triazole-1-carbonyl)piperidin-4-yl)-3,4-bis(3-methoxyphenyl)azetidin-2-one (**5h**).* The title compound was obtained via general procedure D starting from amine **11g** (50 mg, 0.14 mmol) and 1*H*-1,2,4-triazole (20 mg, 0.28 mmol). Purification: 1:1 PE/EtOAc. Yield: 47%, 30 mg, amorphous white solid. ^{1}H NMR (300 MHz, $CDCl_3$) δ 8.74 (s, 1H), 7.97 (s, 1H), 7.29 (m, 2H), 7.04−6.72 (m, 6H), 4.67−4.25 (m, 3H), 4.11 (d, J = 1.9 Hz, 1H), 3.82 (s, 3H), 3.79 (m, 4H), 3.14 (m, 2H), 2.09 (m, 2H), 1.89 (m, 1H), 1.65 (m, 1H). ^{13}C NMR (75 MHz, $CDCl_3$) δ 168.6, 160.5, 160.2, 152.3, 148.6, 146.9, 140.2, 136.5, 130.6, 130.3, 119.6, 118.8, 114.2, 113.4, 113.2, 112.3, 64.6, 63.2, 55.6, 55.5, 50.7, 30.3, 30.1. ESI-MS m/z: 462 [M + H]$^+$, 484 [M + Na]$^+$.

*(±)-trans-1-(1-(1H-1,2,4-Triazole-1-carbonyl)piperidin-4-yl)-4-(benzo[d][1,3]dioxol-5-yl)-3-(3-fluorophenyl)azetidin-2-one (**5i**).* The title compound was obtained via general procedure D starting from amine **11h** (50 mg, 0.14 mmol) and 1*H*-1,2,4-triazole (20 mg, 0.28 mmol). Purification: 20:1 DCM/acetone. Yield: 55%, 36 mg, amorphous white solid. ^{1}H NMR (300 MHz, $CDCl_3$) δ 8.75 (s, 1H), 7.97 (s, 1H), 7.37−7.27 (m, 1H), 7.06−6.91 (m, 3H), 6.88 (s, 1H), 6.84−6.80 (m, 2H), 6.01 (s, 2H), 4.71−4.31 (m, 3H), 4.09 (d, J = 1.9 Hz, 1H), 3.87−3.64 (m, 1H), 3.26−2.98 (m, 2H), 2.19−2.01 (m, 2H), 1.89 (dd, J = 13.2, 2.9 Hz, 1H), 1.71−1.55 (m, 1H). ^{13}C NMR (75 MHz, $CDCl_3$) δ 167.9, 163.2 (d, J_{C-F} = 247.3 Hz), 152.3, 148.9, 148.6, 148.6, 146.9, 137.3 (d, J_{C-F} = 7.4 Hz), 131.9, 130.8 (d, J_{C-F} = 8.4 Hz), 123.1 (d, J_{C-F} = 3.0 Hz), 120.6, 115.0 (d, J_{C-F} = 21.0 Hz), 114.4 (d, J_{C-F} = 21.9 Hz), 109.0, 106.2, 101.7, 64.2, 63.1, 50.7, 30.4, 30.1. ESI-MS m/z: 464 [M + H]$^+$, 486 [M + Na]$^+$.

*(±)-trans-1-(1-(1H-1,2,4-Triazole-1-carbonyl)piperidin-4-yl)-4-(benzo[d][1,3]dioxol-5-yl)-3-(3-methoxy phenyl)azetidin-2-one (**5j**).* The title compound was obtained via general procedure D starting from amine **11i** (50 mg, 0.13 mmol) and 1*H*-1,2,4-triazole (19 mg, 0.26 mmol). Purification: 20:1 DCM/acetone. Yield: 40%, 30 mg, amorphous white solid. ^{1}H NMR (300 MHz, $CDCl_3$) δ 8.76 (s, 1H), 7.98 (s, 1H), 7.36−7.15 (m, 2H), 6.91−6.69 (m, 5H), 6.01 (s, 2H), 4.67−4.23 (m, 3H), 4.07 (d, J = 2.1 Hz, 1H), 3.91−3.67 (m, 4H), 3.31−3.00 (m, 2H), 2.16−2.01 (m, 2H), 1.89 (dd, J = 13.1, 3.5 Hz, 1H), 1.73−1.51 (m, 1H). ^{13}C NMR (75 MHz, $CDCl_3$) δ 168.5, 160.2, 152.3, 148.9, 148.6, 148.5, 136.5, 132.3, 130.3, 129.9, 120.6, 119.6, 113.4, 113.2, 108.9, 106.3, 101.7, 64.7, 63.2, 55.5, 50.6, 30.4, 30.1. ESI-MS m/z: 476 [M + H]$^+$, 498 [M + Na]$^+$.

*(±)-trans-1-(1-(1H-1,2,4-Triazole-1-carbonyl)piperidin-4-yl)-4-(benzo[d][1,3]dioxol-5-yl)-3-phenylazetidin-2-one (**5k**).* The title compound was obtained via general procedure D starting from amine **11j** (50 mg, 0.15 mmol) and 1*H*-1,2,4-triazole (21 mg, 0.30 mmol). Purification: 20:1 DCM/acetone. Yield: 53%, 35 mg, amorphous white solid. ^{1}H NMR (300 MHz, $CDCl_3$) δ 8.75 (s, 1H), 7.98 (s, 1H), 7.44−7.23 (m, 5H), 6.97−6.73 (m, 3H), 6.02 (s, 2H), 4.74−4.32 (m, 3H), 4.11 (d, J = 2.2 Hz, 1H), 3.92−3.63 (m, 1H), 3.29−2.96 (m, 2H), 2.29−1.98 (m, 2H), 1.96−1.79 (m, 1H), 1.79−1.65 (m, 1H). ^{13}C NMR (75 MHz, $CDCl_3$) δ 168.7, 152.3, 148.9, 148.6, 148.5, 146.9, 135.0, 132.3, 129.2, 128.0, 127.4, 120.6, 108.9, 106.3, 101.7, 64.8, 63.4, 50.6, 30.3, 30.1. ESI-MS m/z: 446 [M + H]$^+$, 468 [M + Na]$^+$.

*(±)-Methyl-4-(trans-1-(1-(1H-1,2,4-triazole-1-carbonyl)piperidin-4-yl)-3-(4-fluorophenyl)-4-oxoazetidin-2-yl)benzoate (**5l**).* The title compound was obtained via general procedure D starting from amine **11k** (50 mg, 0.13 mmol) and 1*H*-1,2,4-triazole (19 mg, 0.26 mmol). Purification: 1:1 PE/EtOAc. Yield: 41%, 25 mg, amorphous white solid. ^{1}H NMR (300 MHz, $CDCl_3$) δ 8.74 (s, 1H), 8.10 (d, J = 8.1 Hz, 2H), 7.96 (s, 1H), 7.47 (d, J = 8.1 Hz, 2H), 7.21 (dd, J = 8.3, 5.5 Hz, 2H), 7.05 (t, J = 8.5 Hz, 2H), 4.65−4.26 (m, 3H), 4.12 (d, J = 1.8 Hz, 1H), 3.93 (s, 3H), 3.89−3.70 (m, 1H), 3.11 (dt, J = 23.5, 11.7 Hz, 2H), 2.23−2.06 (m, 2H), 1.87 (d, J = 12.1 Hz, 1H), 1.58 (qd, J = 12.1, 3.8 Hz, 1H). ^{13}C NMR (75 MHz, $CDCl_3$) δ 168.2, 166.6, 162.6 (d, J_{C-F} = 247.4 Hz), 152.3, 148.6, 146.9, 143.5, 131.2, 130.8, 130.4 (d, J_{C-F} = 3.3 Hz), 129.1 (d, J_{C-F} = 8.2 Hz), 126.6, 116.3 (d, J_{C-F} = 21.6 Hz), 64.1, 63.1, 52.6, 51.0, 30.5, 30.2. ESI-MS m/z: 478 [M + H]$^+$, 490 [M + Na]$^+$. HRMS (ESI) m/z [M + H]$^+$ calcd for $C_{25}H_{24}FN_5O_4$ 478.1885, found 478.1871, [M + Na]$^+$; calcd for $C_{25}H_{24}FN_5O_4$ 500.1705, found 500.1688.

*(±)-trans-1-(1-(1H-1,2,3-Triazole-1-carbonyl)piperidin-4-yl)-4-(benzo[d][1,3]dioxol-5-yl)-3-(4-fluoro phenyl)azetidin-2-one (**5m**).* The title compound was obtained via general procedure D starting from amine **11n**[16] (50 mg, 0.14 mmol) and 1*H*-1,2,3-triazole (20 mg, 0.28 mmol). Purification: 1:1 PE/EtOAc. Yield: 60%, 40 mg, amorphous white solid. ^{1}H NMR (300 MHz, $CDCl_3$) δ 7.78 (s, 1H), 7.24−7.12 (m, 2H), 7.08−6.97 (m, 3H), 6.90−6.85 (m, 1H), 6.83−6.78 (m, 2H), 6.00 (s, 2H), 4.55−4.12 (m, 3H), 4.07 (d, J = 1.7 Hz, 1H), 3.90−3.70 (m, 1H), 3.29−2.95 (m, 2H), 2.13−2.03 (m, 2H), 1.86 (d, J = 10.5 Hz, 1H), 1.72−1.52 (m, 1H). ^{13}C NMR (75 MHz, $CDCl_3$) δ 168.4, 162.5 (d, J_{C-F} = 246.6 Hz), 149.1, 148.9, 148.5, 136.3 (2C), 132.1, 130.8 (d, J_{C-F} = 3.3 Hz), 129.1 (d, J_{C-F} = 8.1 Hz), 120.6, 116.2 (d, J_{C-F} = 21.6 Hz), 109.0, 106.2, 101.7, 63.9, 63.4, 50.7, 30.4, 30.1. ESI-MS m/z: 464 [M + H]$^+$, 486 [M + Na]$^+$.

*(±)-trans-1-(1-(1H-Benzo[d][1,2,3]triazole-1-carbonyl)piperidin-4-yl)-3,4-bis(4-fluorophenyl)azetidin-2-one (**5n**).* The title compound was obtained via general procedure D starting from amine **11a** (50 mg, 0.15 mmol) and 1*H*-benzotriazole (35 mg, 0.30 mmol). Purification: 5:1 PE/EtOAc. Yield: 51%, 38 mg, amorphous white solid. ^{1}H NMR (300 MHz, $CDCl_3$) δ 8.07 (d, J = 8.3 Hz, 1H), 7.94 (d, J = 8.3 Hz, 1H), 7.59 (t, J = 7.7 Hz, 1H), 7.49−7.34 (m, 3H), 7.26−7.18 (m, 2H), 7.13 (t, J = 8.6 Hz, 2H), 7.05 (t, J = 8.6 Hz, 2H), 4.63−4.38 (m, 2H), 4.49 (d, J = 2.0 Hz, 1H), 4.10 (d, J = 1.8 Hz, 1H), 3.93−3.77 (m, 1H), 3.39−3.07 (m, 2H), 2.31−2.05 (m, 2H), 1.92 (d, J = 10.4 Hz, 1H), 1.72 (d, J = 9.7 Hz, 1H). ^{13}C NMR (75 MHz, $CDCl_3$) δ 168.4, 163.2 (d, J_{C-F} = 248.4 Hz), 162.6 (d, J_{C-F} = 246.9 Hz), 149.5, 145.6, 134.2 (d, J_{C-F} = 3.2 Hz), 133.4, 130.6 (d, J_{C-F} = 3.3 Hz), 129.7, 129.1 (d, J_{C-F} = 8.2 Hz), 128.4 (d, J_{C-F} = 8.3 Hz), 125.5, 120.1, 116.6 (d, J_{C-F} = 21.8 Hz), 116.2 (d, J_{C-F} = 21.6 Hz), 113.8, 64.2, 62.9, 50.9, 30.6, 30.3. ESI-MS m/z: 488 [M + H]$^+$.

*(±)-trans-1-(1-(1H-Benzo[d][1,2,3]triazole-1-carbonyl)piperidin-4-yl)-3,4-bis(benzo[d][1,3]dioxol-5-yl)azetidin-2-one (**5o**).* The title compound was obtained via general procedure D starting from amine **11b** (50 mg, 0.13 mmol) and 1*H*-benzotriazole (32 mg, 0.26 mmol). Purification: 2:1 PE/EtOAc. Yield: 45%, 30 mg, amorphous white solid. ^{1}H NMR (300 MHz, $CDCl_3$) δ 8.08 (dd, J = 8.3, 1.0 Hz, 1H), 7.95 (dd, J = 8.3, 1.0 Hz, 1H), 7.59 (t, J = 7.7 Hz, 1H), 7.44 (t, J = 7.7 Hz, 1H), 6.91−6.67 (m, 6H), 6.01 (s, 2H), 5.95 (s, 2H), 4.61−4.41 (m, 2H), 4.39 (d, J = 2.1 Hz, 1H), 4.02 (d, J = 1.9 Hz, 1H), 3.93−3.77 (m, 1H), 3.41−3.09 (m, 2H), 2.27−2.10 (m, 2H), 1.94 (dd, J = 13.6, 2.5 Hz, 1H), 1.71 (qd, J = 12.1, 3.7 Hz, 1H). ^{13}C NMR (75 MHz, $CDCl_3$) δ 168.8, 149.5, 148.9, 148.5, 147.4, 145.6, 133.4, 132.3, 129.7, 128.6, 125.5, 120.9, 120.6, 120.1, 113.8, 108.9, 107.7, 106.3, 101.7, 101.4, 64.6, 63.7, 50.7, 30.6, 29.9. ESI-MS m/z: 540 [M + H]$^+$.

https://doi.org/10.1021/acs.jmedchem.3c01278
J. Med. Chem. 2024, 67, 1758−1782

*(±)-trans-1-(1-(1H-Benzo[d][1,2,3]triazole-1-carbonyl)piperidin-4-yl)-3-(benzo[d][1,3]dioxol-5-yl)-4-(4-fluorophenyl)azetidin-2-one (**5p**).* The title compound was obtained via general procedure D starting from amine **11c** (50 mg, 0.14 mmol) and 1*H*-benzotriazole (33 mg, 0.28 mmol). Purification: 4:1 PE/EtOAc. Yield: 48%, 35 mg, amorphous white solid. ^{1}H NMR (300 MHz, $CDCl_3$) δ 8.07 (dd, J = 8.3, 0.8 Hz, 1H), 7.94 (dd, J = 8.3, 0.8 Hz, 1H), 7.59 (t, J = 7.2 Hz, 1H), 7.44 (t, J = 7.4 Hz, 1H), 7.41−7.34 (m, 2H), 7.11 (t, J = 8.5 Hz, 2H), 6.82−6.67 (m, 3H), 5.95 (s, 2H), 4.60−4.37 (m, 2H), 4.47 (d, J = 2.2 Hz, 1H), 4.03 (d, J = 2.2 Hz, 1H), 3.92−3.77 (m, 1H), 3.35−3.07 (m, 2H), 2.25−2.07 (m, 2H), 1.91 (dd, J = 13.2, 3.3 Hz, 1H), 1.66 (dd, J = 28.2, 7.9 Hz, 1H). ^{13}C NMR (75 MHz, $CDCl_3$) δ 168.7, 163.2 (d, J_{C-F} = 248.2 Hz), 149.5, 148.4, 147.5, 145.6, 134.4 (d, J_{C-F} = 3.1 Hz), 133.4, 129.7, 128.4, 128.3 (d, J_{C-F} = 8.3 Hz), 125.5, 120.9, 120.1, 116.6 (d, J_{C-F} = 21.8 Hz), 113.8, 109.0, 107.7, 101.4, 64.8, 63.1, 50.8, 30.6, 30.3. ESI-MS m/z: 514 [M + H]$^+$.

*(±)-trans-1-(1-(1H-Benzo[d][1,2,3]triazole-1-carbonyl)piperidin-4-yl)-3,4-diphenylazetidin-2-one (**5q**).* The title compound was obtained via general procedure D starting from amine **11m**[34] (50 mg, 0.16 mmol) and 1*H*-benzotriazole (36 mg, 0.32 mmol). Purification: 5:1 PE/EtOAc. Yield: 50%, 36 mg, amorphous white solid. ^{1}H NMR (300 MHz, $CDCl_3$) δ 8.08 (dd, J = 8.3, 0.9 Hz, 1H), 7.94 (dd, J = 8.3, 0.9 Hz, 1H), 7.59 (t, J = 7.1 Hz, 1H), 7.49−7.21 (m, 11H), 4.55 (d, J = 2.2 Hz, 1H), 4.63−4.34 (m, 2H), 4.17 (d, J = 1.9 Hz, 1H), 3.94−3.78 (m, 1H), 3.40−3.12 (m, 2H), 2.29−2.20 (m, 2H), 1.93 (dd, J = 13.3, 3.2 Hz, 1H), 1.82−1.62 (m, 1H). ^{13}C NMR (75 MHz, $CDCl_3$) δ 168.8, 149.5, 145.6, 138.6, 135.1, 133.4, 129.6, 129.5, 129.2 (2C), 128.0, 127.5, 126.7, 125.5, 120.1, 113.8, 64.8, 63.5, 50.8, 30.5, 30.3. ESI-MS m/z: 452 [M + H]$^+$, 474 [M + Na]$^+$.

*(±)-trans-1-(1-(1H-Benzo[d][1,2,3]triazole-1-carbonyl)piperidin-4-yl)-4-(benzo[d][1,3]dioxol-5-yl)-3-(3-fluorophenyl)azetidin-2-one (**5r**).* The title compound was obtained via general procedure D starting from amine **11h** (50 mg, 0.14 mmol) and 1*H*-benzotriazole (33 mg, 0.28 mmol). Purification: 4:1 PE/EtOAc. Yield: 46%, 33 mg, amorphous white solid. ^{1}H NMR (300 MHz, $CDCl_3$) δ 8.07 (d, J = 8.3 Hz, 1H), 7.94 (d, J = 8.3 Hz, 1H), 7.59 (t, J = 7.2 Hz, 1H), 7.44 (t, J = 7.2 Hz, 1H), 7.36−7.27 (m, 1H), 7.06−7.00 (m, 1H), 7.00−6.93 (m, 2H), 6.90 (d, J = 1.4 Hz, 1H), 6.85−6.81 (m, 2H), 6.01 (s, 2H), 4.61−4.35 (m, 2H), 4.46 (d, J = 2.3 Hz, 1H), 4.11 (d, J = 2.2 Hz, 1H), 3.93−3.79 (m, 1H), 3.37−3.09 (m, 2H), 2.25−2.10 (m, 2H), 1.95 (dd, J = 13.6, 3.0 Hz, 1H), 1.72 (qd, J = 11.7, 4.0 Hz, 1H). ^{13}C NMR (75 MHz, $CDCl_3$) δ 167.9, 163.3 (d, J_{C-F} = 247.2 Hz), 149.5, 148.9, 148.6, 145.6, 137.3 (d, J_{C-F} = 7.7 Hz), 133.4, 132.0, 130.8 (d, J_{C-F} = 8.4 Hz), 129.7, 125.5, 123.1 (d, J_{C-F} = 3.0 Hz), 120.7, 120.1, 115.0 (d, J_{C-F} = 21.0 Hz), 114.5 (d, J_{C-F} = 21.9 Hz), 113.8, 109.0, 106.2, 101.7, 64.2, 63.1, 50.9, 30.5, 30.2. ESI-MS m/z: 514 [M + H]$^+$, 536 [M + Na]$^+$

*(±)-trans-1-(1-(1H-Benzo[d][1,2,3]triazole-1-carbonyl)piperidin-4-yl)-4-(benzo[d][1,3]dioxol-5-yl)-3-(3-methoxyphenyl)azetidin-2-one (**5s**).* The title compound was obtained via general procedure D starting from amine **11i** (50 mg, 0.13 mmol) and 1*H*-benzotriazole (32 mg, 0.26 mmol). Purification: 2:1 PE/EtOAc. Yield: 52%, 35 mg, amorphous white solid. ^{1}H NMR (300 MHz, $CDCl_3$) δ 8.07 (d, J = 8.3 Hz, 1H), 7.94 (d, J = 8.3 Hz, 1H), 7.59 (t, J = 7.7 Hz, 1H), 7.44 (t, J = 7.6 Hz, 1H), 7.32−7.21 (m, 2H), 6.95−6.74 (m, 5H), 6.01 (s, 2H), 4.63−4.37 (m, 2H), 4.47 (d, J = 2.1 Hz, 1H), 4.09 (d, J = 1.6 Hz, 1H), 3.92−3.80 (m, 1H), 3.79 (s, 3H), 3.39−3.13 (m, 2H), 2.24−2.12 (m, 2H), 1.94 (dd, J = 13.2, 2.7 Hz, 1H), 1.72 (qd, J = 12.2, 4.0 Hz, 1H). ^{13}C NMR (75 MHz, $CDCl_3$) δ 168.5, 160.2, 149.5, 148.9, 148.5, 145.6, 136.5, 133.4, 132.4, 130.3, 129.7, 125.5, 120.7, 120.1, 119.6, 113.8, 113.4, 113.3, 108.9, 106.3, 101.7, 64.7, 63.3, 55.5, 50.7, 30.5, 30.1. ESI-MS m/z: 523 [M + H]$^+$.

*(±)-trans-1-(1-(1H-Benzo[d][1,2,3]triazole-1-carbonyl)piperidin-4-yl)-4-(benzo[d][1,3]dioxol-5-yl)-3-phenylazetidin-2-one (**5t**).* The title compound was obtained via general procedure D starting from mine **11j** (50 mg, 0.15 mmol) and 1*H*-benzotriazole (35 mg, 0.30 mmol). Purification: 4:1 PE/EtOAc. Yield: 55%, 40 mg, amorphous white solid. ^{1}H NMR (300 MHz, $CDCl_3$) δ 8.07 (d, J = 7.6 Hz, 1H), 7.94 (d, J = 8.3 Hz, 1H), 7.58 (t, J = 8.3 Hz, 1H), 7.44 (t, J = 7.7 Hz, 1H), 7.39−7.21 (m, 5H), 7.02−6.74 (m, 3H), 6.01 (s, 2H), 4.63−4.35 (m, 3H), 4.11 (d, J = 2.2 Hz, 1H), 3.95−3.66 (m, 1H), 3.52−2.96 (m, 2H), 2.34−2.11 (m, 2H), 2.03−1.83 (m, 1H), 1.84−1.50 (m, 1H). ^{13}C NMR (75 MHz, $CDCl_3$) δ 168.7, 149.5, 148.9, 148.5, 145.6, 135.1, 133.4, 132.4, 129.7, 129.2, 128.0, 127.5, 125.5, 120.7, 120.1, 113.8, 108.9, 106.3, 101.7, 64.8, 63.4, 50.7, 30.5, 30.3. ESI-MS m/z: 496 [M + H]$^+$, 519 [M + Na]$^+$.

*trans-1-(1-(1H-Benzo[d][1,2,3]triazole-1-carbonyl)piperidin-4-yl)-3-(4-fluorophenyl)-4-(furan-2-yl)azetidine-2-one (**5u**).* The title compound was obtained via general procedure D starting from mine **11l** (25 mg, 0.08 mmol) and 1*H*-benzotriazole (35 mg, 0.30 mmol). Purification: 4:1 PE/EtOAc. Yield: 32%, 9 mg, amorphous white solid. ^{1}H NMR (300 MHz, $CDCl_3$) δ 8.09 (d, J = 8.3 Hz, 1H), 7.95 (d, J = 8.3 Hz, 1H), 7.65−7.56 (m, 1H), 7.53−7.39 (m, 2H), 7.30−7.22 (m, 2H), 7.05 (td, J = 8.6, 1.2 Hz, 2H), 6.46−6.39 (m, 2H), 4.59−4.33 (m, 4H), 3.90 (d, J = 8.4 Hz, 1H), 3.36−3.12 (m, 2H), 2.09 (d, J = 9.5 Hz, 1H), 1.98−1.88 (m, 1H), 1.62 (d, J = 21.5 Hz, 2H). ^{13}C NMR (75 MHz, $CDCl_3$) δ 167.7, 164.2 (d, J_{C-F} = 256.7 Hz), 160.9, 150.3, 149.6, 145.6, 143.7, 133.4, δ 130.5 (d, J = 3.3 Hz), 129.2 (d, J = 8.2 Hz), 129.1, 126.7, 125.5, 120.1, 116.2 (d, J = 21.6 Hz), 113.8, 111.2, 110.2, 60.0, 56.0, 53.7, 50.3, 46.0, 31.1, 30.0. ESI-MS m/z: 460 [M + H]$^+$.

*(±)-trans-1-(1-(1H-Benzo[d][1,2,3]triazole-1-carbonyl)piperidin-4-yl)-4-(benzo[d][1,3]dioxol-5-yl)-3-(4-fluorophenyl)azetidin-2-one (**5v**).* Obtained via general procedure D starting from amine **11n** (50 mg, 0.14 mmol) and 1*H*-benzotriazole (33 mg, 0.28 mmol). Purification: 4:1 PE/EtOAc. Yield: 42%, 30 mg, amorphous white solid. ^{1}H NMR (300 MHz, $CDCl_3$) δ 8.09 (d, J = 8.3 Hz, 1H), 7.95 (d, J = 8.3 Hz, 1H), 7.60 (t, J = 7.7 Hz, 1H), 7.45 (t, J = 7.7 Hz, 1H), 7.23 (m, 2H), 7.05 (t, J = 8.6 Hz, 2H), 6.90 (s, 1H), 6.84 (m, 2H), 6.02 (s, 2H), 4.69−4.38 (m, 3H), 4.10 (d, J = 1.7 Hz, 1H), 3.87 (m, 1H), 3.26 (m, 2H), 2.19 (m, 2H), 1.95 (dd, J = 13.3, 2.5 Hz, 1H), 1.73 (qd, J = 12.8, 2.7 Hz, 1H). ^{13}C NMR (75 MHz, $CDCl_3$) δ 168.5, 162.5 (d, J_{C-F} = 246.7 Hz), 149.5, 148.9, 148.6, 145.6, 133.4, 132.1, 130.8 (d, J_{C-F} = 3.3 Hz), 129.7, 129.1 (d, J_{C-F} = 8.1 Hz), 125.5, 120.6, 120.1, 116.2 (d, J_{C-F} = 21.6 Hz), 113.8, 109.0, 106.3, 101.7, 64.0, 63.5, 50.8, 30.5, 30.3. ESI-MS m/z: 514 [M + H]$^+$, 536 [M + Na]$^+$. HRMS (ESI) m/z [M + H]$^+$ calcd for $[C_{28}H_{25}FN_5O_4]^+$ 514.1885, found 514.1875, [M + Na]$^+$; calcd for $[C_{28}H_{24}FN_5O_4Na]^+$ 536.1704, found 536.1689, [M+K]$^+$; calcd for $[C_{28}H_{24}FN_5O_4K]^+$ 552.1444, found 552.1413.

*(±)-(3R,4S)-1-(1-(1H-Benzo[d][1,2,3]triazole-1-carbonyl)-piperidin-4-yl)-4-(benzo[d][1,3]dioxol-5-yl)-3-(4-fluorophenyl)-azetidin-2-one ((3R,4S)-**5v**).* Spectroscopic data are identical to those reported for (±)-**5v**.

*(3S,4R)-1-(1-(1H-Benzo[d][1,2,3]triazole-1-carbonyl)piperidin-4-yl)-4-(benzo[d][1,3]dioxol-5-yl)-3-(4-fluorophenyl)azetidin-2-one ((3S,4R)-**5v**).* Spectroscopic data are identical to those reported for (±)-**5v**.

*1-Benzyl-N-(pyridin-3-ylmethylene)piperidin-4-amine (**13**).* The title compound was obtained via general procedure A, starting from 3-pyridinecarboxyaldehyde **12** (250 μL, 2.63 mmol). ESI-MS m/z: 280 [M + H]$^+$.

*(±)-trans-1-(1-Benzylpiperidin-4-yl)-3-(4-fluorophenyl)-4-(pyridin-3-yl)azetidin-2-one (**14a**).* The title compound was obtained via general procedure B starting from imine **13** (1091 mg, 2.63 mmol) and 4-fluorophenylacetic acid (608 mg, 3.95 mmol). Purification: 1:1 PE/EtOAc. Yield: 25%, 270 mg, yellow oil. ^{1}H NMR (300 MHz, $CDCl_3$) δ 8.62 (s, 2H), 7.75 (d, J = 7.9 Hz, 1H), 7.36 (dd, J = 7.8, 4.8 Hz, 1H), 7.24−7.16 (m, 7H), 7.04 (t, J = 8.4 Hz, 2H), 4.48 (d, J = 1.6 Hz, 1H), 4.07 (d, J = 1.5 Hz, 1H),3.60 (m, 1H), 3.44 (s, 2H), 2.83 (dd, J = 39.5, 10.8 Hz, 2H), 2.10−1.77 (m, 4H), 1.68 (dd, J = 39.5, 11.6 Hz, 1H), 1.45 (qd, J = 12.0, 4.2 Hz, 1H). ESI-MS m/z: 416 [M + H]$^+$.

*(±)-trans-3-(Benzo[d][1,3]dioxol-5-yl)-1-(1-benzylpiperidin-4-yl)-4-(pyridin-3-yl)azetidin-2-one (**14b**).* The title compound was obtained via general procedure B starting from imine **13** (1162 mg, 2.63 mmol) and (3,4-methylendioxy)phenylacetic acid (710 mg, 3.95 mmol). Purification: 1:1 PE/EtOAc. Yield: 33%, 380 mg, yellow oil. ^{1}H NMR (300 MHz, $CDCl_3$) δ 8.61 (s, 2H), 7.73 (d, J = 7.8 Hz, 1H), 7.36 (dd, J = 7.7, 4.8 Hz, 1H), 7.23 (m, 5H), 6.73 (m, 3H), 5.96 (s, 2H), 4.46 (d, J = 1.5 Hz, 1H), 4.00 (d, J = 1.5 Hz,1H), 3.69−3.55 (m, 1H), 3.43 (s, 2H), 2.82 (dd, J = 40.5, 10.8 Hz, 2H), 2.16−1.79 (m, 4H), 1.67 (d, J = 13.1 Hz, 1H), 1.43 (qd, J = 12.2, 3.8 Hz, 1H). ESI-MS m/z: 442 [M + H]$^+$.

*(±)-trans-1-(1-Benzylpiperidin-4-yl)-3-(4-methoxyphenyl)-4-(pyridin-3-yl)azetidin-2-one (**14c**).* The title compound was obtained

via general procedure B starting from imine **13** (1125 mg, 2.63 mmol) and 4-methoxyphenylacetic acid (650 mg, 3.95 mmol). Purification: 1:1 PE/EtOAc. Yield: 28%, 315 mg, yellow oil. ^{1}H NMR (300 MHz, $CDCl_3$) 8.62 (d, J = 2.2 Hz, 2H), 7.74 (d, J = 7.7 Hz, 1H), 7.35 (dd, J = 7.8, 4.9 Hz, 1H), 7.30−7.22 (m, 5H), 7.15 (d, J = 8.4 Hz, 2H), 6.88 (d, J = 8.5 Hz, 2H), 4.47 (d, J = 1.6 Hz, 1H), 4.04 (d, J = 1.6 Hz, 1H), 3.80 (s, 3H), 3.69−3.55 (m, 1H), 3.44 (s, 2H), 2.82 (dd, J = 39.7, 11.3 Hz, 2H), 2.13−1.88 (m, 4H), 1.75 (dd, J = 44.5, 12.8 Hz, 1H), 1.43 (qd, J = 12.1, 3.2 Hz, 1H). ESI-MS m/z: 428 [M + H]$^+$, 450 [M + Na]$^+$.

*(±)-trans-1-(1-Benzylpiperidin-4-yl)-3-phenyl-4-(pyridin-3-yl)-azetidin-2-one (**14d**).* The title compound was obtained via general procedure B starting from imine **13** (1046 mg, 2.63 mmol) and phenylacetic acid (535 mg, 3.95 mmol). Purification: from 1:1 PE/EtOAc to EtOAc. Yield: 27%, 280 mg, yellow oil. ^{1}H NMR (300 MHz, $CDCl_3$) 8.64 (s, 2H), 7.76 (d, J = 8.0 Hz, 1H), 7.54−7.03 (m, 11H), 4.53 (d, J = 2.0 Hz, 1H), 4.09 (d, J = 1.8 Hz, 1H), 3.82−3.54 (m, 1H), 3.44 (s, 2H), 2.82 (dd, J = 39.8, 10.7 Hz, 2H), 2.17−1.75 (m, 4H), 1.75 (dd, J = 45.0, 13.4 Hz, 1H), 1.45 (qd, J = 12.1, 3.9 Hz, 1H). ESI-MS m/z: 398 [M + H]$^+$, 420 [M + Na]$^+$.

*(±)-trans-1-(1-Benzylpiperidin-4-yl)-4-(4-fluorophenyl)-3-(pyridin-3-yl)azetidin-2-one (**14e**).* The title compound was obtained via general procedure B starting from imine **9a** (390 mg, 1.21 mmol) and 2-(pyridin-3-yl)acetic acid (315 mg, 1.82 mmol). Purification: 1:1 PE/EtOAc. Yield: 38%, 191 mg, yellow oil. ^{1}H NMR (400 MHz, $CDCl_3$) δ 8.53 (d, J = 4.5 Hz, 1H), 8.46 (s, 1H), 7.58 (d, J = 7.8 Hz, 1H), 7.35 (dd, J = 8.4, 5.3 Hz, 2H), 7.30−7.18 (m, 6H), 7.09 (t, J = 8.5 Hz, 2H), 4.47 (d, J = 2.0 Hz, 1H), 4.04 (d, J = 1.5 Hz, 1H), 3.64−3.50 (m,1H), 3.42 (s, 2H), 2.86 (d, J = 11.5 Hz, 1H), 2.73 (d, J = 11.6 Hz, 1H), 2.06−1.82 (m, 4H), 1.66 (d, J = 12.2 Hz, 1H), 1.45 (qd, J = 11.9, 3.8 Hz, 1H). ESI-MS m/z: 416 [M + H]$^+$.

*(±)-trans-4-(Benzo[d][1,3]dioxol-5-yl)-1-(1-benzylpiperidin-4-yl)-3-(pyridin-3-yl)azetidin-2-one (**14f**).* The title compound was obtained via general procedure B starting from **9h**[16] (370 mg, 1.15 mmol) and 2-(pyridin-3-yl)acetic acid (300 mg, 1.73 mmol). Purification: 1:1 PE/EtOAc. Yield: 23%, 117 mg, yellow oil. ^{1}H NMR (400 MHz, $CDCl_3$) δ 8.48 (d, J = 18.3 Hz, 2H), 7.55 (d, J = 7.6 Hz, 1H), 7.34−7.08 (m, 6H), 6.85 (s, 1H), 6.80−6.63 (m, 2H), 5.95 (s, 2H), 4.38 (d, J = 1.9 Hz, 1H), 4.01 (d, J = 1.9 Hz, 1H), 3.53 (d, J = 3.2 Hz, 1H), 3.41 (s, 2H), 3.35−3.27 (m, 1H), 2.78 (dd, J = 46.7, 10.9 Hz, 2H), 2.06−1.80 (m, 3H), 1.68 (d, J = 12.4 Hz, 1H), 1.48 (qd, J = 10.1, 2.4 Hz, 1H). ESI-MS m/z: 442 [M + H]$^+$.

*(±)-trans-3-(4-Fluorophenyl)-1-(piperidin-4-yl)-4-(pyridin-3-yl)-azetidin-2-one (**15a**).* The title compound was obtained via general procedure C starting from **14a** (150 mg, 0.36 mmol). The compound was submitted to the following step without further purification. ESI-MS m/z: 326 [M + H]$^+$, 348 [M + Na]$^+$.

*(±)-trans-3-(Benzo[d][1,3]dioxol-5-yl)-1-(piperidin-4-yl)-4-(pyridin-3-yl)azetidin-2-one (**15b**).* The title compound was obtained via general procedure C starting from **14b** (150 mg, 0.33 mmol). The compound was submitted to the following step without further purification. ESI-MS m/z: 352 [M + H]$^+$.

*(±)-trans-3-(4-Methoxyphenyl)-1-(piperidin-4-yl)-4-(pyridin-3-yl)azetidin-2-one (**15c**).* The title compound was obtained via general procedure C starting from **14c** (150 mg, 0.35 mmol). The compound was submitted to the following step without further purification. ESI-MS m/z: 328 [M + H]$^+$.

*(±)-trans-3-Phenyl-1-(piperidin-4-yl)-4-(pyridin-3-yl)azetidin-2-one (**15d**).* The title compound was obtained via general procedure C starting from **14d** (150 mg, 0.38 mmol). The compound was submitted to the following step without further purification. ESI-MS m/z: 308 [M + H]$^+$.

*(±)-trans-4-(4-Fluorophenyl)-1-(piperidin-4-yl)-3-(pyridin-3-yl)-azetidin-2-one (**15e**).* The title compound was obtained via general procedure C starting from **14e** (50 mg, 0.15 mmol). The compound was submitted to the following step without further purification. ESI-MS m/z: 326 [M + H]$^+$.

*(±)-trans-4-(Benzo[d][1,3]dioxol-5-yl)-1-(piperidin-4-yl)-3-(pyridin-3-yl)azetidin-2-one (**15f**).* The title compound was obtained via general procedure C starting from **14f** (58 mg, 0.13 mmol). The compound was submitted to the following step without further purification. ESI-MS m/z: 352 [M + H]$^+$, 375 [M + Na]$^+$.

*(±)-trans-1-(1-(1H-1,2,4-Triazole-1-carbonyl)piperidin-4-yl)-3-(4-fluorophenyl)-4-(pyridin-3-yl)azetidin-2-one (**6a**).* The title compound was obtained via general procedure D, starting from amine **15a** (47 mg, 0.15 mmol) and 1*H*-1,2,4-triazole (21 mg, 0.30 mmol). Purification 1:1 PE/EtOAc. Yield: 40%, 25 mg, colorless oil. ^{1}H NMR (300 MHz, $CDCl_3$) δ 8.75 (s, 1H), 8.67 (d, J = 1.3 Hz, 1H), 8.17 (s, 1H), 7.96 (m, 1H), 7.76 (d, J = 7.9 Hz, 1H), 7.40 (dd, J = 7.8, 4.8 Hz, 1H), 7.25−7.14 (m, 2H), 7.05 (t, J = 8.5 Hz, 2H), 4.72−4.34 (m, 3H), 4.14 (d, J = 1.5 Hz, 1H), 3.87−3.73 (m, 1H), 3.13 (m, 2H), 2.11−2.02 (m, 2H), 1.89 (dd, J = 39.5, 10.4 Hz, 1H), 1.61 (qd, J = 11.9, 3.9 Hz, 1H). ^{13}C NMR (75 MHz, $CDCl_3$) δ 168.1, 162.7 (d, J_{C-F} = 247.8 Hz), 152.3, 150.9, 148.6, 148.5, 146.9, 134.1, 133.9, 130.2 (d, J_{C-F} = 3.3 Hz), 129.1 (d, J_{C-F} = 8.2 Hz), 124.4, 116.5 (d, J_{C-F} = 21.6 Hz), 64.1, 61.14, 45.6, 30.6, 30.3. ESI-MS m/z: 421 [M + H]$^+$, 443 [M + Na]$^+$. HRMS (ESI) m/z [M + H]$^+$ calcd for [$C_{22}H_{22}FN_6O_2$]$^+$ 421.1783, found 421.1773, [M + Na]$^+$ calcd for [$C_{22}H_{21}FN_6O_2Na$]$^+$ 443.1602, found 443.1593.

*(±)-trans-1-(1-(1H-1,2,4-Triazole-1-carbonyl)piperidin-4-yl)-3-(benzo[d][1,3]dioxol-5-yl)-4-(pyridin-3-yl)azetidin-2-one (**6b**).* The title compound was obtained via general procedure D starting from amine **15b** (50 mg, 0.15 mmol) and 1*H*-1,2,4-triazole (21 mg, 0.30 mmol). Purification: from 4:1 to 2:1 DCM/acetone. Yield: 30%, 20 mg, colorless oil. ^{1}H NMR (300 MHz, $CDCl_3$) δ 8.75 (s, 1H), 8.62 (s, 1H), 8.17 (s, 1H), 7.73 (d, J = 8.0 Hz, 1H), 7.44−7.33 (m, 1H), 7.32−7.13 (m, 1H), 6.84−6.60 (m, 3H), 5.96 (s, 2H), 4.46 (d, J = 1.9 Hz, 1H), 4.00 (d, J = 1.7 Hz, 1H), 3.68−3.53 (m, 1H), 2.83 (dd, J = 39.6, 11.2 Hz, 2H), 2.17−1.79 (m, 4H), 1.67 (d, J = 11.0 Hz, 1H), 1.53−1.34 (m, 1H). ^{13}C NMR (75 MHz, $CDCl_3$) δ 168.6, 150.4, 148.5, 147.6, 134.9, 134.0, 129.3, 128.4, 127.3, 124.2, 122.8, 121.1, 109.0, 107.6, 101.4, 64.6, 63.1, 61.1, 52.3, 46.6, 30.4. ESI-MS m/z: 447 [M + H]$^+$, 469 [M + Na]$^+$. HRMS (ESI) m/z [M + H]$^+$ calcd for [$C_{23}H_{23}N_6O_4$]$^+$ 447.1775, found 447.1764, [M + Na]$^+$ calcd for [$C_{23}H_{22}N_6O_4Na$]$^+$ 469.1595, found 469.1581.

*(±)-trans-1-(1-(1H-1,2,4-Triazole-1-carbonyl)piperidin-4-yl)-3-(4-methoxyphenyl)-4-(pyridin-3-yl)azetidin-2-one (**6c**).* The title compound was obtained via general procedure D starting from amine **15c** (48 mg, 0.15 mmol) and 1*H*-1,2,4-triazole (21 mg, 0.30 mmol). Purification: from 2:1 to 1:1 DCM/acetone. Yield: 32%, 20 mg, colorless oil. ^{1}H NMR (300 MHz, $CDCl_3$) δ 8.75 (s, 1H), 8.65 (s, 2H), 7.97 (s, 1H), 7.76 (d, J = 7.9 Hz, 1H), 7.39 (dd, J = 7.5, 4.7 Hz, 1H), 7.15 (d, J = 8.4 Hz, 2H), 6.90 (d, J = 8.5 Hz, 2H), 4.69−4.34 (m, 3H), 4.11 (d, J = 1.9 Hz, 1H), 3.80 (s, 3H), 3.56−3.39 (m, 1H), 3.26−2.98 (m, 2H), 2.23−1.99 (m, 2H), 1.89 (d, J = 11.2 Hz, 1H), 1.72−1.47 (m, 1H). ^{13}C NMR (75 MHz, $CDCl_3$) δ 168.5, 167.8, 159.5, 152.1, 148.4, 129.8, 128.9, 128.8, 128.3, 126.0, 116.3, 116.0, 114.6, 64.3, 61.0, 55.3, 50.8, 45.4, 30.4. ESI-MS m/z: 433 [M + H]$^+$. HRMS (ESI) m/z [M + H]$^+$ calcd for [$C_{23}H_{25}N_6O_3$]$^+$ 433.1983, found 433.1973, [M + Na]$^+$ calcd for [$C_{23}H_{24}N_6O_3Na$]$^+$ 455.1802, found 455.1790.

*(±)-trans-1-(1-(1H-1,2,4-Triazole-1-carbonyl)piperidin-4-yl)-4-(4-fluorophenyl)-3-(pyridin-3-yl)azetidin-2-one (**6d**).* The title compound was obtained via general procedure D starting from amine **15e** (22 mg, 0.07 mmol) and 1*H*-1,2,4-triazole (17.0 mg, 0.1 mmol). Purification: 1:1 DCM/acetone. Yield: 15%, 4 mg, colorless oil. ^{1}H NMR (400 MHz, $CDCl_3$) δ 8.73 (s, 1H), 8.55 (d, J = 4.7 Hz, 1H), 8.48 (d, J = 1.6 Hz, 1H), 8.18 (s, 1H), 7.95 (s, 1H), 7.60 (d, J = 7.9 Hz, 1H), 7.38 (dd, J = 8.6, 5.2 Hz, 2H), 7.31−7.26 (m, 1H), 7.13 (t, J = 8.5 Hz, 1H), 4.68−4.33 (m, 3H), 4.12 (d, J = 2.0 Hz, 1H), 3.84−3.66 (m, 1H), 3.22−2.97 (m, 2H), 2.09 (dd, J = 11.0, 4.1 Hz, 2H), 1.87 (dd, J = 13.5, 2.2 Hz, 1H), 1.61 (qd, J = 10.1, 2.4 Hz, 1H). ESI-MS m/z: 421 [M + H]$^+$, 443 [M + Na]$^+$.

*(±)-trans-1-(1-(1H-1,2,4-Triazole-1-carbonyl)piperidin-4-yl)-4-(benzo[d][1,3]dioxol-5-yl)-3-(pyridin-3-yl)azetidin-2-one (**6e**).* The title compound was obtained via general procedure D starting from amine **15f** (116 mg, 0.33 mmol) and 1*H*-1,2,4-triazole (78 mg, 0.66 mmol). Purification: 1:1 DCM/acetone. Yield: 23%, 36 mg, colorless oil. ^{1}H NMR (400 MHz, $CDCl_3$) δ 8.71 (d, J = 16.0 Hz, 1H), 8.52 (d, J = 17.5 Hz, 2H), 7.95 (s, 1H), 7.61 (d, J = 7.5 Hz, 1H), 7.37−7.17 (m, 1H), 6.87 (s, 1H), 6.81 (s, 2H), 6.00 (d, J = 2.7 Hz, 2H), 4.63−4.31 (m, 3H), 4.11 (s, 1H), 3.80−3.62 (m, 1H), 3.21−2.95 (m, 2H), 2.20−1.95 (m, 2H), 1.87 (d, 1H), 1.65 (m, 1H). ^{13}C NMR (75 MHz, $CDCl_3$) δ

168.1, 152.2, 149.9, 148.4, 148.3, 147.6, 135.0 (2C), 127.5 (2C), 121.0 (2C), 108.9, 107.5, 101.3, 64.8, 61.1, 51.2, 45.4, 30.7, 30.3. ESI-MS *m/z*: 447 [M + H]$^+$. HRMS (ESI) *m/z* [M + H]$^+$ calcd for [$C_{23}H_{23}N_6O_4$]$^+$ 447.1775 found 447.1763, [M + Na]$^+$; calcd for [$C_{23}H_{22}N_6O_4Na$]$^+$ 469.1595, found 469.1580.

*(±)-trans-1-(1-(1H-Benzo[d][1,2,3]triazole-1-carbonyl)piperidin-4-yl)-3-(4-fluorophenyl)-4-(pyridin-3-yl)azetidin-2-one (**6f**).* The title compound was obtained via general procedure D starting from amine **15a** (117 mg 0.36 mmol) and 1*H*-benzotriazole (85 mg, 0.72 mmol). Purification: from 1:1 PE/EtOAc to 100% EtOAc. Yield: 25%, 42 mg, colorless oil. ^{1}H NMR (300 MHz, $CDCl_3$) δ 8.68 (m, 2H), 8.08 (d, *J* = 8.3 Hz, 1H), 7.95 (d, *J* = 8.3 Hz, 1H), 7.78 (d, *J* = 7.9 Hz, 1H), 7.59 (t, *J* = 7.7 Hz, 1H), 7.48−7.38 (m, 2H), 7.25−7.16 (m, 2H), 7.07 (t, *J* = 8.6 Hz, 2H), 4.55 (d, 3H), 4.16 (d, *J* = 1.9 Hz, 1H), 3.94−3.80 (m, 1H), 3.34−3.12 (m, 2H), 2.29−2.17 (m, 2H), 1.95 (d, *J* = 9.6 Hz, 1H), 1.79−1.66 (m, 1H). ^{13}C NMR (75 MHz, $CDCl_3$) δ 168.2, 162.7 (d, J_{C-F} = 247.4 Hz), 150.9, 149.5, 148.5, 145.6, 134.1, 133.9, 133.4, 130.2 (d, J_{C-F} = 3.4 Hz), 129.7, 129.1 (d, J_{C-F} = 8.2 Hz), 125.6, 124.4, 120.1, 116.4 (d, J_{C-F} = 21.7 Hz), 113.8, 64.1, 61.2, 45.4, 30.7, 30.4. ESI-MS *m/z*: 471 [M + H]$^+$, 493 [M + Na]$^+$.

*(±)-trans-1-(1-(1H-Benzo[d][1,2,3]triazole-1-carbonyl)piperidin-4-yl)-3-(benzo[d][1,3]dixol-5-yl)-4-(piridin-3-yl)azetidin-2-one (**6g**).* The title compound was obtained via general procedure D starting from amine **15b** (116 mg, 0.33 mmol) and 1*H*-benzotriazole (78 mg, 0.66 mmol). Purification: 1:1 PE/EtOAc. Yield: 23%, 37 mg, colorless oil. ^{1}H NMR (300 MHz, $CDCl_3$) 8.66 (s, 2H), 8.08 (d, *J* = 8.3 Hz, 1H), 7.95 (d, *J* = 8.3 Hz, 1H), 7.77 (d, *J* = 7.9 Hz, 1H), 7.59 (t, *J* = 7.2 Hz, 1H), 7.48−7.35 (m, 2H), 6.84−6.66 (m, 3H), 5.97 (s, 2H), 4.65−4.39 (m, 3H), 4.12 (d, *J* = 1.9 Hz, 1H), 3.96−3.79 (m, 1H), 3.36−3.10 (m, 2H), 2.29−2.10 (m, 2H), 2.01−1.85 (m, 1H), 1.79−1.51 (m, 1H). ^{13}C NMR (75 MHz, $CDCl_3$) 168.5, 149.5, 148.6, 147.7, 145.6, 134.0 (2C), 133.4 (2C), 129.7 (2C), 127.9, 125.5, 121.0, 120.1, 113.8, 109.1, 107.6, 101.5, 64.8, 61.4, 51.1, 45.9, 30.4. ESI-MS *m/z*: 497 [M + H]$^+$.

*(±)-trans-1-(1-(1H-Benzo[d][1,2,3]triazole-1-carbonyl)piperidin-4-yl)-3-(4-methoxyphenyl)-4-(pyridin-3-yl)azetidin-2-one (**6h**).* The title compound was obtained via general procedure D starting from amine **15c** (114 mg, 0.35 mmol) and 1*H*-benzotriazole (80 mg, 0.70 mmol). Purification: from 2:1 to 1:1 DCM/acetone. Yield: 27%, 45 mg, colorless oil. ^{1}H NMR (300 MHz, $CDCl_3$) δ 8.65 (s, 2H), 8.08 (d, *J* = 8.3 Hz, 1H), 7.94 (d, *J* = 8.3 Hz, 1H), 7.78 (d, *J* = 8.0 Hz, 1H), 7.59 (t, *J* = 7.4 Hz, 1H), 7.49−7.36 (m, 2H), 7.17 (d, *J* = 8.6 Hz, 2H), 6.90 (d, *J* = 8.6 Hz, 2H), 4.63−4.39 (m, 3H), 4.12 (d, *J* = 1.9 Hz, 1H), 4.00−3.82 (m, 1H), 3.80 (s, 3H), 3.37−3.08 (m, 2H), 2.28−2.08 (m, 2H), 1.94 (d, *J* = 10.3 Hz, 1H), 1.77−1.62 (m, 1H). ^{13}C NMR (75 MHz, $CDCl_3$) δ 168.9, 159.6, 150.7, 149.5, 148.5, 145.6, 134.5, 134.0, 133.4, 129.7, 128.6, 126.4, 125.5, 124.4, 120.1, 114.8, 113.8, 64.4, 61.4, 55.6, 51.0, 45.6, 30.7. ESI-MS *m/z*: 483 [M + H]$^+$. HRMS (ESI) *m/z* [M + H]$^+$ calcd for [$C_{27}H_{27}N_6O_3$]$^+$ 483.2139, found 483.2124, [M + Na]$^+$ calcd for [$C_{27}H_{26}N_6O_3Na$]$^+$ 505.1959, found 505.1943.

*(±)-trans-1-(1-(1H-Benzo[d][1,2,3]triazole-1-carbonyl)piperidin-4-yl)-3-phenyl-4-(pyridin-3-yl)azetidin-2-one (**6i**).* The title compound was obtained via general procedure D starting from amine **15d** (117 mg, 0.38 mmol) and 1*H*-benzotriazole (90 mg, 0.76 mmol). Purification: 1:1 PE/EtOAc Yield: 32%, 55 mg, colorless oil. ^{1}H NMR (300 MHz, $CDCl_3$) 8.67 (d, *J* = 8.3 Hz, 2H), 8.08 (d, *J* = 8.3 Hz, 1H), 7.95 (d, *J* = 8.3 Hz, 1H), 7.79 (d, *J* = 7.0 Hz, 1H), 7.59 (t, *J* = 7.6 Hz, 1H), 7.51−7.29 (m, 4H), 7.26 (m, 3H), 4.75−4.36 (m, 3H), 4.18 (d, *J* = 1.9 Hz, 1H), 3.95−3.82 (m, 1H), 3.38−3.10 (m, 2H), 2.31−2.09 (m, 2H), 1.95 (d, *J* = 13.0 Hz, 1H), 1.81−1.60 (m, 1H). ^{13}C NMR (75 MHz, $CDCl_3$) δ 168.4, 150.8, 149.5, 148.6, 145.6, 134.4, 134.4, 134.0, 133.4, 129.7, 129.4, 128.3, 127.4, 125.5, 124.4, 120.1, 113.8, 64.9, 61.0, 51.1, 45.4, 30.7. ESI-MS *m/z*: 453 [M + H]$^+$. HRMS (ESI) *m/z* [M + H]$^+$ calcd for 453.2034, found 453.2024, [M + Na]$^+$ calcd for $C_{26}H_{24}N_6O_2$ 475.1853 found 475.1842.

*(±)-trans-4-(Benzo[d][1,3]dioxol-5-yl)-1-(piperidin-4-yl)-3-(pyridin-3-yl)azetidin-2-one (**17**).* The title compound was obtained via general procedure A, starting from aldehyde **16** (180 μL, 1.87 mmol). ESI-MS *m/z*: 280 [M + H]$^+$.

*(±)-cis-1-(1-Benzylpiperidin-4-yl)-3-(4-fluorophenyl)-4-(pyridin-4-yl)azetidin-2-one (**18**).* The title compound was obtained via general procedure B starting from imine **17** (523 mg, 1.87 mmol) and 4-fluorophenylacetic acid (432 mg, 2.81 mmol). Purification: from 3:1 to 1:1 PE/EtOAc. Yield 23%, 179 mg, yellow oil. ^{1}H NMR (300 MHz, $CDCl_3$) δ 8.37 (d, *J* = 4.8 Hz, 2H), 7.26 (s, 5H), 7.03−6.89 (m, 4H), 6.78 (t, *J* = 8.5 Hz, 2H), 4.99 (d, *J* = 5.7 Hz, 1H), 4.81 (d, *J* = 5.6 Hz, 1H), 3.73−3.57 (m, 1H), 3.46 (s, 2H), 2.87 (dd, *J* = 30.5, 13.5 Hz, 2H), 2.09−1.87 (m, 4H), 1.77 (d, *J* = 12.7 Hz, 1H), 1.67−1.45 (m, 1H). ESI-MS *m/z*: 416 [M + H]$^+$.

*(±)-cis-3-(4-Fluorophenyl)-1-(piperidin-4-yl)-4-(pyridin-4-yl)-azetidin-2-one (**19**).* The title compound was obtained via general procedure C starting from **18** (80 mg, 0.19 mmol). ESI-MS *m/z*: 326 [M + H]$^+$.

*(±)-cis-1-(1-(1H-1,2,4-Triazole-1-carbonyl)piperidin-4-yl)-3-(4-fluorophenyl)-4-(pyridin-4-yl)azetidin-2-one (**6j**).* The title compound was obtained via general procedure D starting from amine **19** (56 mg, 0.17 mmol) and 1*H*-1,2,4-triazole (42 mg, 0.26 mmol). Purification: 1:1 PE/EtOAc. Yield 23%, 16 mg, amorphous white solid. ^{1}H NMR (300 MHz, $CDCl_3$) δ 8.76 (s, 1H), 8.41 (d, *J* = 4.8 Hz, 2H), 7.97 (s, 1H), 7.05−6.89 (m, 4H), 6.80 (t, *J* = 8.5 Hz, 2H), 5.02 (d, *J* = 5.8 Hz, 1H), 4.86 (d, *J* = 5.8 Hz, 1H), 4.73−4.41 (m, 2H), 3.95−3.77 (m, 1H), 3.24−2.99 (m, 2H), 2.21 (d, *J* = 9.5 Hz, 1H), 2.13−1.94 (m, 2H), 1.73−1.56 (m, 1H). ESI-MS *m/z*: 421 [M + H]$^+$, 443 [M + Na]$^+$.

*tert-Butyl-(1-(1H-1,2,4-triazole-1-carbonyl)piperidin-4-yl)-carbamate (**21**).* 1,1′-Carbonyl-ditriazole (370 mg, 2.25 mmol) was added to a stirred solution of 4-Boc-aminopiperidine **20** (300 mg, 1.50 mmol) in dry DCM (15 mL), and the reaction was stirred at rt for 12 h. Solvent was removed under reduced pressure and the residue was purified by means of chromatography on silica gel 1:1 EtOAc/PE to afford title compound (yield: 84%, 370 mg) as an amorphous white sold. ^{1}H NMR (300 MHz, $CDCl_3$) δ 8.70 (s, 1H), 7.92 (s, 1H), 4.68 (d, *J* = 7.4 Hz, 1H), 4.48−4.21 (m, 2H), 3.71−3.50 (m, 1H), 3.12 (m, 2H), 2.00 (d, *J* = 11.9 Hz, 2H), 1.53−1.41 (m, 2H), 1.37 (s, 9H). ESI-MS *m/z*: 296 [M + H]$^+$, 318 [M + Na]$^+$.

*(4-Aminopiperidin-1-yl)(1H-1,2,4-triazol-1-yl)methanone (**22**).* To a stirred solution of intermediate **21** (370 mg, 1.26 mmol) in MeOH (5 mL), a solution of 1 M HCl in MeOH (3.0 mL) was added, and the solvent was removed under reduced pressure at 40 °C. The solid residue was suspended in DCM and washed with 1N $NaHCO_3$ aqueous solution. The organic layer was dried over Na_2SO_4, filtered, and evaporated. The title compound was used in the next step with any further purification (quantitative yield). ^{1}H NMR (300 MHz, $CDCl_3$) δ 8.76 (s, 1H), 7.99 (s, 1H), 4.59- 4.23 (m, 2H), 3.19 (t, *J* = 11.6 Hz, 2H), 3.10−2.93 (m, 1H), 1.95 (d, *J* = 13.1 Hz, 2H), 1.57−1.34 (m, 4H). ESI-MS *m/z*: 196 [M + H]$^+$, 218 [M + Na]$^+$.

*(4-((Benzo[d][1,3]dioxol-5-ylmethylene)amino)piperidin-1-yl)-(1H-1,2,4-triazol-1-yl)methanone (**23**).* Title compound was obtained via general procedure A, starting from intermediate **22** (274 mg, 1.26 mmol) and (3,4-methylendioxy)benzaldehyde (190 mg, 1.26 mmol). ESI-MS *m/z*: 328 [M + H]$^+$, 350 [M + Na]$^+$.

*(±)-(4-(trans-3-(Benzo[d][1,3]dioxol-5-yl)-1,1-dioxido-4-phenyl-1,2-thiazetidin-2-yl)piperidin-1-yl)(1H-1,2,4-triazol-1-yl)methanone (**7a**).* To a cooled (−5 °C) solution of phenylmethanesulfonyl chloride (120 mg, 0.63 mmol) in dry THF (2 mL), a solution of imine **23** (413 mg, 1.26 mmol) in dry THF (5 mL) was added dropwise. The reaction was stirred at −5 °C for 24 h and then 48 h at 25 °C. The solution was filtered and the solvent was removed under reduced pressure. The crude was purified by means of chromatography on silica gel (5:1 PE/EtOAc) to afford title compound (yield: 15%, 10 mg) as an amorphous white solid. ^{1}H NMR (300 MHz, $CDCl_3$) δ 8.75 (s, 1H), 7.97 (s, 1H), 7.49−7.34 (m, 5H), 7.05 (s, 1H), 6.86 (d, *J* = 7.9 Hz, 1H), 6.75 (d, *J* = 8.0 Hz, 1H), 5.99 (s, 2H), 5.12 (d, *J* = 6.9 Hz, 1H), 4.49−3.97 (m, 3H), 3.78−3.57 (m, 1H), 3.46 (br s, 1H), 3.28 (br s, 1H), 2.23−2.10 (m, 1H), 2.08−1.93 (m, 1H), 1.85−1.73 (m, 1H), 1.65−1.55 (m, 1H). ^{13}C NMR (75 MHz, $CDCl_3$) δ 152.3, 148.9, 148.8, 148.7, 146.8, 131.1, 130.1, 129.3, 128.2, 120.7, 108.9, 106.5, 101.8, 83.5, 59.2, 54.6, 44.2, 31.1, 29.3. ESI-MS *m/z*: 482 [M + H]$^+$, 504 [M + Na]$^+$.

*(±)-trans-4-(Benzo[d][1,3]dioxol-5-yl)-3-(4-fluorophenyl)-1-(piperidin-4-yl)azetidine-2-thione (**24**).* A solution of amine **11n** (50 mg, 0.14 mmol) and Lawesson's reagent (170 mg, 0.42 mmol) in dry toluene (5 mL) was heated at 90 °C for 2 h. The solvent was removed

https://doi.org/10.1021/acs.jmedchem.3c01278
J. Med. Chem. 2024, 67, 1758−1782

under reduced pressure, and the crude was taken up with $NaHCO_3$ saturated solution. The aqueous phase was extracted with DCM (3 × 10 mL) and the combined organic layers were dried over Na_2SO_4, filtered, and evaporated. The crude compound was used in the following step with no further purification. Quantitative yield. ESI-MS m/z: 385 $[M + H]^+$, 407 $[M + Na]^+$.

*(±)-trans-1-(1-(1H-1,2,4-Triazole-1-carbonothioyl)piperidin-4-yl)-4-(benzo[d][1,3]dioxol-5-yl)-3-(4-fluorophenyl)azetidin-2-one (**7b**).* The title compound was obtained via general procedure D starting from amine **11m** (60 mg, 0.16 mmol), 1*H*-1,2,4-triazole (22 mg, 0.32 mmol) and using thiophosgene (25 μL, 0.32 mmol). Purification: 2:1 PE/EtOAc. Yield: 45%, 35 mg, colorless oil. ^{1}H NMR (300 MHz, $CDCl_3$) δ 8.85 (s, 1H), 7.97 (s, 1H), 7.28−7.17 (m, 3H), 7.04 (t, *J* = 8.6 Hz, 2H), 6.95−6.70 (m, 2H), 6.02 (s, 2H), 4.39 (d, *J* = 1.8 Hz, 1H), 4.09 (d, *J* = 1.8 Hz, 1H), 3.95−3.74 (m, 2H), 3.58−3.26 (m, 2H), 2.31−2.13 (m, 2H), 2.00−1.89 (m, 1H), 1.77 (qd, *J* = 11.6, 4.4 Hz, 2H). ESI-MS m/z: 480 $[M + H]^+$.

*(±)-(4-(trans-2-(Benzo[d][1,3]dioxol-5-yl)-3-(4-fluorophenyl)-4-thioxoazetidin-1-yl)piperidin-1-yl)(1H-1,2,4-triazol-1-yl)methanone (**7c**).* The title compound was obtained via general procedure D starting from amine **24** (45 mg, 0.12 mmol), 1*H*-1,2,4-triazole (17 mg, 0.24 mmol). Purification: 2:1 PE/EtOAc. Yield: 55%, 30 mg, colorless oil. ^{1}H NMR (300 MHz, $CDCl_3$) δ 8.75 (s, 1H), 7.97 (s, 1H), 7.24 (m, 2H), 7.04 (t, *J* = 8.5 Hz, 2H), 6.90−6.77 (m, 2H), 6.03 (s, 2H), 4.82 (d, *J* = 1.8 Hz, 1H), 4.51 (t, *J* = 11.7 Hz, 2H), 4.06 (d, *J* = 1.8 Hz, 1H), 3.25−2.87 (m, 2H), 2.24 (d, *J* = 12.4 Hz, 1H), 2.02−1.76 (m, 2H), 1.58−1.36 (m, 2H). ESI-MS m/z: 480 $[M + H]^+$.

*(±)-trans-1-(1-(1H-1,2,4-Triazole-1-carbonothioyl)piperidin-4-yl)-4-(benzo[d][1,3]dioxol-5-yl)-3-(4-fluorophenyl)azetidine-2-thione (**7d**).* The title compound was obtained via general procedure D starting from amine **24** (45 mg, 0.12 mmol), 1*H*-1,2,4-triazole (17 mg, 0.24 mmol) and using thiophosgene solution (20 μL, 0.24 mmol). Purification: 2:1 PE/EtOAc. Yield: 42%, 25 mg, amorphous white solid. ^{1}H NMR (300 MHz, $CDCl_3$) δ 8.87 (s, 1H), 7.97 (s, 1H), 7.36−7.18 (m, 3H), 7.05 (t, *J* = 8.6 Hz, 2H), 6.96−6.76 (m, 2H), 6.03 (s, 2H), 4.83 (d, *J* = 1.7 Hz, 1H), 4.58 (t, *J* = 11.8 Hz, 2H), 4.07 (d, *J* = 1.7 Hz, 1H), 3.41−3.12 (m, 2H), 2.41−2.17 (m, 1H), 2.10−1.80 (m, 2H), 1.67−1.55 (m, 2H). ESI-MS m/z: 496 $[M + H]^+$.

Enzymatic Assays. *FAAH Inhibition Assays.* The effect of compounds on FAAH activity was studied as previously described.[43] AEA hydrolysis was measured by testing the compounds on different enzyme sources (the fresh prepared 10000 g membrane fraction of rat brain [70 μg per sample], and the commercially available human recombinant FAAH [Cayman, 2 μg per sample]). Compounds were coincubated with the enzyme in Tris−HCl 50 mM, at pH 9.5 at 37 °C for 30 min with synthetic *N*-arachidonoyl-[^{14}C]-ethanolamine (55 mCi per mmol, ARC St. Louis, MO) properly diluted with AEA (Tocris Bioscience, Avonmouth, Bristol, UK). In a parallel set of experiments, compounds were preincubated 20 min at 37 °C with the enzyme before adding the [^{14}C]-substrate. The reaction was terminated by organic extraction with ice-cold chloroform/methanol (1:1, vol:vol) and the aqueous phase containing [^{14}C]-ethanolamine was measured by scintillation counting. All data are expressed as the concentration exerting 50% inhibition of [^{14}C]-AEA hydrolysis (IC_{50}) calculated by fitting sigmoidal concentration response curves by Prism (GraphPad Software 9.3.1). Values indicate means of three independent experiments conducted in triplicate.

MAGL Inhibition (Method A). The effect of compounds on MAGL activity was studied as previously described.[28] 2-AG hydrolysis was measured by testing compounds on different enzyme sources (the fresh prepared 10000 g cytosolic fraction of COS-7 cells [100 μg per sample] and the commercially available human recombinant MAGL [Cayman, 10 μg per sample]). Compounds were coincubated with the enzyme in Tris−HCl 50 mM, at pH 7.0 at 37 °C for 20 min and synthetic 2-arachidonoyl-[^{3}H]-glycerol (40 Ci/mmol, ARC St. Louis, MO, USA) properly diluted with 2-AG (Cayman Chemicals, Ann Arbor, MI, USA). In a parallel set of experiments, compounds were preincubated 10 min at 37 °C with the enzyme before adding the [^{3}H]-substrate. After incubation, the amount of [^{3}H]-glycerol produced was measured by scintillation counting of the aqueous phase after extraction of the incubation mixture with 2 volumes of $CHCl_3$/MeOH 1:1 (by volume). All data are expressed as the concentration exerting 50% inhibition of [^{3}H]-2-AG hydrolysis (IC_{50}) calculated by fitting sigmoidal concentration response curves by Prism (GraphPad Software 9.3.1). Values indicate means of three independent experiments conducted in triplicate.

MAGL Inhibition (Method B). *In vitro* MAGL activity was measured as previously described.[44] Briefly, either 10 ng of purified MAGL or 2.5−50 μg of protein from MAGL-transfected HeLa cell lysates were preincubated with inhibitors for 10 min at 37 °C in assay buffer (50 mM Tris-HCl, pH 8.0, 0.5 mg·mL^{-1} bovine serum albumin, fatty acid-free). Following preincubation, 2-oleoylglycerol (2-OG) substrate (10 μM final) was added, and samples were incubated for an additional 30 min at 37 °C. Reactions were stopped with chloroform:methanol (2:1, vol:vol), containing heptadecanoic acid (5 nmol) as an internal standard. Samples were subjected to centrifugation at 2000*g* at 4 °C for 10 min, and the organic layers were collected and dried under a stream of N_2. The residues were suspended in chloroform:methanol (1:3, vol:vol) and the amount of MAGL product, oleic acid, was determined by liquid chromatography/mass spectrometry (LC/MS).

MAGL IC_{50} Measurement. The IC_{50} values of the described ligands were measured using *human*, or *mouse* MAGL.[45,46] Briefly, the compound was prepared in 12 concentrations ranging from 12.5 μM to 0.8 pM. The reaction was carried out in a 384-well plate containing 9 pL of MAGL in assay buffer (50 mM TRIS (GIBCO, 15567−027), 1 mM EDTA (Fluka, 03690), 0.01% Tween, v/v). After incubating with 1 pL compound in various concentrations at room temperature for 15 min, 10 pL of 2-AG in assay buffer was added to initialize the hydrolysis. The plate was incubated at room temperature with gentle shake for further 30 min, followed by the addition of 40 pL of acetonitrile containing 4 pM d_8-arachidonic acid (AA) to quench the reaction. The hydrolytic rate of the enzyme was monitored by an online solid phase extraction (SPE) system (Agilent Rapidfire) coupled to a triple quadrupole mass spectrometry (Agilent 6460) in ESI$^-$ mode, and determined by the intensity of AA (m/z = 303.1−259.1) to d_8-AA (m/z = 311.1−267.0). The IC_{50} values were obtained after fitting the intensity of the AA/d_8-AA under various concentrations into saturation equation. The measured individual IC_{50} values are provided in the Supporting Information.

Receptor Binding Assays. *CB2 by TR-FRET Studies.* Competition binding. To determine the affinity of the MAGL inhibitors, we used a simple competition binding assay approach. The assay buffer used in these experiments consisted of Hanks Balanced Salt Solution (HBSS) containing 0.5% BSA and 5 mM HEPES. fluorescent ligand (700 nM) and increasing concentrations of the competitor are simultaneously added to the CB2R membrane preparation (1 μg total protein per well) in a 40 μL of assay buffer in a 384-well plate incubated at ambient temperature with orbital mixing. The degree of fluorescent ligand bound to the receptor was assessed at equilibrium by HTRF detection. Nonspecific binding was determined as the amount of HTRF signal detected in the presence of SR144528 (1 μM) and was subtracted from total binding, to calculate specific binding for the construction of IC_{50} curves and calculation of affinity values (eqs 1 and 2).

Signal detection and data analysis. Signal detection was performed on a Pherastar FSX (BMG Labtech, Offenburg, Germany). The terbium cryptate donor was always excited with four laser flashes at a wavelength of 337 nm. Time-resolved Forster resonance energy transfer (TR-FRET) signals were collected at 520 (acceptor) and 620 nm (donor surrogate), using the NBD-based fluorescent ligand. Homogeneous time-resolved fluorescence (HTRF) ratios were obtained by dividing the acceptor signal by the donor signal and multiplying this value by 10 000. All experiments were analyzed by nonlinear regression using Prism 9.0 (GraphPad Software, San Diego, USA). Normalized competition displacement binding data were fitted to sigmoidal (variable slope) curves using a "four-parameter logistic equation", The top was fixed to 100, and the bottom to zero, and the Hill coefficient was fixed to −1:

$$Y = \text{bottom} + (\text{top} - \text{bottom})/(1 + 10^{(\log IC50 - X)} \times \text{Hill slope}) \quad (1)$$

https://doi.org/10.1021/acs.jmedchem.3c01278
J. Med. Chem. 2024, 67, 1758−1782

IC_{50} values obtained from the inhibition curves were converted to K_i values using the method of Cheng and Prusoff.

$$K_i = IC_{50}/(1 + [\text{fluorescent tracer concentration}]/K_d) \quad (2)$$

Activity-Based Proteomic Profiling (ABPP) Assay. *Sample Preparation.* Male mouse brain (27 weeks old, C57BI/6J) was homogenized with glass beads (2 × 1 min, bullet blender, speed 8) using cold lysis buffer (20 mM HEPES pH 7.2, 1 mM $MgCl_2$, 2 U/mL benzonase). Membrane and cytosol were separated by centrifugation. Membrane fraction was resuspended in HEPES/DTT buffer (20 mM HEPES pH 7.2, 2 mM DTT). Protein concentration was determined with Bradford Assay, and samples were diluted in HEPES/DTT buffer to a final concentration of 2.0 mg/mL. Samples were snap frozen in liquid nitrogen and stored at −80 °C until further use.

Gel-Based ABPP. Samples of cytosol and membrane fraction were thawed on ice. Samples were divided over tubes and incubated with either vehicle (2.5% DMSO), JZL-184 (10 μM, final concentration), (±)-**4**, (±)-**5v**, or (3*R*, 4*S*)-**5v** (1 or 0.1 μM, final concentration) for 30 min at room temperature. Samples were then incubated with the probe cocktail (MB064 100 nM final and FP-Bodipy 100 nM final) for 10 min at RT.[47] The reaction was quenched with 4× Laemmli buffer for 30 min at room temperature. Samples were resolved by SDS-PAGE (10% AA gel, 15 slots, 0.75 mm, 75 min, 180 V) along with a protein marker. In-gel fluorescence was measured in the Cy3- (MB064, 120 s), Cy2-(FP-Bodipy, 80 s) and Cy5 (Marker, 10 s) channel. Gels were stained with Coomassie for 10 min after scanning and distained overnight in DEMI water for protein loading control.

Time Course and Dilution Assays. For preincubation time course experiment, samples containing MAGL were preincubated with inhibitors for the indicated time at 37 °C in assay buffer (50 mM Tris-HCL, pH 8.0, 0.5 mg mL^{-1} bovine serum albumin, fatty acid-free). Following preincubation, 2-oleoylglycerol (2-OG) substrate (10 μM final) was added, and samples were incubated for an additional 30 min at 37 °C. MAGL activity was determined by LC/MS quantitation of oleic acid. Rapid dilution assays were performed as described by King et al.[48] and Copeland.[49] Briefly, samples containing MAGL (100-fold concentrated compared with standard assays) were preincubated with 10-fold the IC_{50}-equivalent concentration of the azetidin-2-one-based compounds (±)-**5c**, (±)-**5d**, (±)-**5v**, (±)-**4**, or the vehicle (DMSO, final concentration 1%) for 20 min at 37 °C. Samples were then diluted 100-fold with assay buffer containing substrate to initiate reactions, and the time course of product formation over a 60 min period was measured by LC/MS ($n = 3$).

Crystallization, Data Collection, and Structure Determination of the Human MAGL in Complex with Compounds (±)-5d, (±)-5l, and (±)-5r. Human MAGL protein (1−303) with mutations Lys36Ala, Leu169Ser, and Leu176Ser[23] was concentrated to 10.8 mg/mL. Crystallization trials were performed in sitting drop vapor diffusion setups at 21 °C. Crystals appeared within 2 days out of 0.1 M MES pH 6.5, 6−13% PEG MME 5K, 12% 2-propanol. Crystals were soaked for 16 h in crystallization solution supplemented with 10 mM of each compound.

For data collection, crystals were flash cooled at 100 K with 20% ethylene glycol as cryo- protectant added to the soaking solution. X-ray diffraction data were collected using a DECTRIS Pilatus 6 M detector at the beamline X10SA of the Swiss Light Source (Villigen, Switzerland). Data have been processed with XDS[50] and scaled with SADABS (BRUKER). The crystals belong to space group $C222_1$ diffract to resolutions between 1.51−1.73 Å. The structures were determined by molecular replacement with PHASER[51] using the coordinates of PDB 3pe6[23] as search model. Difference electron density was used to place each compound. The structures were refined with programs from the CCP4 suite[52] and BUSTER.[53] Model building was done with COOT.[54] Data collection and refinement statistics are summarized in SI, Table S2. The coordinates of the structures were deposited in the PDB under the accession codes 8PTC, 8PTQ, and 8PTR.

Computational Studies. 3D structures of the ligands used in this work were built in Maestro (Maestro release 2018, Schrödinger, LLC, New York, NY, 2018). Energy minimization was performed using MacroModel application with the OPLS-2005 force field, employing the GBSA model to mimic the solvent effect, with "no cutoff" for nonbonded interactions. The PRCG method (5000 maximum iterations and threshold for gradient convergence = 0.001) was used to minimize the potential energy. The resulting compounds were treated using LigPrep software (LigPrep release 2018, Schrödinger, LLC, New York, NY, 2018) to provide the most probable ionization state at physiological pH (7.4 ± 0.2).

The experimentally solved 3D structure of the MAGL enzyme in complex with (±)-**5d** was used for docking studies [*h*MAGL (PDB 8PTC)], while the other related MAGL enzymes were downloaded from Alphafold [*cyno*MAGL (Alphafold model entry A0A2K5 V664, blue cartoon), *m*MAGL (Alphafold model entry O35678, green cartoon), and *r*MAGL (Alphafold model entry Q8R431, green cartoon)]. The first step was to break the covalent bond between S122 and the crystallized derivative to restore the native arrangement of the enzyme. To prepare the protein for computational experiments, we applied the Protein Preparation Wizard protocol available in Maestro for performing various computational steps to (1) add hydrogens, (2) optimize the orientation of hydroxyl groups of residues, Asn, and Gln, and the protonation state of His, and (3) perform a constrained minimization refinement using the impref utility. Finally, a restrained minimization was accomplished using the Impact Refinement (impref) module to optimize the geometry and minimize the enzyme energy. The minimization was terminated when the energy converged, or the root-mean-square deviation (RMSD) reached a maximum cutoff of 0.30 Å. The other enzymes in this study, *r*FAAH (PDB 3PPM), *h*ABDH6 (PDB 7OTS), and *h*LYPLA2 (PDB 5SYN), were treated using the Protein Preparation Wizard protocol.

Glide software (Glide release 2020, Schrödinger, LLC, New York, NY, 2020) employing the XP scoring function was used to perform all docking studies conducted in this work, The energy grid for docking was prepared using the default value of the protein atom-scaling factor (1.0 Å), with a cubic box centered on the crystallized ligand if present or on the catalytic residues if the ligand was not present. The docked poses considered for the postdocking minimization step were 1000.

Analysis of Metabolic Profiles. *Kinetic Lyophilization Solubility Assay (LYSA).* The test was performed as previously described.[55] The solubility of a test compound in phosphate buffer at pH 6.5 from evaporated DMSO stock solution is measured over time, resulting in the kinetic solubility of the compound. Samples were prepared in duplicate from 10 mM DMSO stock solutions. DMSO was evaporated (1 h) with a centrifugal vacuum evaporator (Genevac Technologies). The residue was dissolved in 0.05 M phosphate buffer (pH 6.5), stirred for 1 h, and shaken for 2 h. Twelve hours later, the solutions were filtered using a microtiter filter plate (Millipore MSDV N65). The filtrate and its 1:10 dilution were analyzed by direct UV measurement or by HPLC-UV. A four-point calibration curve was prepared from the 10 mM DMSO stock solutions and used to determine the solubility of the compounds. Starting from 10 mM stock solution, the measurement range for molecular weight 500 was 0−666 μg/mL.

Microsomal Clearance. For human and mice, pooled commercially available microsome preparations from liver tissues were used (BD UltraPool HLM 150).[56] For human, ultrapooled (150 mixed gender donors) liver microsomes were purchased to account for the biological variance *in vivo*. For the microsome incubations, 96-deep-well plates were applied, which are incubated at 37 °C on a TECAN liquid handling system (Tecan Group Ltd., Switzerland) equipped with Te-Shake shakers and a warming device (Tecan Group Ltd., Switzerland). The incubation buffer was 0.1 M phosphate buffer at pH 7.4. The NADPH regenerating system consisted of 30 mM glucose-6-phosphate disodium salt hydrate; 10 mM NADP; 30 mM $MgCl_2 \cdot 6H_2O$; and 5 mg/mL glucose-6-phosphate dehydrogenase (Roche Diagnostics) in 0.1 M potassium phosphate buffer pH 7.4.

Incubations of a test compound at 1 μM in microsome incubations of 0.5 mg/mL plus cofactor NADPH were performed in 96-well plates at 37 °C. After 1, 3, 6, 9, 15, 25, 35, and 45 min, 40 μL incubation solutions are transferred and quenched with 3:1 (v/v) acetonitrile containing internal standards. Samples were then cooled and centrifuged before analysis by LC-MS/MS. Log peak area ratios (test compound peak area/internal standard peak area) were plotted against incubation time

https://doi.org/10.1021/acs.jmedchem.3c01278
J. Med. Chem. 2024, 67, 1758−1782

using a linear fit. The calculated slope was used to determine the intrinsic clearance: Cl_{int} (μL/min/mg protein) = −slope (min^{-1}) × 1000/[protein concentration (mg/mL)].

Hepatocyte Clearance. Hepatocyte clearance was determined for compounds (±)-**5d**, (±)-**5v**, and (±)-**4** as reported in our previous work.[55] Briefly, for animals, hepatocyte suspension cultures were either freshly prepared by liver perfusion or prepared from cryopreserved hepatocyte batches. For human, commercially available, pooled (5−20 donors), cryopreserved human hepatocytes from nontransplantable liver tissues were used.[57] For suspension cultures, Nunc U96 PP-0.5 mL (Nunc Natural, 267245) plates were incubated in a Thermo Forma incubator from Fischer Scientific (Wohlen, Switzerland) equipped with shakers from Variomag Teleshake shakers (Sterico, Wangen, Switzerland) for maintaining cell dispersion. The cell culture medium was William's media supplemented with glutamine, antibiotics, insulin, dexamethasone, and 10% FCS.

Test compounds were incubated at a concentration of 1 μM in 96 well plates containing suspension cultures 1×10^6 hepatocytes/mL (∼1 mg/mL protein concentration). Plates were shaken at 900 rpm for up to 2 h in a 5% CO_2 atmosphere and 37 °C. After 3, 6, 10, 20, 40, 60, and 120 min, the 100 μL cell suspension in each well was quenched with 200 μL of methanol containing an internal standard. Samples are then cooled and centrifuged before analysis by LC-MS/MS.

Log peak area ratios (test compound peak area/internal standard peak area) or concentrations were plotted against incubation time and a linear fit made to the data with emphasis upon the initial rate of compound disappearance. The slope of the fit was then used to calculate the intrinsic clearance: Cl_{int} (μL/min/1×10^6 cells) = −slope (min^{-1}) × 1000/[1×10^6 cells].

P-Glycoprotein-Mediated Efflux Ratios.[45] The experimental procedure for *in vitro* transport studies with compounds (±)-**5d**, (±)-**5v**, and (±)-**4** was described as previously reported.[58,59] Porcine kidney epithelial LLC-PK1 cells stably transfected with Abcb1a (Mdr1a, mouse P-gp) or Abcb1 (Mdr1, P-gp) were provided by Dr. A. Schinkel (Netherlands Cancer Institute). The cells were cultured with Medium 199 Glutamax (Gibco/Life Technologies) supplemented with 10% fetal bovine serum, 1% penicillin/streptomycin (Amimed, Basel, CH), and 100 ng/mL colchicine (SERVA Electrophoresis Gmbh, Heidelberg, DE) at 37 °C in a humidified 5% CO_2 incubator, and seeded at a density of 1.4×10^5 cells/well on porous poly(ethylene terephthalate) membrane filters 4 days prior to the experiment. On the experimental day, the culture medium was removed from barrier between apical (A) and basolateral (B) compartments and replaced with medium without phenol red. The measurement of transcellular transport was triggered by the addition of 1 μM of the tested compounds to the donor side, corresponding to a total volume of 100 μL on the apical side or 240 μL on the basolateral side, and carried out in both apical-to-basolateral (A → B) and basolateral-to-apical (B → A) directions in triplicates. The resulting inserts were incubated at 37 °C and 5% CO_2 for 3 h. Samples (20 μL) were taken from both donor and receiver sides at the end of the incubation, and the concentration of the test compound was determined by high performance liquid chromatography−tandem mass spectrometry. The apparent permeability (P_{app}) in the basolateral-to-apical direction ($P_{app}^{B\to A}$) and apical-to-basolateral direction ($P_{app}^{A\to B}$) were calculated. The efflux ratios of the compounds were determined as the ratio of $P_{app}^{B\to A}$ to $P_{app}^{A\to B}$. The cell lines were passaged at least three times before the experiments. To ensure Mdr1a functionality, the efflux ratio of ^{3}H-digoxin, a typical Mdr1a substrate, was measured in each incubation plate as a control using scintillation counting. Additionally, the tightness of the cell monolayer was controlled by extracellular marker (Lucifer yellow, Sigma-Aldrich, St. Louis, MO) and quantified using Spectrafluor Plus Reader at 430/535 nm excitation/emission.

Cytochrome P450 (CYP) 3A4, 2C9, and 2D6 Inhibition Assay. The experiments aim to allow some estimation of drug−drug interaction risk, where a compound inhibits one or more cytochrome P450 (CYP) enzymes that are responsible for the metabolism of a comedicated drug molecule. The assays typically generate two end points: IC_{50} value (μM) and percent inhibition at defined or highest acceptable test concentration (typically 50 μM, lower if highest concentration data rejected due to insolubility). Experimental details of the MS-based method have been previously described.[60]

Cell Toxicity and Mutagenicity (Ames Test) Assays. *Cytotoxicity Assays.* This test was performed as described previously.[30] Briefly, for the cytotoxicity assays were performed on mouse immortalized fibroblasts NIH3T3 purchased from the American Type Culture Collection (USA). NIH3T3 cells were maintained in DMEM at 37 °C in a humidified atmosphere containing 5% CO_2. The culture media were supplemented with 10% fetal calf serum (FCS), 1% L-glutamine−penicillin−streptomycin solution, and 1% MEM Non-Essential Amino Acid Solution. Once at the confluence, cells were washed with PBS 0.1 M, taken up with trypsin-EDTA solution, and then centrifuged at 1000 rpm for 5 min. The pellet was resuspended in medium solution (dilution 1:15). The stock solution for each compound was prepared in pure DMSO and diluted with complete culture medium. The solution/suspension obtained was then added to the cell monolayer. Cell viability after 24 h of incubation with the different concentrations of each test compound was evaluated by Neutral Red Uptake by the procedure previously reported.[61] The data processing included the Student's *t* test with $p < 0.05$ taken as the significance level. Three solutions were prepared to determine the percentage of viable cells: (i) Neutral Red (NR) stock solution, 0.33 g of NR dye powder in 100 mL of sterile H_2O; (ii) NR medium, 1.0 mL of NR stock solution +99.0 routine culture medium prewarmed to 37 °C; (iii) NR Desorb solution, 1% glacial acetic acid solution + 50% ethanol + 49% H_2O. After incubation, the routine culture medium was removed from each well, and cells were carefully rinsed with 1 mL of prewarmed D-PBS. Multiwells were then gently blotted with paper towels. NR medium (1.0 mL) was added to each well and further incubated at 37 °C, 95% humidity, and 5.0% CO_2 for 3 h. The cells were checked during the NR incubation for NR crystal formation. After incubation, the NR Medium was removed; cells were carefully rinsed with 1 mL of prewarmed D-PBS. Then, the PBS was decanted and blotted from the wells, and exactly 1 mL of NR Desorb solution was added to each sample. Multiwells were then put on a shaker for 20−45 min to extract NR from the cells and form a homogeneous solution. During this step, the samples were covered in order to protect them from light. Five minutes after the plate shaker removal, the absorbance was read at 540 nm by a UV/visible spectrophotometer (Lambda 25, PerkinElmer).

Mutagenicity Assay: Ames Test. Mutagenetic assays was performed as previously reported.[30] Briefly, TA100 and TA98 strains of *Salmonella typhimurium* and S9 fraction were utilized for the mutagenicity assay. Approximately 107 bacteria were exposed to six concentrations of each test compound, as well as a positive and negative control, for 90 min in a medium containing sufficient histidine to support approximately two cell divisions. After 90 min, the exposure cultures were diluted in a pH indicator medium lacking histidine and aliquoted into 48 wells of a 384-well plate. Within 2 days, cells that had undergone the reversion to His grew into colonies. Metabolism by the bacterial colonies reduced the pH of the medium, changing the color of that well. This color change can be detected visually or by a microplate reader. The number of wells containing reverting colonies were counted for each dose and compared to a zero dose control. Each dose was tested in six replicates. The test was performed both with and without S9 fraction.

Evaluation of Endocannabinoid Levels after *in Vivo* Treatment in Brain. All procedures met the National Institute of Health guidelines for the care and use of laboratory animals and were approved by the Institutional Animal Care and Use Committee at University of California, Irvine. We dissolved compounds (±)-**5c**, (±)-**5d**, and (±)-**5v**, and (±)-**4** in DMSO. JZL-184 (Cayman Chemicals, Ann Arbor, MI, USA) was solubilized in PEG/Tween (4:1). Drugs were intraperitoneally injected to adult male mice. After 1 h from the injection, mice were killed and the brains were taken, cut by half, and immediately frozen for MAGL activity assay and lipid measurement using LC-MS. Procedures for quantitation of endocannabinoid lipids were described previously.[62] Briefly, a half brain sample was homogenized in cold methanol containing the following internal standards: $^2H_4$-anandamide ($^2H_4$-AEA), $^2H_4$-oleoylethanolamide ($^2H_4$−OEA), $^2H_4$-palmitoylethanolamide ($^2H_4$−PEA), $^2H_8$-2-arachidonoyl-*sn*-glycerol ($^2H_8$-2-AG), and [$^2H_8$]-arachidonic acid (Cayman

https://doi.org/10.1021/acs.jmedchem.3c01278
J. Med. Chem. 2024, 67, 1758−1782

Chemicals). Lipids were extracted by adding chloroform and water (2:1, vol:vol) and fractionated through open-bed silica gel columns by progressive elution with chloroform/methanol mixtures. Fractions eluted from the columns were dried under N_2, reconstituted in chloroform/methanol (1:4, vol:vol; 0.1 mL) and subjected to LC/MS.

For monoacylglycerols (MG) and fatty acid ethanolamides (FAE), we used an Agilent 1100-LC system coupled to a 1946D-MS detector equipped with an electrospray ionization (ESI) interface (Agilent Technologies, Inc., Palo Alto, CA, USA). Lipids were separated on a reversed-phase XDB Eclipse C18 column (50 mm × 4.6 mm inner diameter, 1.8 μm, Zorbax, Agilent Technologies). They were eluted with a gradient of methanol in water (from 85% to 90% methanol in 2 min and 90% to 100% in 3 min) at a flow rate of 1.5 mL/min. Column temperature was kept at 40 °C. MS detection was in the positive ionization mode, capillary voltage was set at 3 kV and fragmentor voltage was 120 V. N_2 was used as drying gas at a flow rate of 13 L/min and a temperature of 350 °C. Nebulizer pressure was set at 60 psi. For quantification purposes, we monitored the sodium adducts of the molecular ions $[M + Na]^+$ in the selected ion-monitoring (SIM) mode.

For nonesterified fatty acids, we used a reversed-phase XDB Eclipse C18 column (50 mm × 4.6 mm inner diameter, 1.8 μm, Zorbax, Agilent Technologies) eluted with a linear gradient from 90% to 100% of A in B for 2.5 min at a flow rate of 1.5 mL/min with column temperature at 40 °C. Mobile phase A consisted of methanol containing 0.25% acetic acid and 5 mM ammonium acetate; mobile phase B consisted of water containing 0.25% acetic acid and 5 mM ammonium acetate. ESI was in the negative mode, capillary voltage was set at 4 kV and fragmentor voltage was 100 V. N_2 was used as drying gas at a flow rate of 13 L/min and a temperature of 350 °C. Nebulizer pressure was set at 60 psi. We monitored deprotonated molecular ions $[M - H]^-$ in the SIM mode and $[^2H_8]$-AA (m/z 311) was used as an internal standard.

■ ASSOCIATED CONTENT

Supporting Information

The Supporting Information is available free of charge at https://pubs.acs.org/doi/10.1021/acs.jmedchem.3c01278.

Synthesis of compounds (±)-**6a−j** and (±)-**7a−d**; optimized protocol for the synthesis of compounds (±)-**5d** and (±)-**5v**; enzymatic and receptor binding assays to determine the selectivity profile of compounds (±)-**5d** and (±)-**5v** on a panel of 49 different targets; data collection and refinement statistics for X-ray data; computational studies on the new azetidin-2-one-based MAGL inhibitors; CB_2R receptor profiling by means of TR-FRET-based assays of compounds (±)-**5d** and (±)-**5v**; viability of mouse fibroblasts NIH3T3 after incubation with (±)-**5a**, (±)-**5l**, and (±)-**5v**; Ames test performed on *S. typhimurium* TA98 and TA100 strains for compounds (±)-**5a**, (±)-**5h**, and (±)-**5v**; spectroscopic data for compounds (±)-**5c**, (±)-**5d**, and (±)-**5v**; computational studies (PDF)

Molecular formula strings (CSV)

Accession Codes

The coordinates of the structures were deposited in the PDB under the PDB ID accession codes 8PTC, 8PTQ, and 8PTR. Authors will release the atomic coordinates upon article publication.

■ AUTHOR INFORMATION

Corresponding Authors

Stefania Butini − *Department of Biotechnology, Chemistry and Pharmacy, University of Siena, 53100 Siena, Italy;* orcid.org/0000-0002-8471-0880; Phone: 0039-0577-234161; Email: butini3@unisi.it

Giuseppe Campiani − *Department of Biotechnology, Chemistry and Pharmacy, University of Siena, 53100 Siena, Italy; Bioinformatics Research Center, School of Pharmacy and Pharmaceutical Sciences, Isfahan University of Medical Sciences, Isfahan 81746-7346, Iran;* Email: giuseppe.campiani@unisi.it

Authors

Uwe Grether − *Pharma Research and Early Development, Roche Innovation Center Basel, F. Hoffmann-La Roche Ltd, CH-4070 Basel, Switzerland;* orcid.org/0000-0002-3164-9270

Kwang-Mook Jung − *Department of Anatomy and Neurobiology, University of California Irvine, Irvine, California 92697, United States;* orcid.org/0000-0003-4096-6953

Alessia Ligresti − *Institute of Biomolecular Chemistry, National Research Council of Italy, 80078 Pozzuoli, Italy;* orcid.org/0000-0003-1787-3900

Marco Allarà − *Institute of Biomolecular Chemistry, National Research Council of Italy, 80078 Pozzuoli, Italy*

Annemarieke G. J. Postmus − *Department of Molecular Physiology, Leiden Institute of Chemistry, Leiden University and Oncode Institute, 2300 CC Leiden, Netherlands*

Samuele Maramai − *Department of Biotechnology, Chemistry and Pharmacy, University of Siena, 53100 Siena, Italy;* orcid.org/0000-0001-7499-6961

Simone Brogi − *Department of Pharmacy, University of Pisa, 56126 Pisa, Italy;* orcid.org/0000-0001-9375-6242

Alessandro Papa − *Department of Biotechnology, Chemistry and Pharmacy, University of Siena, 53100 Siena, Italy*

Gabriele Carullo − *Department of Biotechnology, Chemistry and Pharmacy, University of Siena, 53100 Siena, Italy;* orcid.org/0000-0002-1619-3295

David Sykes − *Faculty of Medicine & Health Sciences, University of Nottingham, Nottingham NG7 2UH, United Kingdom; Centre of Membrane Proteins and Receptors (COMPARE), University of Birmingham and University of Nottingham, B15 2TT Birmingham, Midlands, United Kingdom*

Dmitry Veprintsev − *Faculty of Medicine & Health Sciences, University of Nottingham, Nottingham NG7 2UH, United Kingdom;* orcid.org/0000-0002-3583-5409

Stefano Federico − *Department of Biotechnology, Chemistry and Pharmacy, University of Siena, 53100 Siena, Italy;* orcid.org/0000-0002-7478-6128

Alessandro Grillo − *Department of Biotechnology, Chemistry and Pharmacy, University of Siena, 53100 Siena, Italy*

Bruno Di Guglielmo − *Department of Biotechnology, Chemistry and Pharmacy, University of Siena, 53100 Siena, Italy*

Anna Ramunno − *Department of Pharmacy/DIFARMA, University of Salerno, Salerno 84084 Fisciano, Italy;* orcid.org/0000-0003-1089-2439

Anna Floor Stevens − *Department of Molecular Physiology, Leiden Institute of Chemistry, Leiden University and Oncode Institute, 2300 CC Leiden, Netherlands*

Dominik Heer − *Pharma Research and Early Development, Roche Innovation Center Basel, F. Hoffmann-La Roche Ltd, CH-4070 Basel, Switzerland;* orcid.org/0009-0003-2089-4339

Stefania Lamponi − *Department of Biotechnology, Chemistry and Pharmacy, University of Siena, 53100 Siena, Italy*

Sandra Gemma − *Department of Biotechnology, Chemistry and Pharmacy, University of Siena, 53100 Siena, Italy;* orcid.org/0000-0002-8313-2417

Jörg Benz − *Pharma Research and Early Development, Roche Innovation Center Basel, F. Hoffmann-La Roche Ltd, CH-4070 Basel, Switzerland*

Vincenzo Di Marzo − *Institute of Biomolecular Chemistry, National Research Council of Italy, 80078 Pozzuoli, Italy; Centre Nutrition, Santé et Société (NUTRISS), Institut sur La Nutrition Et Les Aliments Fonctionnels (INAF), École de Nutrition, Université Laval, Québec G1V 0A6, Canada; Canada Excellence Research Chair in the Microbiome-Endocannabinoidome Axis in Metabolic Health, Quebec G1V 0A6, Canada; Centre de Recherche de l'Institut de Cardiologie et de Pneumologie de Québec, Faculté de Médecine, Département de Médecine, Université Laval, Québec G1V 4G5, Canada; Unité Mixte Internationale en Recherche Chimique et Biomoléculaire sur le Microbiome et Son Impact Sur la Santé Métabolique et la Nutrition (UMI-MicroMeNu), Université Laval, Quebec G1V 0A6, Canada*

Mario van der Stelt − *Department of Molecular Physiology, Leiden Institute of Chemistry, Leiden University and Oncode Institute, 2300 CC Leiden, Netherlands*

Daniele Piomelli − *Department of Anatomy and Neurobiology, University of California Irvine, Irvine, California 92697, United States;* orcid.org/0000-0002-2983-774X

Complete contact information is available at: https://pubs.acs.org/10.1021/acs.jmedchem.3c01278

Notes

The authors declare no competing financial interest.

■ ACKNOWLEDGMENTS

The technical assistance of Isabelle Kaufmann, Lea Leibrock, Andreas Topp, Matthias Wittwer, Carina Cantrill, Sandrine Simon, and Björn Wagner is greatly acknowledged. Don Wei (MD) is acknowledged for helping in some *in vivo* experiments. Work in the Piomelli lab was supported by grant R21DA053358. S.B. and A.P. thank MIUR-PRIN no. 20175SA5JJ for financial support.

■ ABBREVIATIONS USED

2-AG, 2-arachidonoylglycerol; AA, arachidonic acid; ABHD6, α/β-hydrolase domain-containing 6; ABPP, activity-based protein profiling; AEA, anandamide; BBB, blood−brain barrier; CB_1R, cannabinoid receptor 1; CB_2R, cannabinoid receptor 2; CNS, central nervous system; DBU, 1,5-diazabiciclo(5.4.0)-undec-7-ene; DCM, dichloromethane; DMAP, 4-dimethylaminopyridine; DMSO, dimethyl sulfoxide; ECS, endocannabinoid system; EtOH, ethanol; FAAH, fatty acid amide hydrolase; GPCRs, G protein-coupled receptors; HCl, hydrochloride acid; MeCN, acetonitrile; MeOH, methanol; MS, multiple sclerosis; OEA, oleoylethanolamide; PAMPA, parallel artificial membrane permeability assay; PEA, palmitoylethanolamide; TEA, triethylamine; TFA, trifluoroacetic acid; THF, tetrahydrofuran

■ REFERENCES

(1) Lu, H. C.; Mackie, K. Review of the Endocannabinoid System. *Biol. Psychiatry Cogn. Neurosci. Neuroimaging* **2021**, *6* (6), 607−615.

(2) Papa, A.; Pasquini, S.; Contri, C.; Gemma, S.; Campiani, G.; Butini, S.; Varani, K.; Vincenzi, F. Polypharmacological Approaches for CNS Diseases: Focus on Endocannabinoid Degradation Inhibition. *Cells* **2022**, *11* (3), 471.

(3) Meccariello, R. Endocannabinoid System in Health and Disease: Current Situation and Future Perspectives. *Int. J. Mol. Sci.* **2020**, *21* (10), 3549−3549.

(4) Piomelli, D.; Mabou Tagne, A. Endocannabinoid-Based Therapies. *Annu. Rev. Pharmacol. Toxicol.* **2022**, *62*, 483−507.

(5) Di Marzo, V. Targeting the Endocannabinoid System: To Enhance or Reduce? *Nat. Rev. Drug Discovery* **2008**, *7* (5), 438−455.

(6) Butini, S.; Gemma, S.; Campiani, G. Chapter 8: Natural Compounds and Synthetic Drugs to Target FAAH Enzyme. *RSC Drug Discovery Series* **2020**, *2021*, 337−384.

(7) Bisogno, T.; De Petrocellis, L.; Di Marzo, V. Fatty Acid Amide Hydrolase, an Enzyme with Many Bioactive Substrates. Possible Therapeutic Implications. *Curr. Pharm. Des.* **2002**, *8* (7), 533−547.

(8) Blankman, J. L.; Simon, G. M.; Cravatt, B. F. A Comprehensive Profile of Brain Enzymes That Hydrolyze the Endocannabinoid 2-Arachidonoylglycerol. *Chem. Biol.* **2007**, *14* (12), 1347−1356.

(9) Scalvini, L.; Piomelli, D.; Mor, M. Monoglyceride Lipase: Structure and Inhibitors. *Chem. Phys. Lipids* **2016**, *197*, 13−24.

(10) Mulvihill, M. M.; Nomura, D. K. Therapeutic Potential of Monoacylglycerol Lipase Inhibitors. *Life Sci.* **2013**, *92* (8−9), 492−497.

(11) Ignatowska-Jankowska, B. M.; Ghosh, S.; Crowe, M. S.; Kinsey, S. G.; Niphakis, M. J.; Abdullah, R. A.; Tao, Q.; O'Neal, S. T.; Walentiny, D. M.; Wiley, J. L.; et al. In Vivo Characterization of the Highly Selective Monoacylglycerol Lipase Inhibitor KML29: Antinociceptive Activity without Cannabimimetic Side Effects. *Br. J. Pharmacol.* **2014**, *171* (6), 1392−1407.

(12) Nomura, D. K.; Morrison, B. E.; Blankman, J. L.; Long, J. Z.; Kinsey, S. G.; Marcondes, M. C. G.; Ward, A. M.; Hahn, Y. K.; Lichtman, A. H.; Conti, B.; Cravatt, B. T. Endocannabinoid Hydrolysis Generates Brain Prostaglandins That Promote Neuroinflammation. *Science.* **2011**, *334*, 809−813.

(13) Zhang, J.; Hu, M.; Teng, Z.; Tang, Y. P.; Chen, C. Synaptic and Cognitive Improvements by Inhibition of 2-AG Metabolism Are through Upregulation of MicroRNA-188−3p in a Mouse Model of Alzheimer's Disease. *J. Neurosci.* **2014**, *34* (45), 14919−14933.

(14) Pasquarelli, N.; Porazik, C.; Bayer, H.; Buck, E.; Schildknecht, S.; Weydt, P.; Witting, A.; Ferger, B. Contrasting Effects of Selective MAGL and FAAH Inhibition on Dopamine Depletion and GDNF Expression in a Chronic MPTP Mouse Model of Parkinson's Disease. *Neurochem. Int.* **2017**, *110*, 14−24.

(15) Pasquarelli, N.; Engelskirchen, M.; Hanselmann, J.; Endres, S.; Porazik, C.; Bayer, H.; Buck, E.; Karsak, M.; Weydt, P.; Ferger, B.; et al. Evaluation of Monoacylglycerol Lipase as a Therapeutic Target in a Transgenic Mouse Model of ALS. *Neuropharmacology* **2017**, *124*, 157−169.

(16) Brindisi, M.; Maramai, S.; Gemma, S.; Brogi, S.; Grillo, A.; Di Cesare Mannelli, L.; Gabellieri, E.; Lamponi, S.; Saponara, S.; Gorelli, B.; et al. Development and Pharmacological Characterization of Selective Blockers of 2-Arachidonoyl Glycerol Degradation with Efficacy in Rodent Models of Multiple Sclerosis and Pain. *J. Med. Chem.* **2016**, *59* (6), 2612−2632.

(17) Hernández-Torres, G.; Cipriano, M.; Hedén, E.; Björklund, E.; Canales, Á.; Zian, D.; Feliú, A.; Mecha, M.; Guaza, C.; Fowler, C. J.; et al. A Reversible and Selective Inhibitor of Monoacylglycerol Lipase Ameliorates Multiple Sclerosis. *Angew. Chem.* **2014**, *126* (50), 13985−13990.

(18) Lim, J.; Igarashi, M.; Jung, K. M.; Butini, S.; Campiani, G.; Piomelli, D. Endocannabinoid Modulation of Predator Stress-Induced Long-Term Anxiety in Rats. *Neuropsychopharmacology* **2016**, *41* (5), 1329−1339.

(19) Labar, G.; Bauvois, C.; Borel, F.; Ferrer, J. L.; Wouters, J.; Lambert, D. M. Crystal Structure of the Human Monoacylglycerol Lipase, a Key Actor in Endocannabinoid Signaling. *ChemBioChem.* **2010**, *11* (2), 218−227.

(20) Long, J. Z.; Nomura, D. K.; Cravatt, B. F. Characterization of Monoacylglycerol Lipase Inhibition Reveals Differences in Central and Peripheral Endocannabinoid Metabolism. *Chem. Biol.* **2009**, *16* (7), 744−753.

(21) Bertrand, T.; Augé, F.; Houtmann, J.; Rak, A.; Vallée, F.; Mikol, V.; Berne, P. F.; Michot, N.; Cheuret, D.; Hoornaert, C.; et al. Structural Basis for Human Monoglyceride Lipase Inhibition. *J. Mol. Biol.* **2010**, *396* (3), 663−673.
(22) Flores, C.; Nelen, M. I.; Nulton, E. L.; Prouty, S.; Todd, M.; Zhang, S.-P.Heteroaromatic and Aromatic Piperazinyl Azetidinyl Amides as Monoacylglycerol Lipase Inhibitors. World Patent WO2010124122A1, 2010.
(23) Schalk-Hihi, C.; Schubert, C.; Alexander, R.; Bayoumy, S.; Clemente, J. C.; Deckman, I.; DesJarlais, R. L.; Dzordzorme, K. C.; Flores, C. M.; Grasberger, B.; et al. Crystal Structure of a Soluble Form of Human Monoglyceride Lipase in Complex with an Inhibitor at 1.35 Å Resolution. *Protein Sci.* **2011**, *20* (4), 670−683.
(24) Zanfirescu, A.; Ungurianu, A.; Mihai, D. P.; Radulescu, D.; Nitulescu, G. M. Targeting Monoacylglycerol Lipase in Pursuit of Therapies for Neurological and Neurodegenerative Diseases. *Molecules* **2021**, *26* (18), 5668.
(25) Gil-Ordóñez, A.; Martín-Fontecha, M.; Ortega-Gutiérrez, S.; López-Rodríguez, M. L. Monoacylglycerol Lipase (MAGL) as a Promising Therapeutic Target. *Biochem. Pharmacol.* **2018**, *157* (May), 18−32.
(26) Aaltonen, N.; Savinainen, J. R.; Ribas, C. R.; Rönkkö, J.; Kuusisto, A.; Korhonen, J.; Navia-Paldanius, D.; Häyrinen, J.; Takabe, P.; Käsnänen, H.; et al. Piperazine and Piperidine Triazole Ureas as Ultrapotent and Highly Selective Inhibitors of Monoacylglycerol Lipase. *Chem. Biol.* **2013**, *20* (3), 379−390.
(27) Cisar, J. S.; Weber, O. D.; Clapper, J. R.; Blankman, J. L.; Henry, C. L.; Simon, G. M.; Alexander, J. P.; Jones, T. K.; Ezekowitz, R. A. B.; O'Neill, G. P.; et al. Identification of ABX-1431, a Selective Inhibitor of Monoacylglycerol Lipase and Clinical Candidate for Treatment of Neurological Disorders. *J. Med. Chem.* **2018**, *61* (20), 9062−9084.
(28) Brindisi, M.; Borrelli, G.; Brogi, S.; Grillo, A.; Maramai, S.; Paolino, M.; Benedusi, M.; Pecorelli, A.; Valacchi, G.; Di Cesare Mannelli, L.; et al. Development of Potent Inhibitors of Fatty Acid Amide Hydrolase Useful for the Treatment of Neuropathic Pain. *ChemMedChem.* **2018**, *13* (19), 2090−2103.
(29) Colangeli, R.; Pierucci, M.; Benigno, A.; Campiani, G.; Butini, S.; Di Giovanni, G. The FAAH Inhibitor URB597 Suppresses Hippocampal Maximal Dentate Afterdischarges and Restores Seizure-Induced Impairment of Short and Long-Term Synaptic Plasticity. *Sci. Rep.* **2017**, *7* (1), 1−17.
(30) Grillo, A.; Fezza, F.; Chemi, G.; Colangeli, R.; Brogi, S.; Fazio, D.; Federico, S.; Papa, A.; Relitti, N.; Di Maio, R.; et al. Selective Fatty Acid Amide Hydrolase Inhibitors as Potential Novel Antiepileptic Agents. *ACS Chem. Neurosci.* **2021**, *12* (9), 1716−1736.
(31) Grillo, A.; Chemi, G.; Brogi, S.; Brindisi, M.; Relitti, N.; Fezza, F.; Fazio, D.; Castelletti, L.; Perdona, E.; Wong, A. Development of Novel Multipotent Compounds Modulating Endocannabinoid and Dopaminergic Systems. *Eur. J. Med. Chem.* **2019**, *183*, 111674.
(32) Papa, A.; Pasquini, S.; Galvani, F.; Cammarota, M.; Contri, C.; Carullo, G.; Gemma, S.; Ramunno, A.; Lamponi, S.; Gorelli, B.; Saponara, S.; Varani, K.; Mor, M.; Campiani, G.; Boscia, F.; Vincenzi, F.; Lodola, A.; Butini, S.; et al. Development of Potent and Selective FAAH Inhibitors with Improved Drug-like Properties as Potential Tools to Treat Neuroinflammatory Conditions. *Eur. J. Med. Chem.* **2023**, *246*, No. 114952.
(33) Strelow, J. M. A Perspective on the Kinetics of Covalent and Irreversible Inhibition. *SLAS Discov* **2017**, *22* (1), 3−20.
(34) Federico, S.; Khan, T.; Fontana, A.; Brogi, S.; Benedetti, R.; Sarno, F.; Carullo, G.; Pezzotta, A.; Saraswati, A. P.; Passaro, E.; Pozzetti, L.; Papa, A.; Relitti, N.; Gemma, S.; Butini, S.; Pistocchi, A.; Ramunno, A.; Vincenzi, F.; Varani, K.; Tatangelo, V.; Patrussi, L.; Baldari, C. T.; Saponara, S.; Gorelli, B.; Lamponi, S.; Valoti, M.; Saccoccia, F.; Giannaccari, M.; Ruberti, G.; Herp, D.; Jung, M.; Altucci, L.; Campiani, G.; et al. European Journal of Medicinal Chemistry Azetidin-2-One-Based Small Molecules as Dual h HDAC6/HDAC8 Inhibitors : Investigation of Their Mechanism of Action and Impact of Dual Inhibition Profile on Cell Viability. *Eur. J. Med. Chem.* **2022**, *238*, No. 114409.
(35) Byrne, F. P.; Jin, S.; Paggiola, G.; Petchey, T. H. M.; Clark, J. H.; Farmer, T. J.; Hunt, A. J.; Robert McElroy, C.; Sherwood, J. Tools and Techniques for Solvent Selection: Green Solvent Selection Guides. *Sustain. Chem. Process.* **2016**, *4* (1), 7.
(36) Boddu, S. K.; Ur Rehman, N.; Mohanta, T. K.; Majhi, A.; Avula, S. K.; Al-Harrasi, A. A Review on DBU-Mediated Organic Transformations. *Green Chem. Lett. Rev.* **2022**, *15*, 765−795.
(37) Aaltonen, N.; Kedzierska, E.; Orzelska-Górka, J.; Lehtonen, M.; Navia-Paldanius, D.; Jakupovic, H.; Savinainen, J. R.; Nevalainen, T.; Laitinen, J. T.; Parkkari, T.; et al. In Vivo Characterization of the Ultrapotent Monoacylglycerol Lipase Inhibitor {4-[Bis-(Benzo[d]-[1,3]Dioxol-5-Yl)Methyl]-Piperidin-1-Yl}(1H-1,2,4-Triazol-1-Yl)-Methanone (JJKK-048). *J. Pharmacol. Exp. Ther.* **2016**, *359* (1), 62−72.
(38) Otrubova, K.; Chatterjee, S.; Ghimire, S.; Cravatt, B. F.; Boger, D. L. N-Acyl Pyrazoles: Effective and Tunable Inhibitors of Serine Hydrolases. *Bioorg. Med. Chem.* **2019**, *27* (8), 1693−1703.
(39) Sekhon. Exploiting the Power of Stereochemistry in Drugs: An Overview of Racemic and Enantiopure Drugs. *J. Mod. Med. Chem.* **2013**, 10−36.
(40) Sarott, R. C.; Westphal, M. V.; Pfaff, P.; Korn, C.; Sykes, D. A.; Gazzi, T.; Brennecke, B.; Atz, K.; Weise, M.; Mostinski, Y.; et al. Development of High-Specificity Fluorescent Probes to Enable Cannabinoid Type 2 Receptor Studies in Living Cells. *J. Am. Chem. Soc.* **2020**, *142* (40), 16953−16964.
(41) Bendels, S.; Bissantz, C.; Fasching, B.; Gerebtzoff, G.; Guba, W.; Kansy, M.; Migeon, J.; Mohr, S.; Peters, J.-U.; Tillier, F.; et al. Safety Screening in Early Drug Discovery: An Optimized Assay Panel. *J. Pharmacol. Toxicol. Methods* **2019**, *99*, No. 106609.
(42) Kansy, M.; Senner, F.; Gubernator, K. Screening : Parallel Artificial Membrane Permeation Assay in the Description Of. *J. Med. Chem.* **1998**, *41* (7), 1007−1010.
(43) Ligresti, A.; Silvestri, C.; Vitale, R. M.; Martos, J. L.; Piscitelli, F.; Wang, J. W.; Allarà, M.; Carling, R. W.; Luongo, L.; Guida, F.; et al. FAAH-Catalyzed C−C Bond Cleavage of a New Multitarget Analgesic Drug. *ACS Chem. Neurosci.* **2019**, *10* (1), 424−437.
(44) King, A. R.; Duranti, A.; Tontini, A.; Rivara, S.; Rosengarth, A.; Clapper, J. R.; Astarita, G.; Geaga, J. A.; Luecke, H.; Mor, M.; et al. URB602 Inhibits Monoacylglycerol Lipase and Selectively Blocks 2-Arachidonoylglycerol Degradation in Intact Brain Slices. *Chem. Biol.* **2007**, *14* (12), 1357−1365.
(45) He, Y.; Gobbi, L. C.; Herde, A. M.; Rombach, D.; Ritter, M.; Kuhn, B.; Wittwer, M. B.; Heer, D.; Hornsperger, B.; Bell, C.; et al. Discovery, Synthesis and Evaluation of Novel Reversible Monoacylglycerol Lipase Radioligands Bearing a Morpholine-3-One Scaffold. *Nucl. Med. Biol.* **2022**, *108−109*, 24−32.
(46) He, Y.; Schild, M.; Grether, U.; Benz, J.; Leibrock, L.; Heer, D.; Topp, A.; Collin, L.; Kuhn, B.; Wittwer, M.; et al. Development of High Brain-Penetrant and Reversible Monoacylglycerol Lipase PET Tracers for Neuroimaging. *J. Med. Chem.* **2022**, *65* (3), 2191−2207.
(47) Janssen, A. P. A.; Van Der Vliet, D.; Bakker, A. T.; Jiang, M.; Grimm, S. H.; Campiani, G.; Butini, S.; Van Der Stelt, M. Development of a Multiplexed Activity-Based Protein Profiling Assay to Evaluate Activity of Endocannabinoid Hydrolase Inhibitors. *ACS Chem. Biol.* **2018**, *13* (9), 2406−2413.
(48) King, A. R.; Lodola, A.; Carmi, C.; Fu, J.; Mor, M.; Piomelli, D. A Critical Cysteine Residue in Monoacylglycerol Lipase Is Targeted by a New Class of Isothiazolinone-Based Enzyme Inhibitors. *Br. J. Pharmacol.* **2009**, *157* (6), 974−983.
(49) Copeland, R. A. Evaluation of Enzyme Inhibitors in Drug Discovery. A Guide for Medicinal Chemists and Pharmacologists. *Methods Biochem. Anal.* **2005**, *46*, 1−265.
(50) Kabsch, W. Integration, Scaling, Space-Group Assignment and Post-Refinement. *Acta Crystallogr. Sect. D* **2010**, *66* (2), 133−144.
(51) McCoy, A. J.; Grosse-Kunstleve, R. W.; Adams, P. D.; Winn, M. D.; Storoni, L. C.; Read, R. J. {\it Phaser} Crystallographic Software. *J. Appl. Crystallogr.* **2007**, *40* (4), 658−674.
(52) Winn, M. D.; Ballard, C. C.; Cowtan, K. D.; Dodson, E. J.; Emsley, P.; Evans, P. R.; Keegan, R. M.; Krissinel, E. B.; Leslie, A. G. W.;

McCoy, A.; et al. Overview of the {\it CCP}4 Suite and Current Developments. *Acta Crystallogr. Sect. D* **2011**, *67* (4), 235−242.

(53) Dengl, S.; Fenn, S.; Georges, G.; Moelleken, J.; Ros, F.; Koenigsberger, E. Anti-Vegf antibodies and methods of use. WO2019129677A1

(54) Emsley, P.; Lohkamp, B.; Scott, W. G.; Cowtan, K. Features and Development of{\it Coot}. *Acta Crystallogr. Sect. D* **2010**, *66* (4), 486−501.

(55) Porter, R. F.; Szczesniak, A.-M.; Toguri, J. T.; Gebremeskel, S.; Johnston, B.; Lehmann, C.; Fingerle, J.; Rothenhäusler, B.; Perret, C.; Rogers-Evans, M. Selective Cannabinoid 2 Receptor Agonists as Potential Therapeutic Drugs for the Treatment of Endotoxin-Induced Uveitis. *Molecules* **2019**, *24* (18), 3338.

(56) Di, L.; Keefer, C.; Scott, D. O.; Strelevitz, T. J.; Chang, G.; Bi, Y. A.; Lai, Y.; Duckworth, J.; Fenner, K.; Troutman, M. D.; et al. Mechanistic Insights from Comparing Intrinsic Clearance Values between Human Liver Microsomes and Hepatocytes to Guide Drug Design. *Eur. J. Med. Chem.* **2012**, *57*, 441−448.

(57) LeCluyse, E. L.; Witek, R. P.; Andersen, M. E.; Powers, M. J. Organotypic Liver Culture Models: Meeting Current Challenges in Toxicity Testing. *Crit. Rev. Toxicol.* **2012**, *42* (6), 501−548.

(58) Caruso, A.; Alvarez-Sánchez, R.; Hillebrecht, A.; Poirier, A.; Schuler, F.; Lavé, T.; Funk, C.; Belli, S. PK/PD Assessment in CNS Drug Discovery: Prediction of CSF Concentration in Rodents for P-Glycoprotein Substrates and Application to in Vivo Potency Estimation. *Biochem. Pharmacol.* **2013**, *85* (11), 1684−1699.

(59) Schwab, D.; Fischer, H.; Tabatabaei, A.; Poli, S.; Huwyler, J. Comparison of in Vitro P-Glycoprotein Screening Assays: Recommendations for Their Use in Drug Discovery. *J. Med. Chem.* **2003**, *46* (9), 1716−1725.

(60) Fowler, S.; Zhang, H. In Vitro Evaluation of Reversible and Irreversible Cytochrome P450 Inhibition: Current Status on Methodologies and Their Utility for Predicting Drug-Drug Interactions. *AAPS J.* **2008**, *10* (2), 410−424.

(61) Lamponi, S.; Aloisi, A. M.; Bonechi, C.; Consumi, M.; Donati, A.; Leone, G.; Rossi, C.; Tamasi, G.; Ghiandai, L.; Ferrini, E.; et al. Evaluation of in Vitro Cell and Blood Compatibility and in Vivo Analgesic Activity of Plant-Derived Dietary Supplements. *J. Integr. Med.* **2019**, *17* (3), 213−220.

(62) Astarita, G.; Piomelli, D. Lipidomic Analysis of Endocannabinoid Metabolism in Biological Samples. *J. Chromatogr. B. Analyt. Technol. Biomed. Life Sci.* **2009**, *877* (26), 2755−2767.

https://doi.org/10.1021/acs.jmedchem.3c01278
J. Med. Chem. 2024, 67, 1758−1782